icct
THE INTERNATIONAL COUNCIL ON CLEAN TRANSPORTATION

SEPTEMBER 2025

Aviation Vision 2050

The potential for climate-neutral growth

XINYI SOLA ZHENG, JAYANT MUKHOPADHAYA PH.D., JONATHAN BENOIT, SUPRAJA N. KUMAR, DAN RUTHERFORD PH.D., DENIZ RHODE, DANIEL SITOMPUL

ACKNOWLEDGMENTS

The authors thank ICCT researchers Ana Beatriz Rebouças and Gabe Alvarez for their thoughtful feedback. We are also grateful to the external reviewers—Tim Johnson (Transport & Environment), Marc Shapiro (Breakthrough Energy), Tom Opderbeck and Sarah Chou (American Airlines), and Jerrold Cline (GE Aerospace Research)—for their valuable inputs. This work was conducted with generous support from Climate Imperative Foundation.

International Council on Clean Transportation
1500 K Street NW, Suite 650
Washington, DC 20005

communications@theicct.org | www.theicct.org | @TheICCT

EXECUTIVE SUMMARY

Aviation is a growing contributor to climate change, with effects extending beyond carbon dioxide (CO_2) emissions to include short-lived climate pollutants (SLCPs) such as nitrogen oxides, black carbon, and contrail cirrus. In 2022, the International Civil Aviation Organization agreed to achieve net-zero CO_2 emissions by 2050, but the industry is not on track to deliver the scale of fuel efficiency improvements, sustainable aviation fuel (SAF) uptake, and zero-emission aircraft development required to meet that goal. Recent advances in the scientific understanding of SLCPs have attracted attention to the potential rapid reductions in aviation-attributable warming through contrail mitigation. But no deep decarbonization roadmaps for aviation have been updated to reflect SLCP controls.

This report updates the ICCT's *Vision 2050* decarbonization roadmap for the aviation sector by quantifying how SLCP mitigation can complement greenhouse gas (GHG) strategies to align aviation with the Paris Agreement. Using a high-fidelity 2023 flight emission inventory (JETSTREAM), an emission projection model (PACE 2.0), and a simplified climate model (FaIR), the report estimates aviation's warming potential through 2050 across five scenarios that span the full range of GHG and SLCP control: Historical Trends, Current Commitments, GHG Forward, SLCP Forward, and Full Breakthrough.

The Paris Agreement, adopted in 2015, commits countries to limit global warming to well below 2 °C and to pursue efforts to limit the temperature increase to 1.5 °C above pre-industrial levels. This report compares aviation's warming contributions to the remaining 1.7 °C warming budget, reflecting recent findings that global warming is likely to surpass the 1.5 °C threshold before 2030.

As shown in Figure ES1, under the Historical Trends scenario, we project an additional 60 millidegrees Celsius (mC), or 0.06 °C, of warming from aviation activity between 2025 and 2050, which is double its contribution to temperature change over its entire history from 1940 to 2024. The Current Commitments scenario, which accounts for policies to curb aviation GHG emissions announced to date, projects an 11 mC (19%) reduction in warming by mid-century. The GHG Forward case, which models maximum levels of GHG mitigation through SAF uptake, zero-emission planes (ZEPs), and improved fuel efficiency, is projected to cut future warming by 29 mC, or 48% below the Historical Trends case. However, aviation would double its historical 4% share of global warming, to 9% of the remaining 1.7 °C budget, under this scenario.

Figure ES1

Aviation's projected contribution to global warming by scenario, 1940 to 2050

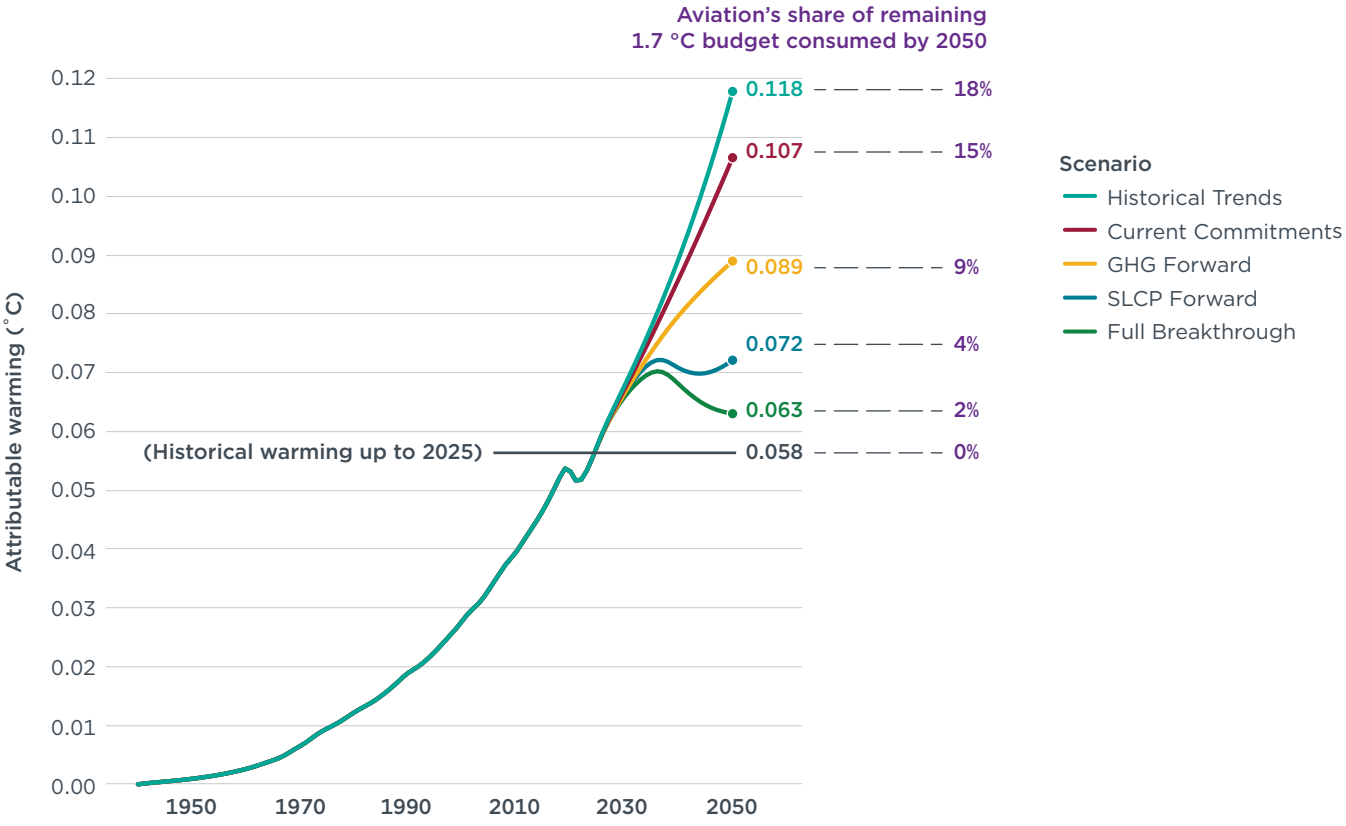

THE INTERNATIONAL COUNCIL ON CLEAN TRANSPORTATION **THEICCT.ORG**

Larger reductions are modeled via the SLCP Forward scenario, which adds contrail avoidance, fuel quality improvements, and advanced engines to the Current Commitments scenario; in this scenario, additional warming is reduced by 46 mC, or 76% below Historical Trends. The SLCP Forward scenario keeps aviation to a 4% share of the remaining 1.7 °C climate budget until 2050, but the share will likely increase beyond 2050 as unmitigated GHG emissions continue to drive warming. In the Full Breakthrough scenario, which blends maximum GHG and SLCP mitigation, aviation's contribution to global warming is cut by 91% below the Historical Trends scenario and limits aviation's share of additional contribution to the remaining 1.7 °C budget to 2%.

By comparing the Historical Trends and Full Breakthrough scenarios, we can characterize the relative contribution that different mitigation levers may play in curbing aviation's climate impact. Table ES1 summarizes the relative contribution of each mitigation lever to avoidable warming in 2050. The share of total warming by mitigation lever is shown at the far right; the breakdown of GHG versus SLCP control is shown at the bottom of the table.

Table ES1

Share of avoidable warming by mitigation lever in 2050 under the Full Breakthrough scenario

Rank	Mitigation lever	Avoided warming (mC)			% of total
		GHGs	SLCPs	Total	
1	**Contrail avoidance**	0.07	-23.4	-23.3	42.5%
2	**Sustainable aviation fuel**	-5.90	-5.68	-11.6	21.1%
3	**Hydrotreating**	0.05	-6.35	-6.30	11.5%
4	**Operational efficiency**	-1.37	-4.58	-5.95	10.8%
5	**Low NO_x/nvPM engines**	0.00	-4.39	-4.39	8.0%
6	**Technical efficiency**	-0.84	-1.80	-2.64	4.8%
7	**Demand response**	-0.12	-0.30	-0.42	0.8%
8	**Modal shift**	-0.07	-0.17	-0.25	0.5%
9	**Zero-emission planes**	-0.02	-0.02	-0.05	0.1%
	Total	**-8.20**	**-46.6**	**-54.9**	**100%**
	% of total	**15%**	**85%**	**100%**	

As shown in the table, contrail avoidance contributes the largest share (23 mC, or more than 40%) of all potential avoidable warming. That includes a small (0.07 mC) temperature increase due to the fuel burn penalty of rerouting. The use of SAF contributes 21% of avoided temperature increase, the second largest amount. Hydrotreating and operational efficiency are the third and fourth most important levers, both contributing about 11% of the total avoidable warming; three-quarters of the operational efficiency-enabled mitigation comes from SLCPs due in part to a reduction in kilometers flown. Other levers, including low NO_x and low non-volatile particulate matter (nvPM) engines, hydrotreating, technical efficiency, ZEPs, demand response, and modal shift contribute only modestly to avoidable warming. Overall, 85% of the avoided temperature increase is linked to SLCPs. Because contrail abatement technologies would take less time to develop and scale compared to SAF, and at lower cost ($5–$20 per tonne CO_2e, versus more than $300 per tonne CO_2e), SLCP reduction emerges as a more feasible option with large potential in mitigating aviation's climate impact.

Key conclusions of this work include:

» **A 2050 net-zero CO_2 target is a necessary but not sufficient condition to align aviation with the Paris Agreement.** While a maximum level of GHG mitigation through aircraft and fuels is estimated to cut additional aviation warming by 48% below the Historical Trends scenario, we still project a 31 mC temperature rise due to aviation in 2050, with continuing warming afterwards. Given a remaining climate budget of 340 mC to achieve 1.7 °C (Forster et al., 2024), aviation would consume 9% of the remaining 1.7 °C climate budget under a maximum GHG reduction scenario, more than double its historical share of 4%.

» **SLCP controls, notably contrail avoidance, can complement GHG mitigation by delivering substantial near-term reductions via easier-to-implement technology solutions.** Contrail avoidance in particular is modeled to be the most impactful and cost-effective lever, accounting for 40% of total avoidable warming by 2050

in the Full Breakthrough scenario, with mitigation costs orders of magnitude lower than for SAFs. Still, without additional action on lower carbon planes and fuels, the short-term cooling due to SLCP cuts is projected to be overwhelmed by 2045 due to accumulating GHGs in the atmosphere, driving more warming.

- **Aggressive GHG and SLCP controls will be needed to contain aviation's contribution to global warming and achieve climate-neutral growth.** Combining aggressive GHG and SLCP controls under the Full Breakthrough scenario is projected to cut more than 90% of additional aviation-attributable warming by 2050 compared with the Historical Trends scenario, limiting aviation's share of the remaining 1.5 °C climate budget consumed by 2050 to 4% and its share of the remaining 1.7 °C budget consumed to 2%. This reduction can be achieved despite a 150% increase in traffic compared with 2023, resulting in climate-neutral growth between 2035 and 2050—and potentially beyond with further GHG controls.
- **Four mitigation levers—contrail avoidance, SAFs, hydrotreating, and operational efficiency—account for nearly 90% of avoidable warming in 2050.** Policymakers could prioritize measures to mature these key technologies, such as widescale avoidance trials coordinated by air navigation service providers, mandates and incentives for SAF and hydrotreating fossil jet fuel, and carbon pricing policies to promote more fuel-efficient operations. Deployment of SAF in particular would deliver both GHG and SLCP mitigation benefits.
- **Control of SLCP is estimated to result in a climate benefit despite the expected increase in GHG emissions from their implementation.** The benefit of reducing SLCPs is projected to outweigh the increased fuel consumption from applying SLCP control measures. This is still true when assuming the climate impact of SLCPs is at the lower end of the 95% confidence interval from our uncertainty analysis.

The report concludes that current actions focused on GHG emissions are insufficient to align aviation with the Paris Agreement. To achieve mid-term climate stabilization, policymakers can incentivize SLCP controls—especially contrail mitigation—while continuing to develop GHG-reduction technologies for reducing long-term climate impact.

TABLE OF CONTENTS

LIST OF TABLES

LIST OF FIGURES

INTRODUCTION

Aircraft are a large and growing source of greenhouse gas (GHG) emissions, accounting for 2.4% of annual anthropogenic CO_2 emissions in 2018 (Lee et al., 2021) and 4% of anthropogenic global warming to date (Klower et al., 2021).[1] While industry and governments have been focusing on reaching net-zero carbon dioxide (CO_2) emissions by 2050, less attention has been paid to the role of short-lived climate pollutant (SLCP) mitigation in aligning aviation with the Paris Agreement. This is in part due to the scientific uncertainty around the warming impacts of aviation SLCPs, but even at the lower end of estimated effects, mitigation would deliver substantial near-term climate benefits. Contrail activity is highly concentrated over certain regions and flight corridors, making targeted mitigation both feasible and cost-effective with technologies that can be implemented relatively quickly.

To capture the full suite of climate mitigation levers available to the aviation sector, this report updates the ICCT's *Vision 2050* decarbonization roadmap for the aviation sector by quantifying how SLCP mitigation can complement GHG reduction strategies to align aviation with the Paris agreement. This study is organized as follows. We first provide background on aviation's climate impacts and the current state of technology and policy roadmaps. The next section describes the methodology, including emissions inventory development, climate modeling, and scenario design. Next, we present aviation's projected emissions through 2050 and its projected contribution to global warming across five scenarios. We close with discussion on the implications of these findings for climate policy design and future research.

1 In the context of Kyoto Protocol greenhouse gases, aviation's GHG emissions are composed almost entirely of carbon dioxide (CO_2), with small amounts of nitrous oxide (N_2O) and methane (CH_4). Besides GHGs, aviation's contribution to climate change also involve short-lived climate pollutants (with atmospheric lifetimes of less than 20 years) such as contrails, NO_x, nvPM, water vapor, and sulfur oxides.

BACKGROUND

In 2021, the aviation industry established a goal to achieve net-zero CO_2 emissions from operations by 2050. This voluntary commitment was subsequently codified for international aviation by the UN's International Civil Aviation Organization (ICAO) in 2022 (ICAO, 2022b). Underlying ICAO's agreement are technology roadmaps for deep decarbonization. According to the International Air Transport Association (IATA)'s synthesis of all major 2050 net-zero CO_2 roadmaps, including the ICCT's *Vision 2050* (Graver et al., 2022), more than half of cumulative CO_2 reductions through 2050 would need to come from sustainable aviation fuels (SAFs); about 30% from fuel efficiency; and the balance from a combination of economic measures, CO_2 removal, and demand reduction (IATA, 2024a). Some technology roadmaps include hydrogen-powered aircraft, which emit no CO_2 during operation and very little CO_2 on a life-cycle basis when the fuel is produced from renewable power.

The ICCT's previous *Vision 2050* report included four potential scenarios for how aviation's CO_2 emissions may evolve through 2050 (Graver et al., 2022). Under the report's Breakthrough scenario, early, aggressive, and sustained government intervention was assumed to trigger widespread investments in zero-carbon aircraft and fuels, which would peak fossil fuel use in 2025 and end its use by 2050. As a result, cumulative aviation CO_2 would decline by about 55% through 2050, and more than 90% compared with the report's Historical Trends scenario that year. The resulting emission trajectory is consistent with a 1.75 °C warming goal, subject to the constraint that aviation does not increase its share of emissions over time.

In aggregate, the various net-zero roadmaps for aviation imply that aircraft CO_2 emissions will need to peak this decade to achieve net-zero emissions in 2050 (Mithal & Rutherford, 2023). Unfortunately, evidence is building that aviation is unlikely to follow the ambitious technology uptake needed to achieve this goal (Rutherford, 2024). Market data suggest that SAFs accounted for only 0.3% of global jet fuel use in 2024 (IATA, 2024b), or about one-fiftieth of what will be required in 2030 under a net-zero pathway. Legally binding SAF requirements in Brazil, Europe, Japan, and the United Kingdom are consistent with 2% global SAF uptake by 2030.

Similar delays have been seen for zero-emission planes (ZEPs) powered by electricity and hydrogen. Electric aircraft, which could cover a small (up to 0.2%) share of aviation revenue passenger kilometers (RPKs) by 2050, have hit turbulence (Mukhopadhaya & Graver, 2022), with many startups pivoting to hybrid designs. Airbus has rolled back plans to develop a narrowbody hydrogen aircraft and is now focusing on putting a smaller regional aircraft into service (Kaminski-Morrow, 2024). Most recently, Airbus announced that its plan to develop hydrogen aircraft by 2035 would be delayed (Hepher, 2025).

In the absence of low-emission aircraft and fuel deployment at large scale, the primary opportunity for reducing GHG emissions lies in fuel efficiency, mostly through the introduction of new aircraft. Airbus and Boeing are working to develop next-generation narrowbody planes that reduce fuel burn by 20%–25% relative to current aircraft types (Airbus, 2025). That is well short of the fuel burn reductions envisioned under the *Vision 2050* Breakthrough scenario. Hameed & Rutherford (2025) found that the major commercial airframers are certifying fewer of the new aircraft types that drive fuel efficiency improvements. Counting variants within a family, new type introductions fell from a peak of 6 per year in the late 1990s to only 1 per year after 2020.

Given that in-sector CO_2 abatement alone is unlikely to meet the net-zero goal, much less align aviation with a 1.5 °C pathway, interest in climate mitigation through reductions in SLCPs is growing. SLCPs cause transient warming that dissipates quickly once emissions cease (Smith et al., 2018; Berntsen & Fuglestvedt, 2008). This is in contrast to CO_2, whose long atmospheric lifetime commits the planet to persistent warming. Because of their short atmospheric lifetime, SLCP reductions can produce a faster climate benefit—helping to slow near-term warming and buy time for longer-term CO_2 strategies to take effect.

The major source of SLCPs from aviation is condensation trails (contrails) generated by aircraft operating in cold, humid areas of the troposphere, which may drive at least as much global warming as CO_2 alone (Burkhardt & Kärcher, 2011; Lee et al., 2021; Teoh et al., 2024). An estimated 2%–5% of flights crossing ice super-saturated regions—atmospheric zones with relative humidity greater than 100% over ice—cause 80% of short-lived contrail-cirrus warming. Estimates for the marginal cost of contrail abatement range from less than $5/tonne of carbon dioxide equivalent (CO_2e) to $25/tonne of CO_2e, compared with more than $300/tonne for SAFs (Google Research, 2023; Andrews et al., 2024; Transport & Environment, 2024).[2]

Following contrails, NO_x is the SLCP with the second-largest climate impact in the aviation sector. Cruise-phase NO_x emissions lead to the formation of tropospheric ozone and the reduction of methane levels in the atmosphere. At present, the net impact of these emissions is expected to be warming, but future temperature response will depend on background concentrations of these gases (Terrenoire et al., 2022).[3] Non-volatile particulate matter (nvPM), or black carbon, is also expected to have a net warming impact and play a key role in contrail formation. Thus, aircraft engine standards to reduce cruise-phase NO_x emissions and fuels with higher hydrogen content to reduce black carbon emissions may help mitigate aviation's climate impact.

Klöwer et al. (2021) investigated the potential for SLCP cuts to make substantial short-term reductions in climate change. Using a simplified climate model, the authors investigated two scenarios: 1) long-term cuts in traffic of 2.5% per annum, and 2) the adoption of SAFs with low life-cycle carbon and high hydrogen content up to a 90% blend. Under both scenarios, aviation's contribution to global warming was halted this decade at about 0.04 °C, compared with increases of about 0.09 °C in 2050 under a case of 3% traffic growth. Integral to these findings is that quick short-term cuts in radiative forcing (RF)—that is, the net change in Earth's energy balance due to climate forcers, including atmospheric adjustments—from SLCPs can offset longer-term RF impacts from accumulating CO_2 emissions.[4] Klöwer's work, while notable, did not fully explore all mitigation levers (e.g., fuel efficiency improvement and contrail avoidance) and used simplified representations of aircraft technology and operations. Moreover, it generated only global average results and cannot be linked to concrete policies to support the adoption of low GHG and SLCP technologies and practices.

2 All monetary values in this report are in U.S. dollars.

3 The climate impact of aviation cruise-phase NO_x is dependent on the net forcing resulting from increases in ozone and decreases in methane, which is currently warming. However, this could become negative in the future due to changing emissions from other sectors affecting background methane concentrations.

4 The term "radiative forcing" has been used in International Panel on Climate Change assessments to denote an externally imposed perturbation in the radiative energy budget of the Earth's climate system. Such a perturbation can be caused by changes in the concentrations of radiatively active species, the solar irradiance incident, or surface reflection properties. This imbalance in the radiation budget can lead to changes in climate parameters and result in a new equilibrium state of the climate system (Albritton et al., 2001).

METHODOLOGY

SCENARIOS MODELED

This report considers five scenarios—a Historical Trends scenario plus four action scenarios—to model how aviation emissions might evolve over the next 25 years. These scenarios are described below and summarized in Table 1.

- **Historical Trends**: This is a counterfactual scenario in which governments take no additional action to address aviation's climate impact. Only nominal market-driven improvements in fuel efficiency and existing aircraft and engine standards are modeled. The existing ICAO Committee on Aviation Environmental Protection (CAEP) standards include the CAEP/10 CO_2 standard, CAEP/8 NO_x standard, and CAEP/11 nvPM standard (ICAO, 2023d; ICAO, 2017).
- **Current Commitments**: This scenario projects emissions given existing government and industry goals, measures, and commitments. These include declared manufacturer plans to develop new aircraft types through 2035 (including a regional hydrogen fuel-cell aircraft) and announced SAF mandates in Brazil, the European Union, Japan, and the United Kingdom. This scenario is used to measure progress to date.
- **GHG Forward**: This scenario estimates the impacts of dedicated efforts by governments and industry to shift from fossil fuel use to low-carbon aircraft and fuels, peaking GHG emissions in 2030 and nearly halving 2050 aviation CO_2 compared with 2023 levels. Because progress towards net-zero has not been aligned with the 2025 peak of aviation emissions modeled in the ICCT's previous *Vision 2050* report, the Transformation scenario was selected to present the maximum potential for GHG reductions from aircraft and fuels in this study (Rutherford, 2024). Specifically, SAFs achieve an 8% market share globally in 2030, rising to 71% in 2050. Aircraft manufacturers develop more fuel efficient widebody and narrowbody aircraft types by 2035, and a hydrogen combustion narrowbody aircraft in 2040.
- **SLCP Forward**: This scenario assumes that government intervention, supported by voluntary industry efforts, drives new technologies and operational practices to reduce the impact of short-lived climate pollutants beginning in 2030. Relevant policies include engine standards to reduce NO_x and fine particulate matter, standards requiring hydrotreating of fossil jet fuel in Europe, and the promotion of contrail avoidance maneuvers on routes to and from high- and upper-middle-income countries. Greenhouse gas emissions are projected as under the Current Commitments scenario.
- **Full Breakthrough**: This scenario projects emissions assuming early, targeted, and sustained interventions by governments rapidly advance technologies to reduce both short- and long-lived climate pollutants. Greenhouse gases are projected per the GHG Forward scenario, and SLCPs per the SLCP Forward scenario. This serves as the most ambitious scenario of this report.

Table 1
Scenarios investigated

Scenario	Definition	Role
Historical Trends	Counterfactual	Baseline aviation warming with no dedicated action
Current Commitments	Announced policies and industry goals	Indicate progress to date
GHG Forward	Maximum GHG reduction through aircraft and fuels	Investigate temperature reductions from dedicated GHG cuts
SLCP Forward	Maximum mitigation of NO_x, nvPM, and contrails	Investigate temperature reductions from dedicated SLCP cuts
Full Breakthrough	Maximum mitigation of both short- and long-lived climate pollutants	Investigate maximum temperature reductions possible Determine relative importance of GHG versus SLCP control

Table 2 summarizes the high-level modeling assumptions for each scenario pertaining to annual fuel efficiency improvements, global SAF share, entry into service (EIS) years for ZEPs and advanced engine technologies, share of hydrotreating, and share of contrail avoidance.

Table 2
Modeling assumptions by scenario

		Historical Trends	Current Commitments	GHG Forward	SLCP Forward	Full Breakthrough
Technical efficiency (MJ/RTK)	2023–2050 (improvement per year)	-0.8%	-1.1%	-1.5%	-1.1%	-1.5%
Operational efficiency (MJ/RTK)	2023–2050 (improvement per year)	-0.2%	-0.5%	-0.8%	-0.5%	-0.8%
Global sustainable aviation fuel share (%)	2030	–	2%	8%	2%	8%
	2050	–	9%	71%	9%	71%
ZEPs entry into service	Electric commuter	–	2030			
	Hydrogen regional	–	2035			
	Hydrogen narrowbody	–	–	2045	–	2045
Advanced engines entry into service	Regional jets/narrowbody	–	2035			
	Widebody	–	2040	2035	2040	2035
	Freighters	–	2045	2040	2045	2040
Avoided contrail radiative forcing (global)	2035	–	–	–	15%	
	2050	–	–	–	90%	
Share of hydrotreated kerosene	2027	–	–	–	5%	
	2035	–	–	–	100%	

Notes: Commuter aircraft have no more than 19 seats; regional jets have fewer than 100 seats; narrowbody aircraft are single-aisle aircraft with 100 seats or more; widebody aircraft are double-aisle aircraft with 100 seats or more; freighters are aircraft dedicated to cargo transport.

As shown, annual fuel burn reductions, including technical, payload, and traffic efficiency improvements (Graver, 2022), range from 1.3% under the Historical Trends scenario to 2.3% under the GHG Forward and Full Breakthrough scenarios. In the latter scenarios, more fuel-efficient new type aircraft are introduced beginning in 2035, in addition to increased payload and traffic efficiency from airlines, including formation flying. Uptake of SAF varies from 0% to 71% in 2050, with the Current Commitments and SLCP Forward scenarios representing modest (9%) global uptake in 2050. That aligns with expected SAF uptake under existing mandates, notably ReFuelEU, which assume 70% SAF blending in 2050 for flights departing EU airports.

Regarding advanced airframes and engines, every action scenario (i.e., all but the Historical Trends scenario) assumes the introduction of electric commuter aircraft in 2030 and a hydrogen fuel-cell regional aircraft in 2035. Under the GHG Forward and Full Breakthrough scenarios, we also model the introduction of a liquid hydrogen-powered narrowbody aircraft entering service in 2045. Advanced engines with reduced NO_x and nvPM emissions are introduced between 2035 and 2045, entering regional jet, narrowbody, and widebody designs first, followed by freighter applications. In the GHG Forward and Full Breakthrough scenarios, this transition takes 5 years; in the Current Commitments and SLCP Forward scenarios, it takes 10 years.

We assume the gradual introduction of contrail avoidance maneuvers starting in 2030, with a focus on high- and upper-middle-income countries. Those practices are scaled up over time, reducing global effective RF by 15% in 2035 and 90% in 2050. Finally, hydrotreatment of fossil jet fuel on flights departing high-income countries is phased in starting in 2027 at 5% of fuel use, increasing linearly from that year until reaching 100% of fuel supply in 2035; hydrotreating in middle-income countries is delayed by 5 years, and no hydrotreating is modeled for lower-income countries.

A detailed rationale for all modeling assumptions can be found below.

CLIMATE IMPACT INVENTORY

The base 2023 inventory was developed using the ICCT's (n.d.-a) global aviation emissions model, the Jet and Turboprop Simulations for Trajectory-based Emissions And Meteorological effects (JETSTREAM) model. The model estimates fuel burn, GHG, and SLCP emissions from commercial aircraft operations by integrating flight trajectories, aircraft and engine performance data and models, and meteorological data. The model also simulates contrail cirrus formation using a python-based contrail process model.

Aircraft trajectories

We used the Spire (n.d.) Automatic Dependent Surveillance-Broadcast (ADS-B) database from 2023 as our primary data source for flight trajectories. The dataset includes trajectory data for all global flight movements that were equipped with ADS-B transmitters captured by ground or satellite receivers and were not removed from the dataset based on the U.S. Federal Aviation Administration's Limiting Aircraft Data Displayed regulation. The dataset contains 62 million unique flight trajectories and metadata about the flights, including arrival and departure airports, arrival and departure times, airline name and IATA code, aircraft type name and ICAO code, ICAO address, tail number, and aircraft role. Extensive data cleaning processes were implemented to discard incomplete or incorrect data, fill missing trajectory and metadata, and correct unrealistic waypoints and metadata.

The modeled flights were matched to the 36.4 million scheduled commercial flights according to flight schedule data for 2023 from OAG (n.d.). Of the scheduled flights, 79% had direct matches with the trajectory data for origin, destination, airline, and aircraft; 9% of scheduled flights could only be matched on origin, destination, and aircraft; and 11% could only be matched on aircraft type. For the 1% of flights for which there was no match, the average fuel burn across the entire inventory for the flight distance was used.

Meteorological data

Data from the fifth generation global climate and weather model (ERA5) by the European Centre for Medium-Range Weather Forecasts were used to provide information about the atmosphere in the vicinity of flights (Hersbach et al., 2023). The data were downloaded at longitude–latitude grid resolution of 0.25° × 0.25° over 37 pressure levels (from sea level to 42,000 feet above sea level) and at a 1-hour time resolution. A key variable in determining the formation and lifetime of a contrail is the relative humidity with respect to ice (RH_i) in the atmosphere. ERA5 has been shown to overestimate the RH_i compared with radiosonde data (Agarwal et al., 2022) and underestimate it when compared with in-situ measurements taken by the In-Service Aircraft for a Global Observing System (IAGOS; IAGOS, n.d.) fleet. In addition, ERA5 data rarely capture the high-supersaturation (RH_i > 120%) that the in-situ sensors measure. Thus, a correction to the RH_i field is required to make it more closely resemble real-world data. We used a correction developed by Teoh et al. (2024) that calibrates ERA5 data such that the probability density of the RH_i more closely resembles that seen by the IAGOS aircraft.

Aircraft performance model

BADA3, developed by Eurocontrol (n.d.), was selected as the aircraft and engine performance model for estimating cruise fuel burn and emissions. It combines aerodynamic data, thrust models, and phase-specific fuel consumption formulas to deliver performance simulation outputs across a variety of aircraft types and different operational scenarios. For the aircraft types not currently covered by BADA3, comparable aircraft that are similar in weight, performance, and mission were identified and used in the modeling.

Fuel burn and emissions

For each flight, cruise emissions were calculated using the BADA3 aircraft performance model. Landing and take-off emissions were modeled using the ICAO Engine Emissions Databank (EEDB) for turbofan engines and a mix of Eurocontrol (2023) and European Union Aviation Safety Agency (n.d.) datasets for turboprops engines. For each engine, emissions of NO_x, fine particulate matter ($PM_{2.5}$), carbon monoxide (CO), and hydrocarbons (HC) were calculated for the four landing and take-off modes—taxi/idle, take-off, climb-out, and approach—using engine-specific fuel flow rates and time-in-mode assumptions from ICAO and U.S. Environmental Protection Agency (EPA) guidance. When direct measurements were unavailable, emissions were estimated using surrogate engines, thrust class interpolation, or conversion from smoke number via the SCOPE11 method (Agarwal et al., 2019). Statistics for the aircraft-to-engine mapping are provided in Table 3.

Table 3

Engine mapping applied for engine emission estimates

Engine type	Total flights	% of total	Category	Flights	% of engine type
Jet	35,839,376	88%	Same engine name	27,459,793	76.60%
			Different generation	8,077,771	22.50%
			Equivalent engine thrust	301,812	0.90%
Turboprops	5,047,592	12%	Eurocontrol	4,503,712	90%
			Constant (EPA & ICAO)	543,880	10%

Cruise-phase NO_x emissions were modeled using Fuel Flow Method 2, which adjusts ground-based emission indices from the EEDB for altitude effects (DuBois & Paynter, 2006). For engines not in the EEDB, JETSTREAM applies constant emission indices derived from literature. Cruise nvPM was modeled using the T4/T2 method, which interpolates emissions from certified engine data using thermodynamic parameters (Teoh, Schumann, Gryspeerdt, et al., 2022).

To model the total climate impact of aviation, in addition to CO_2, we tracked and projected NO_x, soot, SO_x, and water vapor emissions. The fuel burn and emission quantities by ICAO region of departure for 2023 are presented in Table 4. North America and Europe make up nearly 50% of the world's aviation traffic.

Table 4

Fuel burn and pollutant emissions by departure region

ICAO departure region	Fuel (10^9 kg)	Fuel burn (share of global)	NO_x (10^9 kg)	nvPM mass (10^6 kg)	nvPM number (10^{26})	SO_x (10^6 kg)	H_2O (10^9 kg)
North America	69.1	25.6%	1.04	5.91	0.612	84.6	85.1
Europe	62.5	23.1%	0.948	5.41	0.562	76.6	77.0
China	40.3	14.9%	0.611	3.42	0.377	49.3	49.6
Pacific South East Asia	25.6	9.48%	0.397	2.35	0.237	31.4	31.6
Middle East	19.5	7.22%	0.319	1.83	0.180	23.9	24.0
North Asia	15.8	5.86%	0.251	1.43	0.145	19.4	19.5
South West Asia	11.5	4.27%	0.176	1.01	0.113	14.1	14.2
South America	10.5	3.88%	0.164	0.95	0.093	12.8	12.9
Central America	7.90	2.92%	0.116	0.65	0.074	9.67	9.72
Africa	7.51	2.78%	0.112	0.67	0.067	9.20	9.25
Global	270	100%	4.13	23.6	2.46	331	333

Contrail modeling

Aviation activities can generate contrail cirrus, which are ice clouds formed from aircraft exhaust in ice super-saturated regions. These clouds trap outgoing radiation, causing temporary net warming, which differs from the sustained warming caused by

greenhouse gases. For this study, contrail impacts were modeled using the pycontrails (v0.54.6) implementation of the Contrail Cirrus Prediction (CoCiP) process model (Shapiro et al., 2023). The CoCiP model simulates the properties of a contrail for its entire lifecycle (i.e., formation, persistence, and dissipation). The model, described in Schumann et al. (2012), uses aircraft trajectory and engine data, in addition to meteorological inputs, to estimate the initial properties of the contrail. It tracks key properties of the contrail, such as the width and optical depth, and combines this with information about incoming and outgoing radiation to calculate the amount of energy the contrail traps.

The annual climate impact of contrails is measured by how they change the balance of incoming and outgoing radiation to cause RF, typically expressed in milliwatts per square meter (mW/m^2). To determine the aggregate annual RF from contrails, the energy that is trapped by all contrails over the course of year is divided by the number of seconds in a year and the surface area of the Earth.

Since the CoCiP models contrails at the flight level, it also provides a spatiotemporal distribution of the contrail RF, shown in Figure 1. Contrail RF is most concentrated over Europe and North America, particularly along the transatlantic corridor, due to a combined effect of dense flightpaths and atmospheric conditions that favor persistent contrails (i.e., cold, humid, and stable air at cruising altitudes). Combined, flights departing these two regions contributed 64% of the effective RF from contrails in 2023, larger than their share of global air traffic and CO_2 emissions (less than 50%).

Figure 1
Contrail cirrus annual mean net radiative forcing, 2023

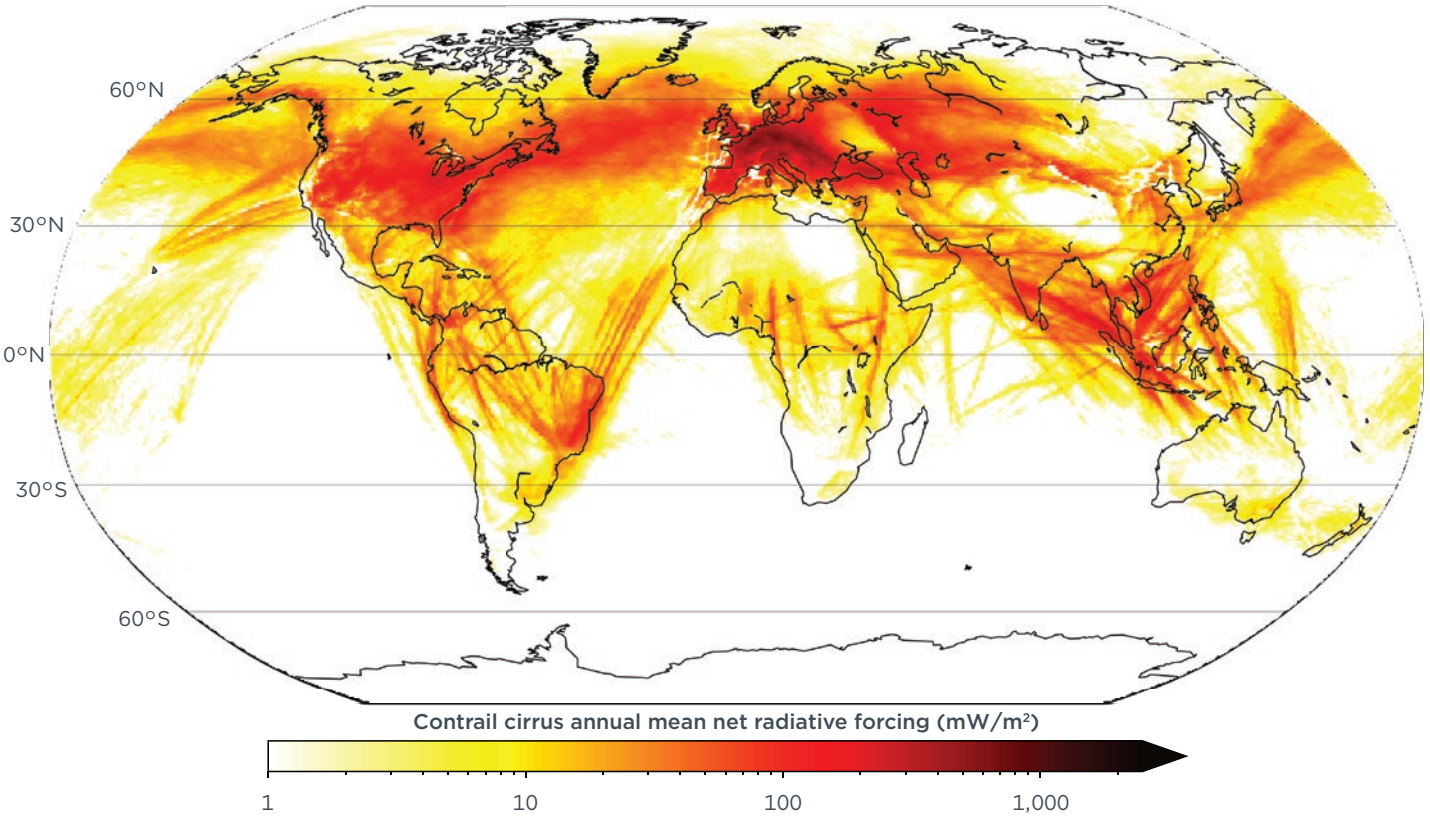

THE INTERNATIONAL COUNCIL ON CLEAN TRANSPORTATION **THEICCT.ORG**

Southeast Asia was the second-largest hotspot for persistent contrails in 2023, making the Pacific Southeast Asia the third largest ICAO region in terms of contrail RF. China, despite being the third largest market and accounting for 13% of the total traffic volume in 2023, contributed 7% of global contrail RF in 2023. Even though China has a high volume of domestic air traffic, large inland parts of China were free of persistent contrails because of dry upper atmosphere conditions and strong vertical mixing that are unfavorable to contrails.

Because contrails occur over short periods of time and are dispersed across the world, contrail RF is not as effective as CO_2 in raising Earth's surface temperature. The climate can, to a certain extent, make rapid adjustments that reduce the efficacy of contrail RF in creating surface temperature change. The net energy flux change at the top of the atmosphere after accounting for these rapid adjustments is defined as effective radiative forcing (ERF); it is used for measuring contrail's warming impacts in this report. This efficacy factor of contrails is uncertain (Ponater et al., 2005; Rap et al., 2010; Bickel et al., 2020; Bickel, 2023). For this report, we used a triangular distribution to represent the efficacy of contrail warming, with a minimum of 0.14, a midpoint of 0.36, and a maximum of 0.7. More details are provided in Appendix C.

Additionally, quantification of contrail ERF is characterized by large uncertainties due to year-on-year variations in atmospheric conditions and the complex, nonlinear interactions between aircraft emissions, atmospheric conditions, and radiative processes. A meta-analysis of ERF per flight kilometer estimates in the recent literature was conducted to quantify the contrail ERF uncertainty ranges for the purpose of this report. Details of the uncertainty quantification process can be found in Appendix C.

Our analysis using the CoCiP model and 2023 aviation trajectory data yielded a 2023 annual net RF of 42.3 mW/m^2 and an ERF of 17.8 mW/m^2. Based on the flight trajectory data, we calculated that 56.8 million km were flown in 2023. This results in an ERF per flight kilometer of 3.13E-10 mW/m^2/km globally. The meta-analysis yielded an ERF per flight km value 2.25 times higher, of 7.03E-10 mW/m^2/km, with a 95% confidence interval of (1.04E-10, 20.1E-10). This is approximately 25% lower than the central estimate of 9.36E-10 mW/m^2/km from Lee et al. (2021). The 95% confidence interval is also wider than the 5%–95% confidence interval calculated by Lee et al. (2021), of (2.77E-10, 15.98E-10). When the results of the meta-analysis are applied to 2023, the ERF estimate increases from 17.8 mW/m^2 to 39.9 mW/m^2 with a 95% confidence interval of 6.9 mW/m^2 to 114.4 mW/m^2.

Since we assumed that contrail impact scales linearly with flight kilometers by region, we are mostly interested in the ERF per flight kilometer metric. We calculated the ERF per flight kilometer for each departure and arrival region, reflecting the regional variation in contrail formation described above (Table 5). Our projections of commercial aviation relied on varied growth rates for revenue tonne-kilometers (RTK) for each region pair. For contrail projections, we applied payload and operational efficiency improvements to the RTK growth rate to simulate growth in flight kilometers, rather than RTK. For any projected year, the flight kilometers between a region pair are multiplied by the contrail ERF per flight kilometer for that region pair to calculate the contrail ERF for that region pair.

Table 5

Share of revenue tonne-kilometers and contrail effective radiative forcing by ICAO departure region, 2023

ICAO departure region	RTK		Contrail ERF	
	Value (billions)	Share of total	Value (mW/m²)	Share of total
Europe	267	25%	15.6	38%
North America	262	24%	10.7	26%
Pacific-Southeast Asia	105	10%	3.2	8%
China	145	13%	2.7	7%
North Asia	66	6%	2.2	5%
Middle East	81	8%	1.9	5%
South America	41	4%	1.2	3%
Central America	34	3%	1.2	3%
Southwest Asia	46	4%	1.1	3%
Africa	30	3%	1.0	2%
Global	1,077	100%	39.9 [6.9, 114.4][a]	100%

[a] Bracketed values denote upper and lower bound of 95% confidence interval, respectively.

Non-contrail SLCPs

Other than contrails, we tracked emissions of NO_x, nvPM, SO_x, and water vapor. Each of these pollutants create RF through distinct physical and chemical processes (Lee et al., 2021). For these pollutants, we relied on global-average ERFs from Lee et al. (2021).

Non-contrail SLCPs were treated differently than our contrail estimates to reflect the evolving literature. The contrail ERF estimate reported in Lee et al. (2021) was based on four studies, whereas at least eight additional estimates have been published since, warranting an updated meta-analysis. In contrast, Lee et al. (2021) based ERF estimates for NO_x on 20 studies, for water vapor on 9 studies, and for soot/nvPM aerosol-radiation interactions on 10 studies. Table 6 lists the ERF per annual emission values in teragrams (Tg, equivalent to one million tonnes) and the associated 5%–95% bounds. ERF per annual emission values were multiplied by the annual emission of the pollutant to get the resulting annual global ERF for that year.

Table 6

ERF values and their ranges for non-contrail SLCPs

Pollutant	Central estimate for ERF (mW/m²/Tg/yr)	Lower bound for ERF (mW/m²/Tg/yr)	Upper bound for ERF (mW/m²/Tg/yr)
NO_x	12.25	0.41	19.91
SO_x	-19.91	-49.78	-6.87
nvPM	100.67	7.95	428.65
Water vapor	0.0052	0.0021	0.0083

Since Lee et al. (2021) was published, more recent work has studied the net NO_x impact from future aviation emissions and found that the net NO_x effect could be reduced, or even become negative, indicating a cooling effect (Skowron et al., 2021; Terrenoire et al., 2022). This is expected to happen due to the increasing background concentrations of NO_x and methane in the future. However, these studies are not included in this analysis due to differing assumptions of temperature change scenarios and the warming efficacy of methane.

Commercial operations data

We mapped flight-level emissions to commercial airline schedules purchased from OAG (n.d.) using a hierarchical matching process, combining exact matches with modeled estimates based on aircraft type and route distance. Load factors and cargo weights were assigned using route or airline specific data from the U.S. Department of Transportation (DOT) Form T-100 (as supplied by Airline Data Inc., n.d.), the ICAO Data+ Traffic by Flight Stage database (ICAO, n.d.-b), and ch-aviation (n.d.). Results were validated against ICAO CORSIA data (ICAO, n.d.-a) and airline fuel use reported in DOT (n.d.) Form 41 and flight-level data from Brazil's National Civil Aviation Industry (n.d.).

For full methodological details, including emission factor sources, fallback procedures, and validation results, please refer to the JETSTREAM documentation (ICCT, 2025).

PROJECTION OF AVIATION CLIMATE EFFECTS MODEL

Model structure

Version 1.0 of the Projection of Aviation Carbon Emissions (PACE) model underlying the GHG analysis in ICCT's previous *Vision 2050* roadmap (Graver et al., 2022) was expanded in version 2.0 to include the projection of SLCPs to 2050. PACE 2.0 was also updated to enable the projection of freight emissions at the region pair and traffic segment levels (ICCT, n.d.-b). Segments are defined by unique combinations of ICAO region pair, trip destination (domestic or international), aircraft class, and flight distance band. Figure 2 presents the model flow of PACE 2.0, with red text signifying newly added modeling capabilities.

Figure 2
PACE 2.0 model flow

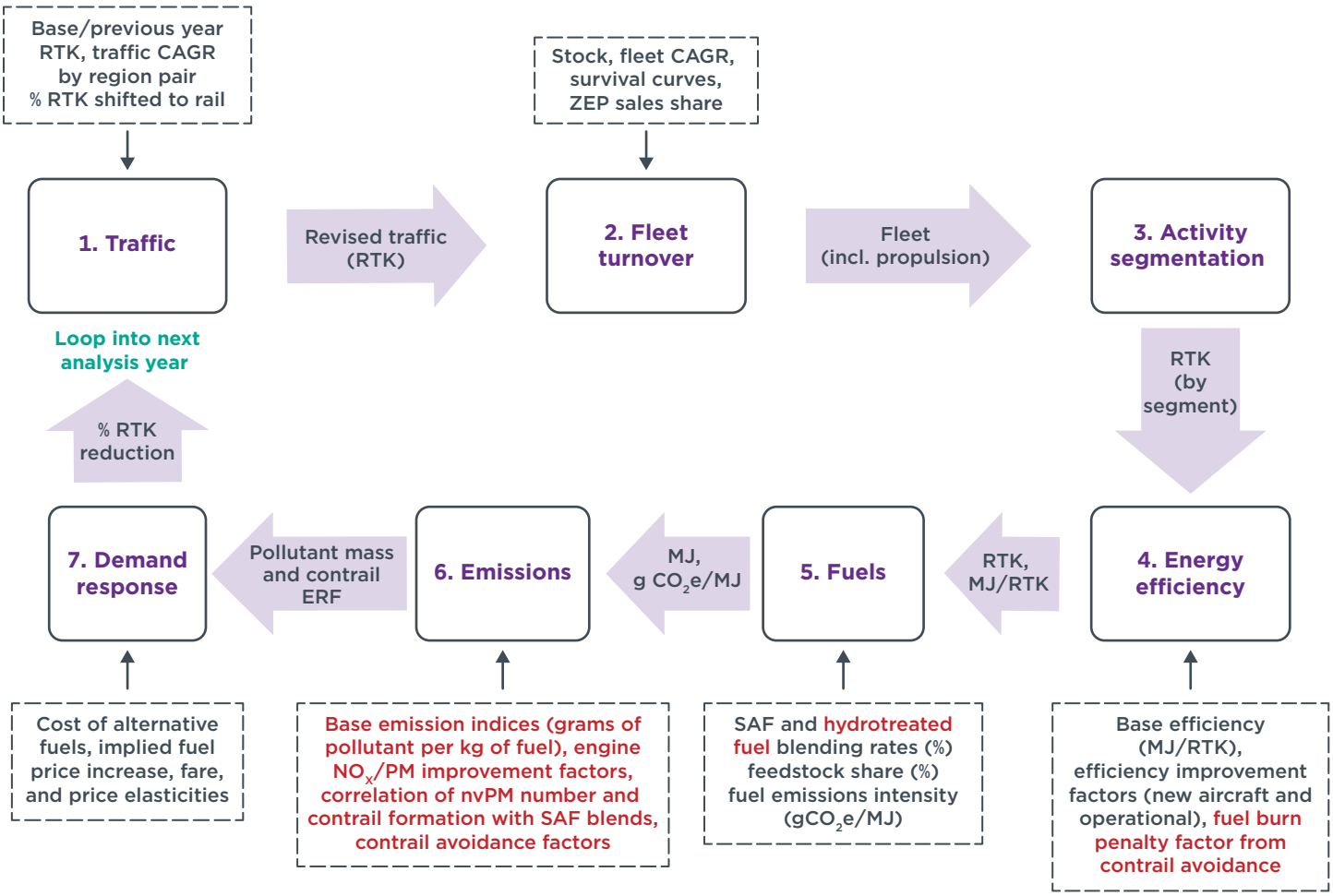

Note: Red text denotes newly added modeling capabilities; CAGR = compound annual growth rate.

To project traffic, emissions, and associated warming to 2050, GHG-related inputs were updated in the PACE model to reflect more recent trends, and new assumptions were derived for short-lived climate pollutants. Details on these inputs are provided below.

Existing inputs update

Four existing variables were updated to reflect the most recent understanding of technology and policy trends: traffic growth, fuel efficiency, SAFs, and ZEPs. Unchanged model inputs include bio-SAF feedstock split, bio-SAF and e-SAF cost, modal shift, fleet renewal curves, airfare, and demand elasticities. Implied carbon price varies with SAF blending assumptions.

Traffic growth

The ICCT's previous *Vision 2050* aviation roadmap modeled decarbonization pathways using a central traffic growth scenario (assuming a 3% compound annual growth rate) and tested the sensitivity of the results to higher (3.7%) and lower (2.4%) rates

between 2019 and 2050. Since then, air traffic has rebounded quickly from the impacts of the COVID-19 pandemic. Traffic growth rates were thus updated to capture both the actual air traffic volume from 2023 to 2024 (11% year-on-year RPK growth) and estimated volume for 2025 (8% year-on-year RPK growth) released by IATA (2024c), as well as post-COVID long-term growth rates projected by ICAO (2023b) by ICAO region pair for passenger and cargo transport (Table 7).

Table 7

Passenger and freight traffic assumptions for all scenarios, 2025 to 2050

Traffic type	Metric	Year	Case		
			Low	Central	High
Passenger	Annual increase	2025–2050	+2.8%	+3.4%	+3.7%
	Trillion RPK	2025		9.78	
		2050	19.5	22.6	24.3
		2050/2025 (ratio)	1.99	2.31	2.48
Freight	Annual increase	2025–2050	+3.1%	+3.6%	+3.9%
	Billion freight tonne-kilometers	2025		291	
		2050	624	705	758
		2050/2025 (ratio)	2.15	2.42	2.60

The updated annual growth rates vary from 2.8% to 3.7% for passengers and from 3.1% to 3.9% for freighters, with a central case of a 3.4% annual growth rate for passengers and 3.6% annual growth rate for freight. This translates to a central case of about 130% growth for passengers and 140% growth for freight in 2050, compared with 2025. Owing to better data about the actual traffic recovery post-COVID, the updated forecasts project less uncertainty in 2050 traffic compared to the previous *Vision 2050* study, with the variance between the High and Low traffic cases falling in half, from 48% in the 2022 study to only 24% here.

The central traffic assumptions were adopted across all main analyses. Sensitivity of results to high and low traffic cases can be found in Appendix A.

Fuel efficiency

The technical efficiency (TE) assumptions for fuel were updated to reflect a more realistic fleet adoption timeline as well as policy commitments. They were derived from historical aircraft performance trends using data from an ICCT fuel burn study (Hameed & Rutherford, 2025). Fuel efficiency is measured in grams of fuel per tonne-kilometer and reflects two categories of improvements: 1) incremental reductions in fuel burn from new in-production (InP) aircraft types, and 2) step function reductions in fuel burn from new aircraft types entering into service.

InP aircraft are from aircraft families that have already been type certified and continue to be delivered. These include models with performance improvement packages—such as engine improvements, aerodynamic refinements, and system upgrades—without entirely new airframes. Fuel burn reductions from InP aircraft may also be achieved from the introduction of new "stretch" variants within an aircraft family.

In-production improvement cycles were chosen based on observed periods of relatively stable but consistent efficiency gains, typically over a span of 15–20 years prior to the introduction of new aircraft models (IATA, n.d.). In contrast, EIS cycles represent the market transition periods following the introduction of completely new aircraft types. These were selected based on real-world timelines observed for fleet adoption after new aircraft become available, accounting for the gradual phase-out of older models and scaling up of newer ones, capturing the typical fleet turnover behavior in commercial aviation.

These InP and EIS cycles were used to define year-on-year fuel efficiency improvements and inform transition dynamics in each scenario. Scenario-specific assumptions reflect varying timelines and magnitudes of efficiency gains—for example, a 25%–35% TE improvement with the introduction of new aircraft in the 2030s—tailored to align with industry trends and policy ambition levels. Baseline assumptions have no new aircraft being introduced until 2050, with continued yearly improvement (Table 8).

Table 8

Technical efficiency assumptions by aircraft class

Technical efficiency assumption	Scenario	Aircraft class			
		Regional jets	Narrowbody	Widebody	Freighter
New aircraft introduction	Historical Trends	–			2026
	Current Commitments + SLCP Forward	2035		2040	2026, 2045
	GHG and Full Breakthrough			2035	2026, 2040
TE improvement at EIS	Historical Trends	–			–
	Current Commitments + SLCP Forward	15%	25%		20%, +25% [a]
	GHG and Full Breakthrough	25%	35%		20%, +35% [a]
InP TE gain (% per year)	All scenarios	0.15% p.a.	0.81% p.a.	0.38% p.a.	–
EIS cycle (years)	All scenarios	4	6	9	5

[a] The technical efficiency improvements for the next EIS cycle are expressed relative to the resulting values of the most recent EIS.

The scenario-specific TE improvement assumptions outlined in Table 7 are based on original equipment manufacturer announcements and demonstration projects that provide empirical evidence for both the magnitude and timing of efficiency gains. For regional aircraft, ATR's EVO concept (planned for around 2030) targets a 20% reduction in fuel burn compared with relatively older ATR 72-600 models (ATR, n.d.), while Embraer's Energia hybrid-electric program highlights similar step-change improvements of up to 25%, supporting the 15%–25% values assumed across scenarios (Embraer Commercial Aviation, n.d.). For narrowbodies, CFM's RISE open-fan engine promises "at least 20% lower fuel consumption than today's LEAP engines," aligning with the 25% Current Commitments assumption when coupled with additional aerodynamic refinements (CFM International, n.d.). Looking further ahead, NASA's X-66A truss-braced wing demonstrator with Boeing suggests that approximately 30% reductions in fuel burn are feasible, which justifies the 35% assumption under the GHG Forward scenario when coupled with other advancements in material science and technology (O'Shea, 2023). For widebodies, Rolls-Royce's UltraFan demonstrator is

designed for a 25% fuel burn reduction versus the first-generation Trent engine (Rolls-Royce, n.d.), supporting the 25% efficiency steps in the Current Commitments scenario. More ambitious 35% step changes become credible with advanced concepts such as the JetZero blended-wing-body concept backed by the U.S. Air Force, or boundary layer ingestion (JetZero, n.d.).

While it is impossible to predict technical efficiency improvements with certainty, these assumptions are intended to reflect a balanced view based on manufacturer announcements and independent academic studies. They represent realistic averages given the likelihood of technology readiness in the corresponding EIS years within the context of each scenario. These scenario-specific values are then embedded within historical InP and EIS cycle structures, ensuring that the assumed efficiency gains not only reflect manufacturer and academic expectations but also align with observed fleet transition patterns over the past two decades.

For in-production aircraft cycle years, we selected 2009 to 2024 for regional jets, 2001 to 2015 for narrowbody aircraft, and 1996 to 2014 for widebodies. During these periods, performance improvement packages and variants of existing aircraft types generated annual improvements of 0.15% for regional jets, 0.81% for narrowbodies, and 0.38% for widebodies. Historical EIS cycles for regional jets (2004–2008), narrowbodies (2016–2022), and widebodies (2014–2023) identified EIS phase-ins of 4, 6, and 9 years, respectively.

For freighters, all scenarios assumed 2026 as the EIS year for freighter variants of current-generation aircraft, with an expected fuel efficiency improvement of approximately 20%. As performance improvement package cycles are uncommon for this class of aircraft, no related annual efficiency improvements were included. For next-generation freighter aircraft, the EIS year was assumed to occur 5 years after the corresponding widebody EIS year within each scenario, with corresponding technical efficiency improvements. The improvements in TE for each EIS cycle were estimated using methods detailed in Appendix A.

The assumptions regarding TE improvements were compared with 2019 technology levels referenced in the previous *Vision 2050* report. The estimated improvements were subsequently normalized to reflect 2023 conditions (Figure 3).

Figure 3

Technical efficiency assumptions by scenario for regional, narrowbody, widebody, and freighter aircraft

THE INTERNATIONAL COUNCIL ON CLEAN TRANSPORTATION **THEICCT.ORG**

Operational efficiency assumptions, including payload efficiency and en-route efficiency, were imported from the previous *Vision 2050* report; the previously modeled efficiency gains between 2019 and 2025 were applied to the period 2023 to 2050, as there were minimal efficiency improvements between 2019 and 2023 due to the COVID-19 pandemic. Market-driven improvements of 0.33% per annum, equivalent to the Action scenario in the previous *Vision 2050* report, were assumed in the Historical Trends scenario. For the Current Commitments and SLCP Forward scenarios, operational efficiency improves linearly at 0.5% per annum, equivalent to the Transformation scenario in the previous report. For the GHG Forward and Full Breakthrough scenarios, operational efficiency improves linearly at 0.8% per annum, equivalent to the Breakthrough scenario in the previous report. That reflects the introduction of formation flying covering 5% of global passenger flight traffic in 2030 and almost half of global passenger traffic in 2050 (Graver et al., 2022).

Sustainable aviation fuels

The Current Commitments scenario captures four SAF policies:

- **European Union**: Under the ReFuelEU Aviation regulation, fuel suppliers must blend SAF into aviation fuel, starting at 2% in 2025 and increasing to 70% by 2050 (European Commission, n.d.).[5]
- **United Kingdom**: Beginning in 2025, the United Kingdom mandates that 2% of jet fuel be SAF, with targets rising to 10% by 2030 and 22% by 2040 (UK Department for Transport, 2024).[6]
- **Brazil**: A GHG intensity standard was enacted as part of the Fuel of the Future Law, requiring a 1% annual reduction in aviation fuel GHG intensity with SAF use starting in 2027, aiming for a 10% reduction by 2037 (Government of Brazil, 2024).
- **Japan**: A mandate that SAF comprise 10% of aviation fuel supplied for all flights departing from Japanese airports by 2030 is under discussion in the country (Japan Ministry of Economy, Trade and Industry, 2025).

The SAF blend at the end of the effective period of these policies is held constant for that respective market until 2050. For example, the SAF blend in the United Kingdom is held constant at 22% between 2040 and 2050. Proposed SAF mandates in several other countries are not included in our modeling (4AIR, 2025). The SLCP Forward scenario follows the same SAF assumptions as in the Current Commitments scenario. Meanwhile, the SAF inputs for both the GHG Forward and Full Breakthrough scenarios are taken from the Transformation scenario of ICCT's previous *Vision 2050* roadmap, which represents the maximum GHG reduction potential through aircraft and fuels considering progress towards the net-zero goal to date.

Since the announced policies mandate either SAF blending rates or fuel GHG intensity reductions rather than an absolute volume of SAF use, the PACE 2.0 model was switched to SAF blends as an input format to calculate global average blend rates based on the regional policies. Global average blending rates for all scenarios are summarized in Table 2. Assumptions concerning the SAF feedstock split, life-cycle GHG emissions of each SAF pathway, and cost of each SAF pathway are the same as in the previous *Vision 2050* report.

Zero-emission planes

ZEPs have faced strong headwinds since 2021 (Rhode, 2025). Airbus has pushed back its ZEROe program to introduce hydrogen-powered commercial aircraft in 2035 (Norris & Warwick, 2025), citing a mix of infrastructure challenges and slower-than-expected technology development (Graham, 2025). Universal Hydrogen, a U.S.-based company that flew the largest aircraft ever on hydrogen-electric power, shut down in 2024 after failing to secure enough funding to continue research and development (Hemmerdinger & Hardee, 2023; Aerospace Testing International, 2024). Eviation, an electric-plane startup based in Washington state, has paused its Alice program and laid off most of its employees (Boyle, 2025). ZeroAvia is currently pursuing certification of its 600 kW fuel-cell powertrain for a 10–20 seat aircraft that they aim to enter service in 2026, with a 40–80 seat aircraft, which would require a ~2 MW powertrain, entering

5 There is sub-mandate for the share of synthetic fuels in the overall SAF mix, starting at 1.2% in 2030 and rising to 35% by 2050.

6 The power-to liquid obligation will be introduced from 2028 at 0.2% of total jet fuel demand and will reach 3.5% of total jet fuel demand in 2040.

service in 2028. We do not expect these timelines to be feasible for commercialization given the smaller engine is not yet certified and the slow progress discussed above.

For these reasons, we have updated the EIS of ZEP assumptions in the following manner:

- We include fuel-cell regional aircraft, both in the form of retrofit turboprops (Mukhopadhaya, 2023) and clean-sheet designs (Debney et al., 2022). These are assumed to enter service in 2035 in the Current Commitments, GHG Forward, SLCP Forward, and Full Breakthrough scenarios.
- The introduction of liquid hydrogen-powered narrowbody aircraft has been delayed from 2035 to 2040 and these aircraft are only introduced in the GHG Forward and Full Breakthrough scenarios.

In addition to changing the EIS years, we have changed how the delivery numbers for each year are calculated. Previously, we assumed a certain share of new deliveries of each aircraft class would be hydrogen powered, with the number of new deliveries being determined by the fleet turnover calculations within the model. We also capped the share of operational ZEPs to be less than the share of global RPK addressable by ZEPs, based on previous technical and performance analyses. For example, our modeling showed that a family of liquid hydrogen-powered narrowbody aircraft could replace fossil-fueled variants on 37.5% of the global RPK based on 2019 data. Thus, the share of liquid hydrogen-powered narrowbody aircraft in the global narrowbody fleet does not increase past 37.5%.

We maintained these rules as upper limits for the number of new deliveries of ZEPs each year. We also added new limits on the pace of introduction in the first 10 years from each aircraft's EIS to simulate lower-than-typical aircraft manufacturing numbers. This is due to limited availability of hydrogen infrastructure and the challenge of producing an entirely new aircraft. To this end, we assumed that:

- For an electric commuter aircraft, the number of deliveries in a year is set to 10 units in the first year of service (2030) and increases by 10 each year, reaching 200 units per year in 2050. In addition, the maximum share of new deliveries of commuter aircraft that can be electric is set to 5% for the first year of service (2030), linearly increasing to 100% in 2050.
- For a fuel-cell regional turboprop, the number of deliveries in a year is set to 5 units in the first year of service (2035) and increases by 5 each year, reaching 80 units per year in 2050. Further, the maximum share of new deliveries of regional aircraft that can be fuel-cell powered is set to 10% for the first year of service (2030), linearly increasing to 25% in 2050.
- For a liquid hydrogen-powered narrowbody aircraft, the number of deliveries in a year is set to 10 units in the first year of service (2045), 20 units in the second year of service, and increases by 20 each year thereafter, reaching 100 units per year in 2050. In addition, the maximum share of new deliveries of regional aircraft that can be fuel-cell powered is set to 3% for the first year of service (2030), linearly increasing to 10% in 2050.

The final delivery number for a year is taken to be the lower of the maximum possible deliveries and the maximum share of new deliveries that are ZEPs in a given year.

New model inputs

Reductions in NO_x and nvPM emissions from engine technologies

NO_x and nvPM emissions from new engine technologies across the five scenarios were defined using engine certification data in the EEDB, targets set by the ICAO CAEP/11 Independent Experts Review, and emission targets for project engines that are currently being developed by manufacturers (ICAO, n.d., 2019). New engines are assumed to enter service in the same timelines described above for new aircraft types.

First, the average cruise-phase NO_x emissions indices (EI NO_x) in the 2023 global fleet were extracted from JETSTREAM and used as the baseline for each aircraft class. In the Historical Trends scenario, it is assumed that no further NO_x improvements are achieved, and an annual fleetwide EI NO_x increase of 0.61% occurs, obtained from averaging trends in literature assessing historical NO_x emissions (Baughcum et al., 1999; Grobler, 2024; Quadros et al., 2022). This increase in NO_x emissions reflects the tradeoff from achieving fuel efficiency improvements through overall pressure ratio (OPR) increases in modern engine designs.

In the Current Commitments and GHG Forward scenarios, the EI NO_x for new deliveries was calculated by applying the 0.61% annual increase to the best performing in-production engine in each aircraft class until the EIS of new aircraft types. The annual increase is assumed to occur fleetwide through 2050. These two scenarios assume an ambitious NO_x standard is set at the upcoming ICAO CAEP/14 meeting in 2028, in line with the current best-in-service engine NO_x technology.

In the SLCP Forward and Full Forward scenarios, improvements were applied to the current best-performing engines, and it was assumed that OPR increases do not continue in future engine designs. This implies that NO_x reductions are prioritized during engine development, and fuel efficiency improvements are achieved through design changes other than OPR increases. A 10% EI NO_x reduction is assumed for regional jets, and a 25% reduction is assumed for narrowbody and widebody aircraft, entering service starting in 2035.[7]

In all scenarios, the EI NO_x of new freighter deliveries are assumed to behave similarly to those of widebody aircraft with a 5-year delay applied. The NO_x assumptions for new aircraft deliveries in each scenario are defined in Table 9.[8]

Table 9

Cruise-phase NO_x emission indices by aircraft class and scenario for new deliveries (g NO_x/kg fuel)

Aircraft class	Scenario				
	Historical Trends	Current Commitments	GHG Forward	SLCP Forward	Full Breakthrough
Regional jet	13.96	10.41		8.71	
Narrowbody	15.81	10.12		7.1	
Widebody	17.68	12.80	12.41	8.66	

7 The climb-out measurement points at 85% rated thrust in the ICAO EEDB were used to approximate engine EIs in the cruise phase.

8 Entry years for engines with emissions indices presented in Tables 6, 7, and 8 are aligned with EIS of new type aircraft in each scenario (from 2035–2045). For the Historical Trends scenario, since there is no entry of new aircraft types, emission indices are presented for each aircraft class in 2035.

The average cruise-phase nvPM number EIs in the 2023 global fleet were extracted to define the baseline for each aircraft class. In the Historical Trends, Current Commitments, and GHG Forward scenarios, it is assumed that no further technological improvements are made to achieve nvPM reductions. This is because there is no current workplan in place to update the ICAO CAEP/11 landing and take-off nvPM standard, and no cruise-phase nvPM standard is in place.

In the SLCP Forward and Full Breakthrough scenarios, the average nvPM number EIs for narrowbody and widebody aircraft were set to be equal to the current best performing engine in the 2023 inventory. This assumes a 99% reduction for narrowbody and widebody aircraft coming from future low-soot engine designs.[9] There is no assumed improvement for regional jets because of the technical challenges associated with achieving nvPM reductions for smaller engine geometries. The nvPM number EI and nvPM mass EI assumptions for new aircraft deliveries starting in 2035 for each scenario are defined in Table 10 and Table 11.

Table 10

nvPM number emission indices by aircraft class and scenario for new deliveries (# of particles/kg fuel)

Aircraft class	Scenario				
	Historical Trends	Current Commitments	GHG Forward	SLCP Forward	Full Breakthrough
Regional jet	9.79×10^{14}				
Narrowbody	9.28×10^{14}			2.81×10^{10}	
Widebody	9.71×10^{14}			1.06×10^{11}	

Table 11

nvPM mass emission indices by aircraft class and scenario for new deliveries (mg nvPM/kg fuel)

Aircraft class	Scenario				
	Historical Trends	Current Commitments	GHG Forward	SLCP Forward	Full Breakthrough
Regional jet	84.4				
Narrowbody	82.9			9.87×10^{-3}	
Widebody	103			2.16	

Relationships between fuel composition, nvPM emissions, ice particle number, and contrail radiative forcing

The impacts of fuel composition, namely fuel hydrogen content, on SLCPs are informed by a compilation of studies detailing modeling approaches and in-flight testing. Because research assessing these effects can consider different variables and geographical scopes, we chose to average the findings across studies to capture a range of potential impacts. A three-step approach was taken, as detailed below.

9 In-service lean-burn engines using TAPS combustors have nvPM emissions levels that are orders of magnitude lower than their rich-burn counterparts, in the range of 98%–99% lower nvPM for narrowbody and widebody aircraft.

First, the change in nvPM emissions as a function of SAF blend was defined using data points from Teoh, Schumann, Voigt, et al. (2022) and Markl et al. (2024), and these were fitted to a polynomial curve. This correlation results in a 31% reduction in nvPM number EI for a 50% SAF blend and a 43% reduction for 100% SAF (Appendix B). Hydrotreated jet fuel was assumed to have the same fuel composition as SAF, and therefore the same relationship with nvPM emissions.

Given limited data on changes in nvPM mass across a range of SAF blends due to varying particle size distributions across engine technologies, nvPM mass was modeled to have similar percentage reductions due to SAF as nvPM number. nvPM mass and number reductions from fuel composition were combined with those coming from engine technologies across the fleet in a given year to estimate a total reduction in nvPM emissions for that year.

A similar approach leveraging Teoh, Schumann, Voigt, et al. (2022) and Markl et al. (2024) was used to define the relationship between reductions in nvPM number and reductions in ice crystal number for rich-burn engines. In this case, a linear fit was used, resulting in a correlation between percent change in ice crystal number and in nvPM number EI (Appendix B). This correlation results in a 50% reduction in ice particle number for a 43% reduction in nvPM number EI.

Finally, using results from Teoh, Schumann, Voigt, et al. (2022), Burkhardt et al. (2018), Bock and Burkhardt (2019), and Markl et al. (2024), a relationship between percent change in ice crystal number and in annual mean net contrail RF was extracted (Appendix B). Using these three correlations, PACE converted annual changes in the fuel mix, nvPM emissions, and ice crystal number into a resulting change in annual mean contrail RF, as shown in Figure 4. PACE estimates a reduction of 30% in annual mean contrail RF for 100% SAF.

Figure 4

SAF blend percentage versus percent change in annual net mean radiative forcing

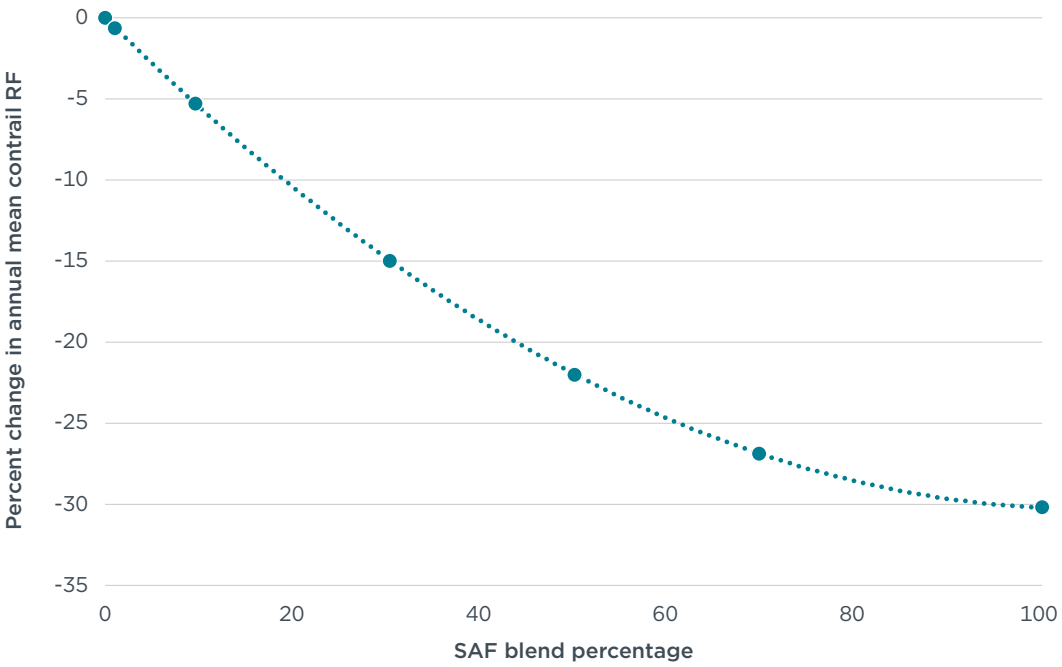

THE INTERNATIONAL COUNCIL ON CLEAN TRANSPORTATION **THEICCT.ORG**

Hydrotreating

In the SLCP Forward and Full Breakthrough scenarios, we assumed that an increasing share of fossil jet fuel is hydrotreated, which increases the fuel hydrogen content and reduces the naphthalene, sulfur, and aromatic content of fossil jet fuel. This lowers the resulting soot emissions and the likelihood of forming persistent contrails. Specifically, 5% of flights departing high-income countries were assumed to utilize hydrotreated fossil jet fuel starting in 2027, with this share increasing linearly to reach full (100%) hydrotreated fuel usage by 2035. The same ramp-up rate applies to middle-income countries but is delayed by five years; no hydrotreating is assumed for low-income countries. Once 100% hydrotreating was reached in high- and middle-income countries, it was held constant through 2050 and makes up approximately 80% of the modeled global fuel consumption in 2050.[10]

SLCP reductions from hydrotreated fossil jet fuel were assumed to be identical to those from SAF. However, hydrotreatment would incur an additional 3.35 g CO_2e/MJ of fuel unless green hydrogen (i.e., hydrogen produced using additional renewable electricity) was deployed for the process, resulting in a life-cycle GHG intensity of 92.35 g CO_2e/MJ, or a 3.8% penalty (Barrett et al., 2021). This GHG penalty is a tradeoff for reduced contrail RF and local air quality benefits incurred from hydrotreated jet fuel, as aircraft engine emissions have been linked to significant human health impacts (Yim et al., 2015; Seters et al., 2024).

Starting in 2040, it was assumed that 100% green hydrogen was used for hydrotreatment, so a well-to-wake carbon intensity equal to fossil jet fuel at 89 g CO_2e/MJ was assumed for hydrotreated fuel from there on. This is in line with the EU's renewable fuels of non-biological origin mandate and Renewable Energy Directive, which sets targets for uptake of renewable hydrogen use in transport and industrial processes (Buffi et al., 2022).

A 2023 study commissioned by the ICCT (Mathpro Inc., 2023) concluded that hydrotreating could control naphthalenes at a cost of $0.09–$0.12 per gallon for conversion refineries, which are the dominant suppliers of jet fuel in most regions of the world. The average price premium of $0.10 per gallon compared to the price of conventional fossil jet fuel (Jet A) was used to quantify the cost of hydrotreating in this study.

Contrail avoidance

Contrail avoidance is implemented in the SLCP Forward and Full Breakthrough scenarios. We assumed that only countries classified as high income and upper-middle income according to the World Bank (n.d.) implement avoidance. High-income countries start the implementation in 2032, with upper-middle-income countries starting implementation 5 years later, in 2037. In both cases, the scale-up takes 10 years and reaches an effectiveness of 95% (i.e., avoiding 95% of the warming impact of contrails from flights departing those regions). The scale-up is modeled as an S-curve and is shown in Figure 5.

10 The magnitude of hydrotreating modeled in the Full Breakthrough scenario can be lower than its maximum capacity. This is because, when the total capacity of SAF and hydrotreating is greater than the total kerosene demand in a year, SAF is prioritized due to its GHG benefits.

Figure 5

Scale-up of contrail avoidance by high-income and upper-middle-income countries

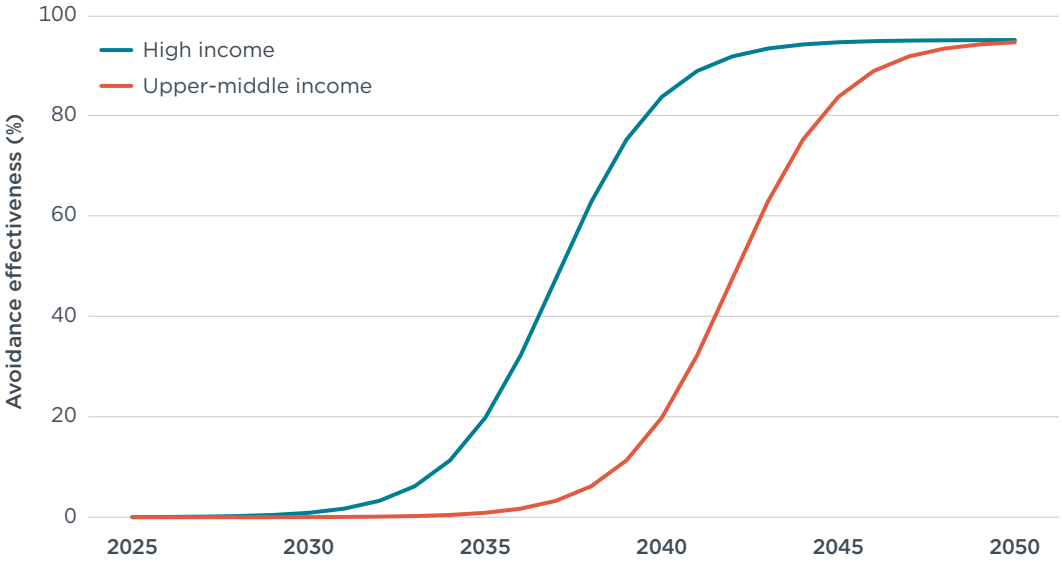

THE INTERNATIONAL COUNCIL ON CLEAN TRANSPORTATION **THEICCT.ORG**

The split between implementation timelines by income mirrors the current technology adoption trajectory, where high-income regions and countries like the European Union, the United Kingdom, and the United States are leading the testing of avoidance measures. Flights departing low-income and lower-middle-income countries contribute only 5% of global contrail warming and thus contrail avoidance is expected to be considered a lower priority. The start dates of 2032 and 2037 acknowledge that contrail avoidance is not a fully mature technology. The intervening 7 years are assumed to be needed to scale up trials and prove the climate benefit of implementing contrail avoidance in entire airspaces.

The assumed maximum effectiveness of 95% is higher than the 54% reduction in contrail length that was achieved by a contrail avoidance trial in the continental United States (Sonabend-W et al., 2024). Higher effectiveness is expected as the technology develops and forecasting of where and when a contrail will form improves (Platt et al., 2024).

A scale-up period of 10 years is faster than typical aircraft lifetimes (20–30 years) and expected SAF scale-up timelines. However, unlike aircraft and SAF production, which require producing physical assets, contrail avoidance technology is primarily a software technology. Although training the software will take time, it is still expected to be faster than the scale-up of SAF. The S-curve is used to simulate the slower initial implementation of contrail avoidance as the tools are adopted. This is followed by a rapid increase as relatively few flights (3%) are expected to be responsible for a large proportion (80%) of the warming based on our 2023 JETSTREAM inventory. Adoption slows towards the end of the scale-up period as double the number flights would need to be rerouted to increase contrail reduction from 80% to 95%. We do not expect a 100% reduction as there will always remain some uncertainty in forecasting contrail formation.

Contrail avoidance is likely to incur a fuel burn penalty. Recent flight trials have shown a 2% increase in fuel burn for an avoidance flight compared with the planned route

while achieving a 54% reduction in contrail length (Sonabend-W et al., 2024). However, these trials have been limited in scope as they were performed by individual airlines. To reap climate benefits, contrail avoidance would need to be implemented across entire airspaces, with all operating aircraft avoiding areas with high likelihood of contrail formation. Such coordinated avoidance may incur higher fuel burn penalties due to air traffic capacity reductions in the designated avoidance areas.

We assumed that flights performing avoidance incur a 2%–5% fuel burn penalty, which transitions linearly as the scale of avoidance increases. The upper limit of 5% is assumed to be enforced in the flight planning process, and only avoidance maneuvers that incur a penalty of less than 5% would be allowed. To calculate the fleetwide fuel burn penalty, we sorted all flights by their contrail impact and applied a fuel burn penalty to all flights required to reach the desired avoidance effectiveness. The additional fuel burn was summed and compared with the fleet's total fuel burn to provide the fleetwide penalty. Figure 6 shows the fleetwide fuel burn penalty when the per-flight fuel burn penalty is 2% (blue line) and 5% (brown line). This study uses a combined fuel burn penalty (red line), which transitions the per-flight fuel burn penalty from 2% to 5%. On a fleetwide basis, the combined penalty is about a 1% increase in fuel burn for avoiding 95% of contrails formed by flights leaving high- and upper-middle-income countries.

Figure 6
Fleetwide fuel burn penalty based on desired avoidance effectiveness

THE INTERNATIONAL COUNCIL ON CLEAN TRANSPORTATION **THEICCT.ORG**

TEMPERATURE RESPONSE

Climate modeling framework

We utilized the Finite Amplitude Impulse Response (FaIR) model v2.2.2 to quantify the global warming response from aviation climate forcers (Leach et al., 2021). FaIR is a reduced-complexity climate model that provides a computationally efficient alternative to complex Earth system models while maintaining fidelity to CMIP6 modeling—the

current gold standard and primary reference used in major climate assessments—in its representation of Earth's temperature, carbon cycle, and non-CO_2 responses.

The model's simplified structure enables assessment of climate impacts across multiple scenarios and emission species, making it well-suited to combine various aviation climate forcers—each with varying atmospheric lifetimes and radiative properties—into a single global warming metric each year. Modeling includes both the immediate impacts of short-lived climate pollutants and the cumulative effects from longer-lived pollutants.

Scenario configuration and baseline assumptions

Our analysis was conducted against a baseline climate scenario consistent with a below 2 ˚C warming pathway in 2100. The emissions input for this baseline comes from the CMIP6 SSP119 scenario and reflects significant advancements in climate intervention globally (Intergovernmental Panel on Climate Change [IPCC], 2022). We implemented 66 climate configuration scenarios to capture variability in climate sensitivity, following the ensemble approach recommended in the FaIR documentation. The results represent the ensemble mean across all configurations.

Modeling aviation climate forcers

Aviation climate forcers were modeled in FaIR using two distinct approaches based on their atmospheric behavior:

Emissions-based inputs: CO_2, nvPM, CH_4, and SO_2 were input using FaIR's emissions option to calculate their radiative forcing and subsequent temperature response over many years. FaIR accounts for the cumulative warming effects of long-lived emissions by tracking their atmospheric persistence over time and emulating impacts on Earth's carbon cycle.

Effective radiative forcing inputs: For climate forcers that do not persist beyond a year, it is appropriate to use the effective radiative forcing input. For contrails, the ERF from PACE outputs is input directly into the model. Stratospheric NO_x and stratospheric water vapor were also input directly as an RF time series after conversion using factors from Lee et al. (2021). For stratospheric water vapor, the conversion factor is 0.0052 mW m^{-2} per Tg H_2O per year. NO_x emissions were first converted from NO_x to N using their molecular weight, assuming the weight of NO_2, then to effective radiative forcing using 12.25 mW m^{-2} per Tg N per year.

Aviation-attributable warming calculation

All scenarios were run as emission reductions from the CMIP6 SSP119 baseline. To quantify aviation-attributable warming for each scenario and pollutant, we ran additional scenarios in which each scenario-pollutant combination was fully removed. These scenarios were then subtracted from the full temperature trajectory for each climate configuration, scenario, and pollutant combination to determine scenario- and pollutant-specific warming attribution.

Regional considerations and limitations

In using a reduced-complexity climate model, our analysis assumes globally averaged climate impacts for each aviation emission species and contrails. Regional responses to global warming are expected to vary significantly from the global mean, as many short-lived climate impacts are not well dispersed, and local atmospheric properties may affect the intensity of impacts.

POLLUTANT EMISSIONS

Fuel efficiency and fuel mix trends

Based on our projection, a combination of aircraft technical efficiency improvements and operational efficiency improvements reduce the energy intensity of commercial air transport, measured in megajoules of energy per RTK (MJ/RTK), by between 24% and 46% in 2050 compared with 2023 levels (Figure 7). The smallest reductions were seen in the Historical Trends scenario, with market-driven efficiency improvements and no additional policy interventions. Under the Current Commitments and SLCP Forward scenarios, energy per RTK falls by about 14% below the Historical Trends case in 2050, or 34% below 2023 levels. The GHG Forward and Full Breakthrough scenarios showed accelerated efficiency gains as a result of larger leaps in fuel efficiency and earlier widebody EIS modeled, with MJ/RTK falling by 45% below 2023 levels in 2050.

Figure 7
Aviation fuel efficiency by scenario, 2023–2050

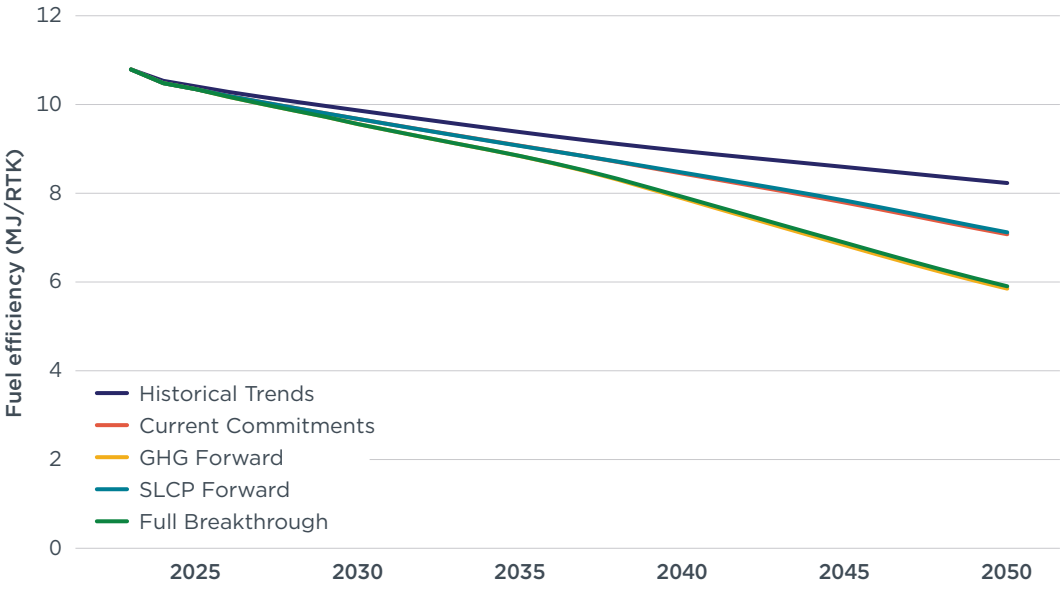

THE INTERNATIONAL COUNCIL ON CLEAN TRANSPORTATION **THEICCT.ORG**

The share of Jet A used globally is projected to fall over time in all action scenarios as a function of bio-SAF, e-fuel, or hydrotreatment deployment (Figure 8). Under the Current Commitments and SLCP Forward scenarios (overlapping in the figure), announced SAF mandates in Brazil, the European Union, Japan, and the United Kingdom deliver global average SAF usage of 2% in 2030 and 9% in 2050. This blending rate is much lower than the least ambitious policy scenario in our previous *Vision 2050* modeling, which entailed 50% SAF blending in 2050, reflecting slow progress toward the large-scale SAF deployment required for aviation decarbonization. The GHG Forward and Full Breakthrough scenarios (overlapping in the figure) assume a SAF blending rate of 8% in 2030 and 71% in 2050, which corresponds to the *Vision 2050* Transformation scenario, representing the minimum level of fuel switch needed to trend towards net-zero in 2050. The 71% SAF blending in

2050 is also consistent with a case in which the ReFuelEU ambition for SAF production was adopted globally.

Figure 8

Jet A share of global aviation kerosene consumption by scenario, 2023–2050

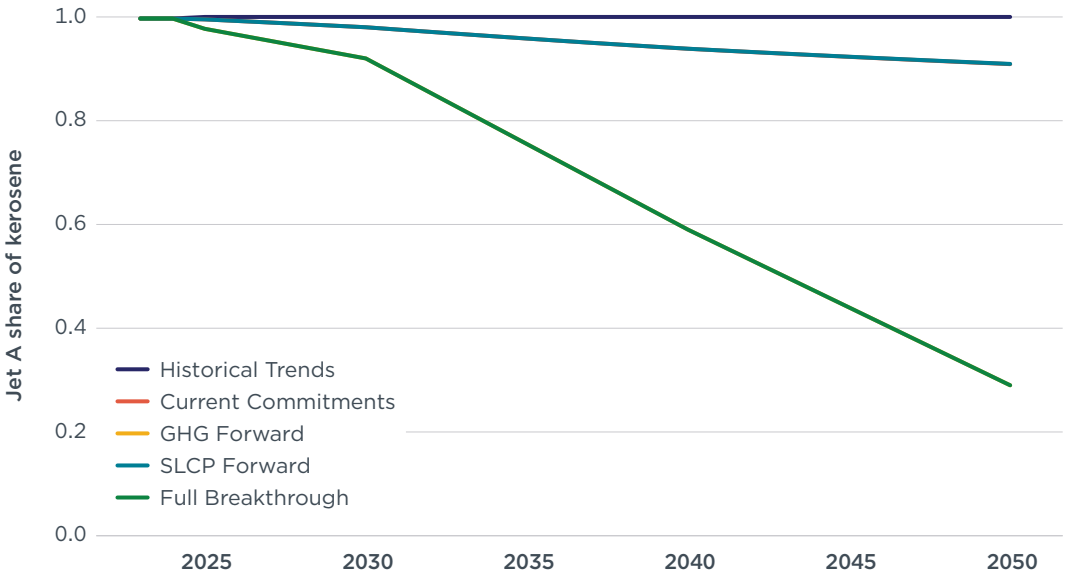

THE INTERNATIONAL COUNCIL ON CLEAN TRANSPORTATION **THEICCT.ORG**

Hydrotreated fossil jet fuel makes up a substantial amount of kerosene supply modeled in the SLCP Forward and Full Breakthrough scenarios (Figure 9), due to the assumed 8-year ramp-up from 5% to 100%. In the SLCP Forward scenario, hydrotreating reaches the maximum level in 2040 (i.e., 80% of total kerosene demand, or 100% of high- and middle-income countries' kerosene demand), delivering most of the contrail and nvPM reductions, as SAF blending is low in this scenario. In the Full Breakthrough scenario, the scale of hydrotreating peaks at 62% of global kerosene demand in 2037, as the capacity of hydrotreating exceeds the demand of fossil Jet A, prioritizing SAF use, which provides both GHG and SLCP mitigation.

Figure 9

Share of kerosene feedstock in SLCP Forward (left) and Full Breakthrough (right) scenarios

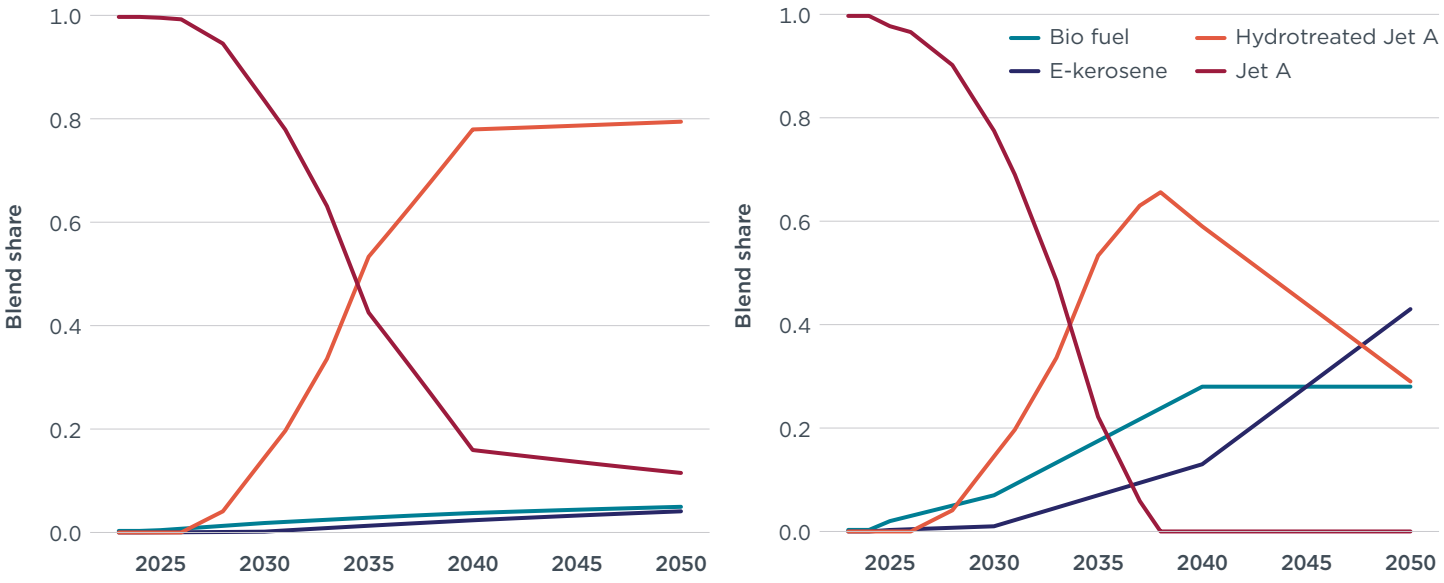

THE INTERNATIONAL COUNCIL ON CLEAN TRANSPORTATION **THEICCT.ORG**

GHG and SLCP emission trends

By design, the GHG Forward and Full Breakthrough scenarios exhibit nearly identical annual GHG emissions, as do the Current Commitments and SLCP Forward scenarios.[11] Under current industry commitments and announced policies, GHG emissions are projected to continue to rise through 2050, reaching about 1,630 million metric tonnes (Mt) of CO_2e in 2050, a 58% increase from 2023 levels (Figure 10). The GHG Forward and Full Breakthrough scenarios limit GHG emissions to under 500 Mt in 2050, or a 70% cut from the Current Commitments scenario. The level of maximum GHG mitigation assumed in this study would not enable the industry to reach net-zero by 2050 goal; this reflects the current trend of delayed fossil jet fuel peaking, which would need to occur by 2025 in a net-zero compatible scenario. Instead, our maximum GHG reduction scenarios peak fossil jet fuel consumption by 2030. Under the Current Commitments scenario, airlines emit about 38.9 Gt CO_2e from 2023 to 2050. Cumulative GHG emissions from 2023 to 2050 under the GHG Forward and Full Breakthrough scenarios, meanwhile, sum to 26.5 Gt CO_2e, or about a 40% reduction compared with the Historical Trends scenario.

11 Very minor differences in GHG emissions are seen for the fuel burn penalty of contrail avoidance and upstream emissions associated with the hydrotreating of jet fuel on flights departing EU airports.

Figure 10

Annual (left) and cumulative (right) GHG emissions by scenario, 2023–2050

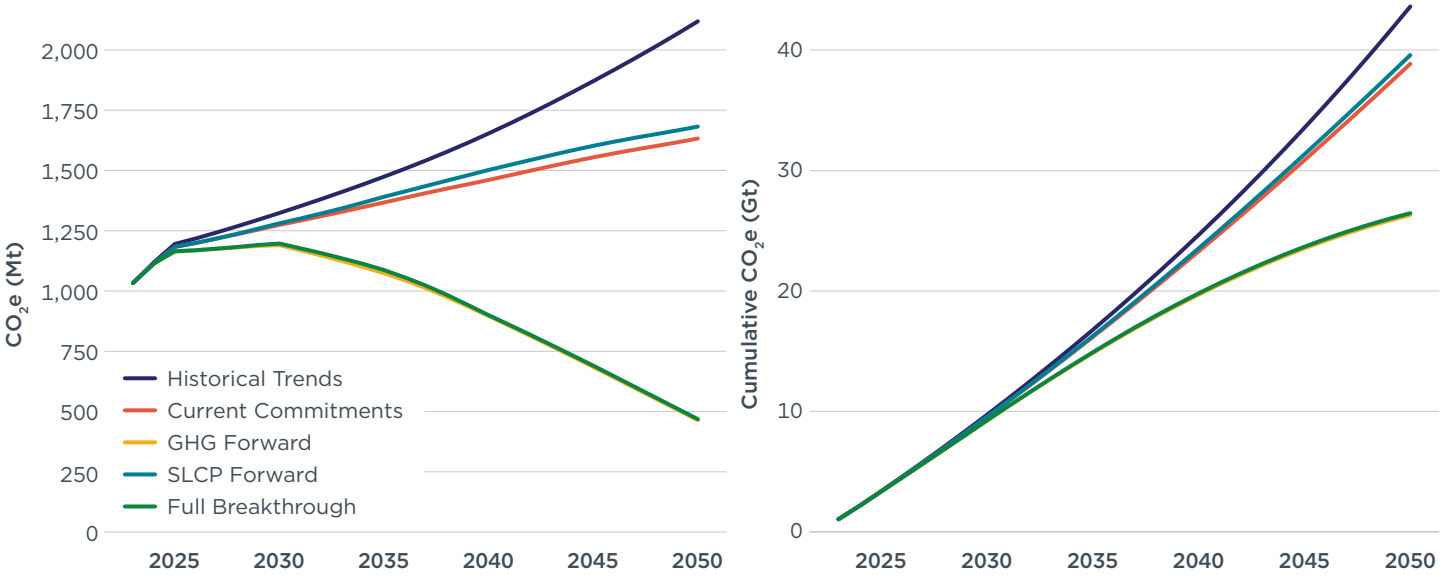

THE INTERNATIONAL COUNCIL ON CLEAN TRANSPORTATION **THEICCT.ORG**

The GHG Forward scenario is projected to cut absolute NO_x emissions more than the SLCP Forward scenario (Figure 11). Although the reduction in NO_x EI is faster in the SLCP Forward scenario than in the GHG Forward scenario, the larger fuel efficiency gains in GHG Forward (combined with significant reductions in EI) cut more NO_x overall. Without standards requiring the adoption of best-in-class engine technology, NO_x emissions would increase over time due to increasing traffic and EI. In the GHG Forward scenario, aviation is projected to emit about 5.3 Mt of NO_x in 2050, a 23% reduction from the Current Commitments scenario, surpassing the SLCP Forward scenario (which results in a 17% reduction from the Current Commitments scenario). The Full Breakthrough scenario is projected to provide the largest reduction (39%), with the combined effect of large fuel efficiency gains and steep reductions in EI with advanced engine technologies.

For nvPM emissions, we observe large reductions in the GHG Forward, SLCP Forward, and Full Breakthrough scenarios from the Current Commitments scenario (of 51%–82% in 2050). While no engine-level nvPM improvement is expected under the Current Commitments and GHG Forward scenarios, high SAF blend rates and fuel efficiency improvements assumed in the GHG Forward scenarios substantially reduce nvPM emissions intensity, allowing the scenario to deliver steep reductions. The SLCP Forward scenario, which is characterized by low SAF blends and fuel efficiency gains but large improvements in engine technology and hydrotreating capacity, is projected to result in even larger reductions. The combination of these measures in the Full Breakthrough Scenario enables nvPM emissions reductions of 82% below the Current Commitment scenario.

Figure 11

NO_x and nvPM emissions by scenario, 2023–2050

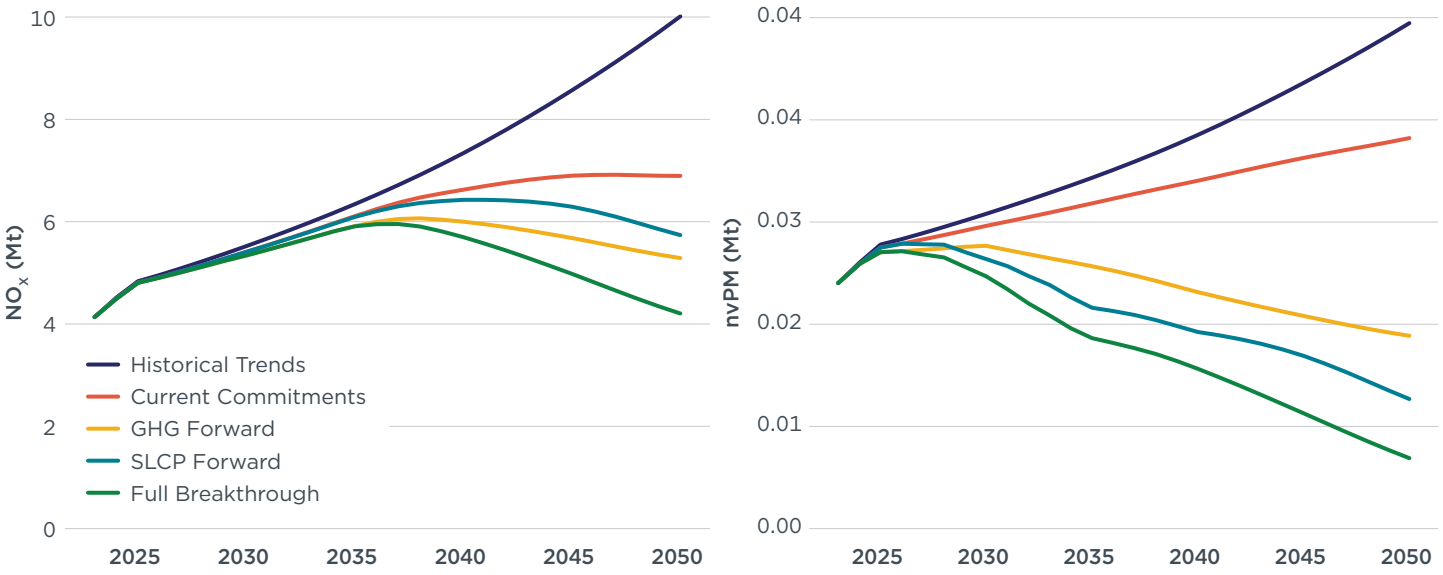

THE INTERNATIONAL COUNCIL ON CLEAN TRANSPORTATION **THEICCT.ORG**

Reductions in contrail ERF are achieved through a combination of SAF blending, hydrotreatment, low-soot engines, improved efficiency, and avoidance maneuvers. In the Current Commitments and GHG Forward scenarios, no contrail avoidance or hydrotreating is modeled, so contrail mitigation is driven by SAF blending and operational efficiency gain alone (Figure 12). The 9% SAF blending rate in 2050 in the Current Commitments scenario would deliver a 5% reduction in contrail ERF compared with the Historical Trends scenario, while operational efficiency improvements decrease flight distance per unit of transport work and reduce contrail formation by an additional 8%; the total contrail ERF reduction in the Current Commitments scenario amounts to 13%. In the GHG Forward scenario, a 71% SAF blend in 2050 is projected to deliver a 30% reduction in contrails; the total reduction amounts to 38%, with 8% due to operational efficiency improvement. Contrail reductions are much larger in the SLCP Forward and Full Breakthrough scenarios, at 93% and 94% reductions from the Historical Trends scenario in 2050, respectively. The reduction rate is similar between the two scenarios despite large differences in SAF blending; this is because avoidance maneuvers dominate the mitigation of contrails in these two scenarios.

Figure 12

Annual contrail effective radiative forcing by scenario, 2023–2050

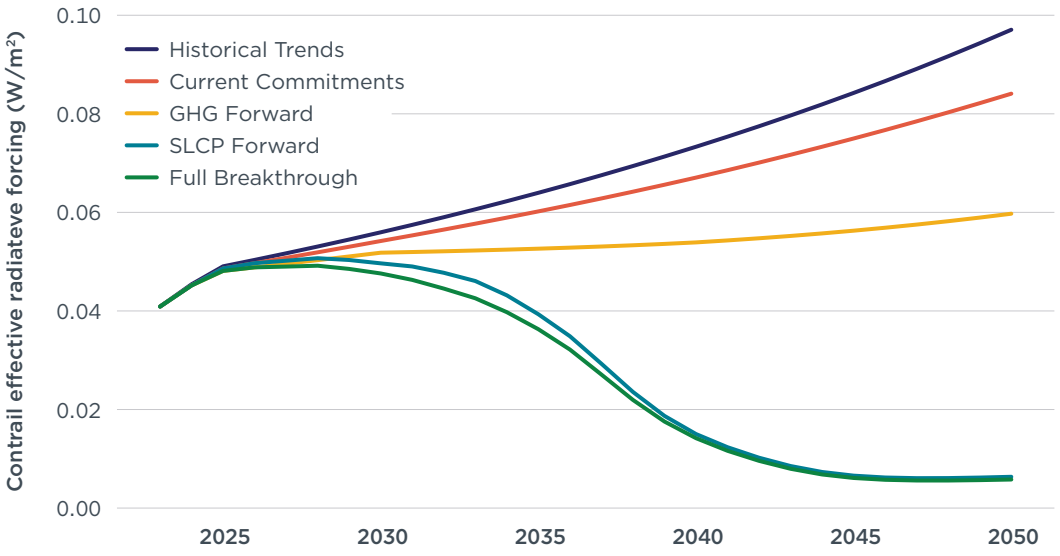

THE INTERNATIONAL COUNCIL ON CLEAN TRANSPORTATION **THEICCT.ORG**

Since contrail warming, contrail avoidance, and SAF uptake vary regionally, mitigated warming also varies regionally. Figure 13 shows the projected contrail ERF mitigation over time for each ICAO departure region in the Full Breakthrough scenario. Europe and North America experience the largest savings, with smaller contributions from Pacific South East Asia, China, the Middle East, and North Asia. South West Asia is the only region that shows an increase in contrail ERF between 2023 and 2050; this is primarily because low-income and lower-middle-income countries make up 80% of the contrail warming in this region and are assumed not to implement contrail avoidance.

Figure 13

Annual ERF for flights departing each region in the Full Breakthrough scenario

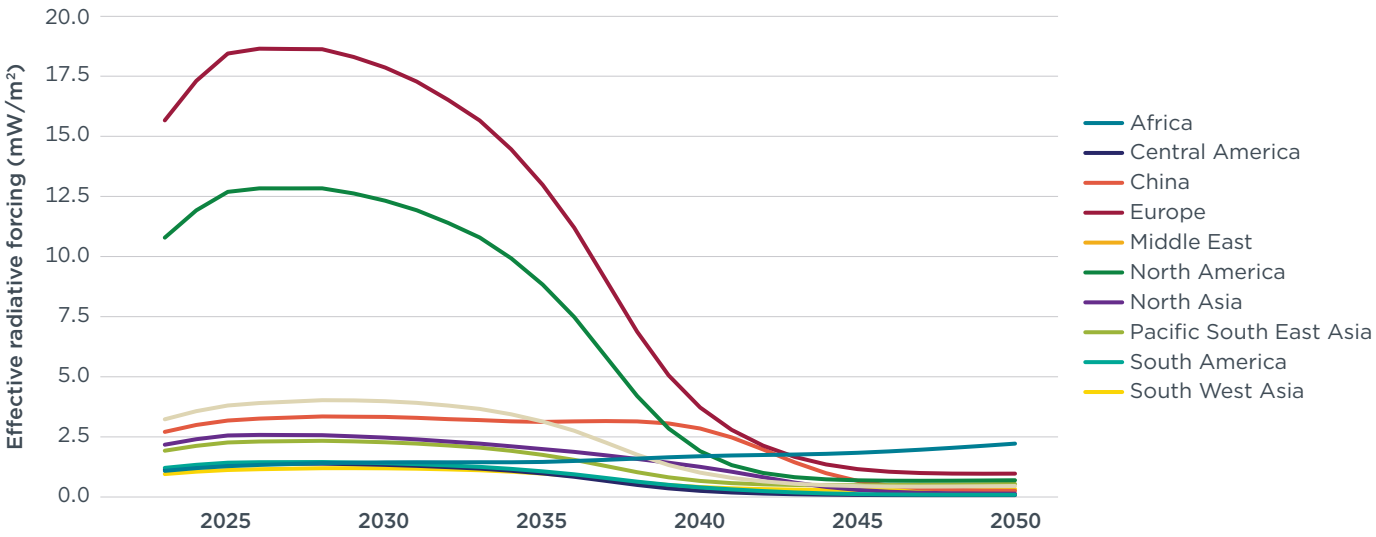

THE INTERNATIONAL COUNCIL ON CLEAN TRANSPORTATION **THEICCT.ORG**

TEMPERATURE RESPONSE

Aviation-attributable warming

Figure 14 summarizes the results of the modeled temperature response for the five scenarios. Aviation's projected contribution to global warming was also evaluated, by its share of the remaining 1.7 °C budget of 340 mC, based on 1.36 °C of warming to date (Forster et al., 2024).

Figure 14
Aviation's historical and contribution to global warming by scenario, 1940–2050

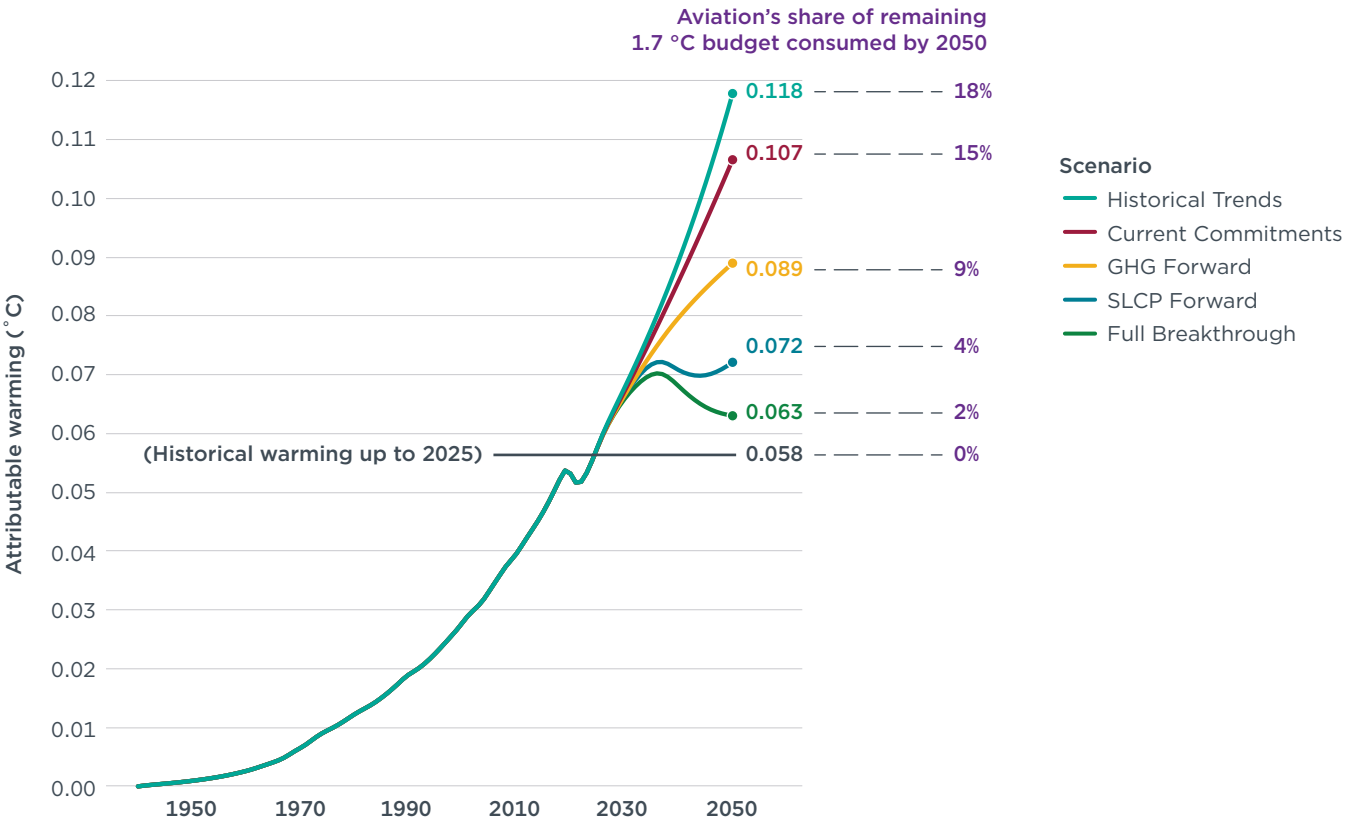

THE INTERNATIONAL COUNCIL ON CLEAN TRANSPORTATION **THEICCT.ORG**

As shown, relative to 2025 values (0.058 °C), we project a 103% increase in aviation-attributable warming through 2050 under the Historical Trends scenario (0.118 °C) and a near doubling under the Current Commitments case (0.107 °C). Under the latter scenario, aviation would triple its 4% share of historical warming to consume 15% of the remaining 1.7 °C budget (Table 12). Under the GHG Forward scenario, accelerated investments in SAF and fuel efficiency reduce additional warming by 29 mC (0.029 °C) in 2050, a 48% reduction from the 60 mC additional warming in the Historical Trends scenario. Aviation would consume 22% of the remaining 1.5 °C budget in this case, more than 5 times its historical share and double its share under a 1.7 °C budget.

Table 12

Aviation-attributable warming and share of remaining climate budget under each scenario

Scenario	Total warming 1940–2050 (°C)	Additional warming 2025–2050 (°C)	% of remaining budget		
			1.5 °C (0.14 °C)	1.7 °C (0.34 °C)	2 °C (0.64 °C)
Historical Trends	0.118	0.0603	43%	18%	9%
Current Commitments	0.107	0.0493	35%	15%	8%
GHG Forward	0.089	0.0313	22%	9%	5%
SLCP Forward	0.072	0.0143	10%	4%	2%
Full Breakthrough	0.063	0.0053	4%	2%	1%

Accelerated implementation of SLCP controls in the form of avoided contrails, advanced engine technologies, and hydrotreating jet fuel, could reduce additional warming in 2050 by about 46 mC, or approximately 1.5 times that of the GHG Forward scenario. The SLCP Forward scenario would mitigate three-quarters (76%) of the expected additional warming beyond 2025 in the Historical Trends scenario. Although the SLCP Forward scenario limits aviation's warming contribution by 2050 to 4% of the global total, an inflection point is projected to occur around 2045 when warming from the continued accumulation of aviation CO_2 in the atmosphere overpowers short-term cooling from SLCP control, suggesting a high probability of continued warming beyond 2050 and an increased aviation share of global warming.

Under the Full Breakthrough scenario, combining both GHG and SLCP control, additional warming from aviation relative to 2025 peaks around 2036 and gradually decreases through 2050 to 5.3 mC, or a 91% reduction from the 60 mC additional warming modeled in the Historical Trends scenario. This offers the potential for climate-neutral growth, since traffic is anticipated to increase by about 150% above 2023 levels by 2050 while aviation's contribution to global warming is trending downward. This maximum-ambition scenario also limits aviation's share of the remaining 1.5 °C budget consumed by 2050 to 4% and reduces its share of a 1.7 °C budget to 2%. However, the stabilization of aviation's climate contribution beyond 2050 would depend on whether and how quickly GHG emissions can reach zero, as well as potential contrail formation in conditions with low nvPM emissions.

Figure 15 shows aviation's historical and projected contribution to global warming under each scenario from 1940 to 2050 by pollutant. It is arranged from highest warming impact (CO_2, top left) to lowest warming impact (cooling from sulfates, bottom right). The two largest contributors, CO_2 and contrails, have 7 times the expanded scale compared with the minor contributors. Contrails are projected to account for the majority of potential abated warming under the SLCP Forward and Full Breakthrough scenarios, as indicated by the gap between the Historical Trends and these two scenarios. This is because contrails can be mitigated quickly by today's technology (rerouting and hydrotreating) and their warming effects are transient, while technologies to mitigate GHG emissions (SAF and direct use of hydrogen) remain nascent and emitted CO_2 remains in the atmosphere for hundreds of years.

Figure 15

Aviation's historical and projected contribution to global warming by pollutant and scenario, 1940–2050

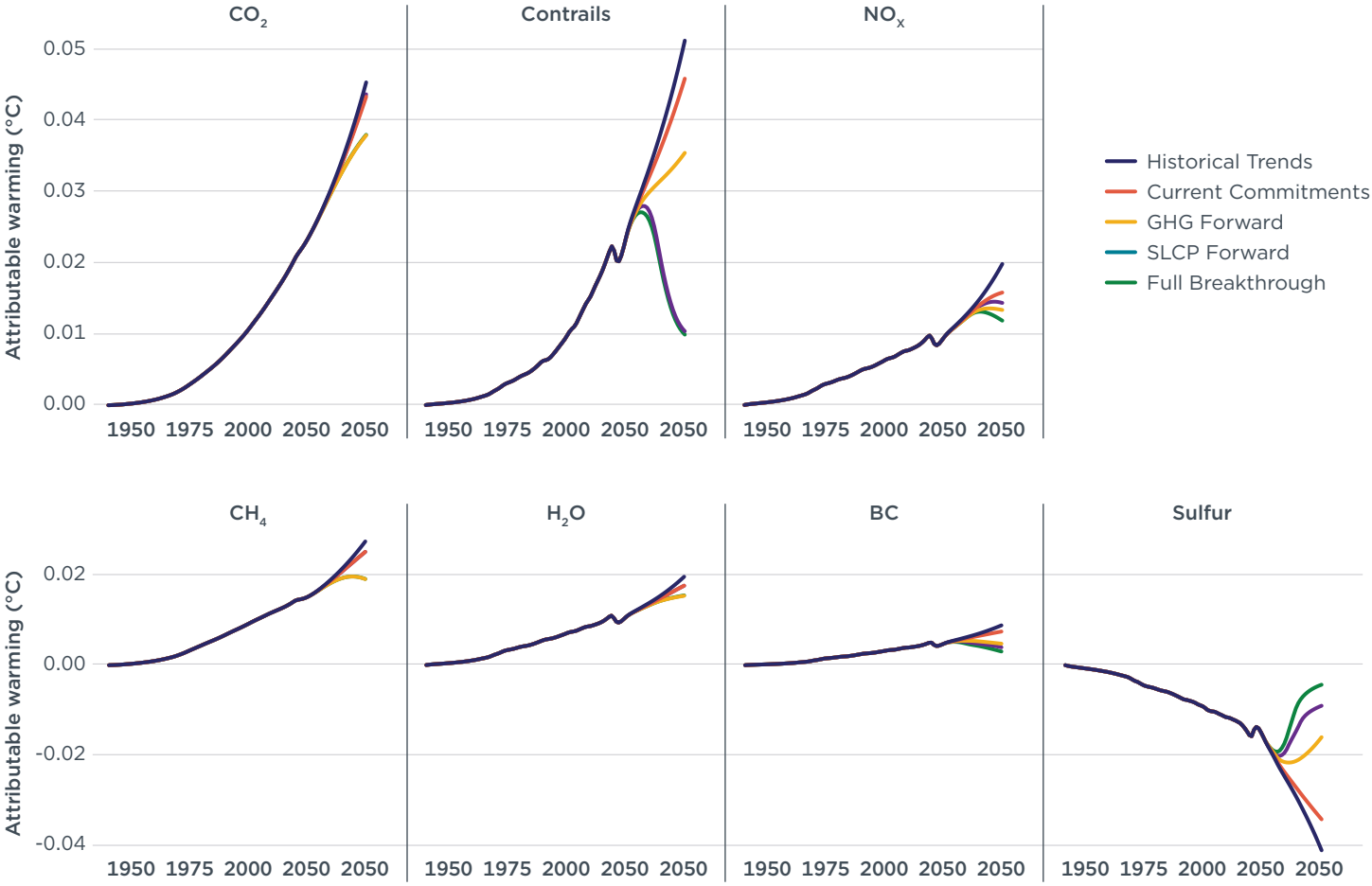

THE INTERNATIONAL COUNCIL ON CLEAN TRANSPORTATION **THEICCT.ORG**

As shown in Figure 15, we projected contrails and CO_2, followed by NO_x, to be the dominant climate warmers from aviation in 2050 under the Historical Trends scenario. Other species contribute only moderately to warming, with sulfates providing a cooling impact approximately one-fifth the amount of warming from NO_x. The warming impact of reducing fuel sulfur via the use of SAFs and hydrotreatment, on the order of about 4 mC, is modest compared with the cooling impact from their reduced GHG emissions.

Figure 16 shows aviation's historical and projected contribution to global warming under the SLCP Forward scenario, stacking the effects of GHGs and SLCPs. The figure highlights how targeted SLCP controls—such as contrail avoidance and hydrotreatment—can achieve a pronounced short-term slowdown in aviation-attributable warming beginning in the 2030s. However, the cumulative effect of continued CO_2 emissions causes total aviation warming to begin rising again toward mid-century, despite deep SLCP reductions. This illustrates the limits of relying on SLCP controls alone: while they can deliver significant near-term cooling, lasting climate stabilization still requires deep cuts in CO_2 emissions.

Figure 16

Aviation's historical and projected contribution to global warming by GHG and SLCP under the SLCP Forward scenario, 1940–2050

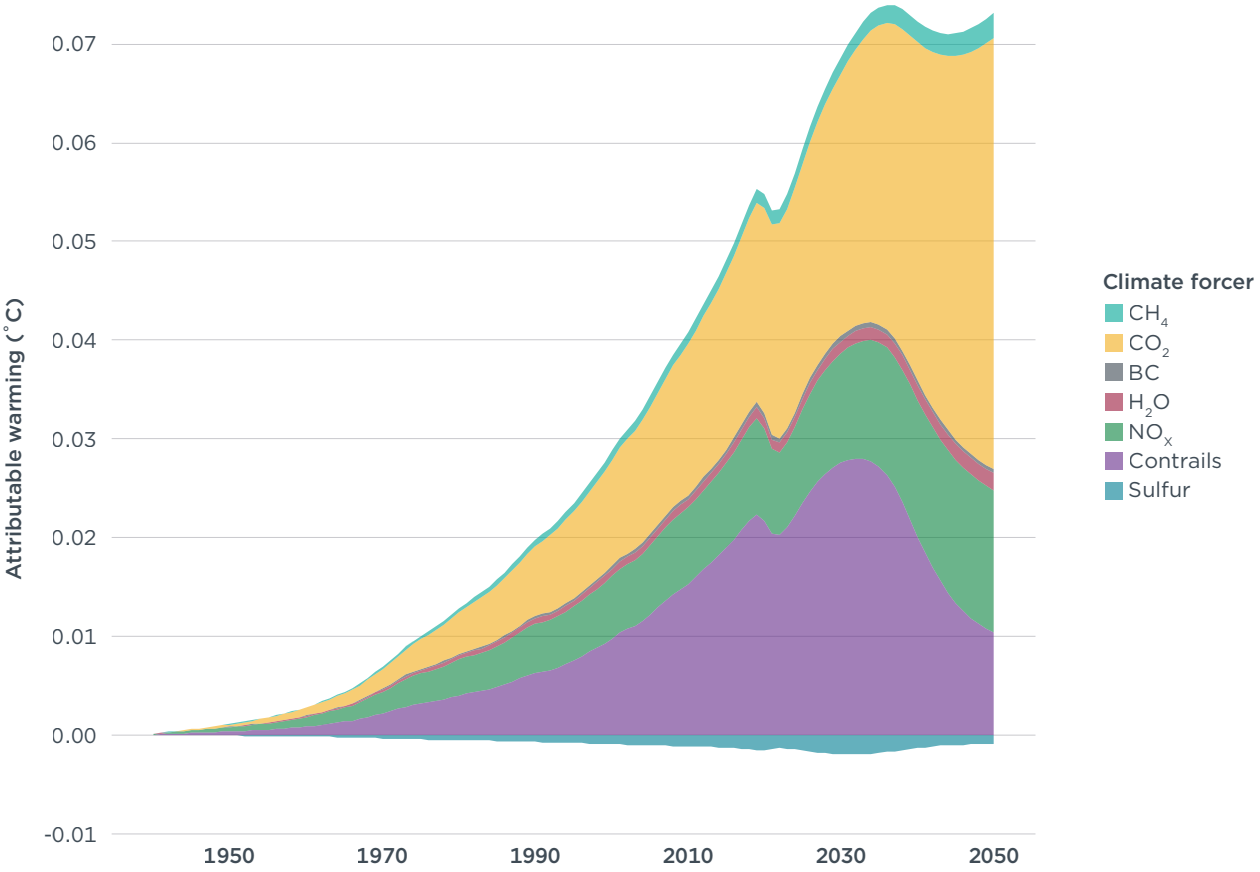

THE INTERNATIONAL COUNCIL ON CLEAN TRANSPORTATION **THEICCT.ORG**

Warming contribution by pollutant and contrail uncertainties

Figure 17 shows aviation-induced warming by pollutant (left) and aggregate long-lived GHGs versus SLCP groups (right) in 2050. The figure on the left shows only the mean expected contribution from each pollutant, while the figure on the right also shows the 95% confidence interval for the SLCP temperature response. As shown at left, contrails account for about 40% of total warming from 1940 to 2050 under the Historical Trends, Current Commitments, and GHG Forward scenarios. That share falls under the SLCP Forward and Full Breakthrough scenarios to about one-seventh of total warming due to contrail avoidance and hydrotreating. In aggregate (right), without dedicated control, SLCPs together account for approximately 60% of total warming between 1940 and 2050. That share falls to around 40% in the SLCP Forward and Full Breakthrough scenarios, while GHG's warming contribution remains relatively stable across scenarios, highlighting the opportunity for rapid SLCP reductions alone to almost halve aviation's contribution to global warming.

Figure 17

Total warming by pollutant from 1940 to 2050 (left) and GHG versus SLCP warming in 2050 (right)

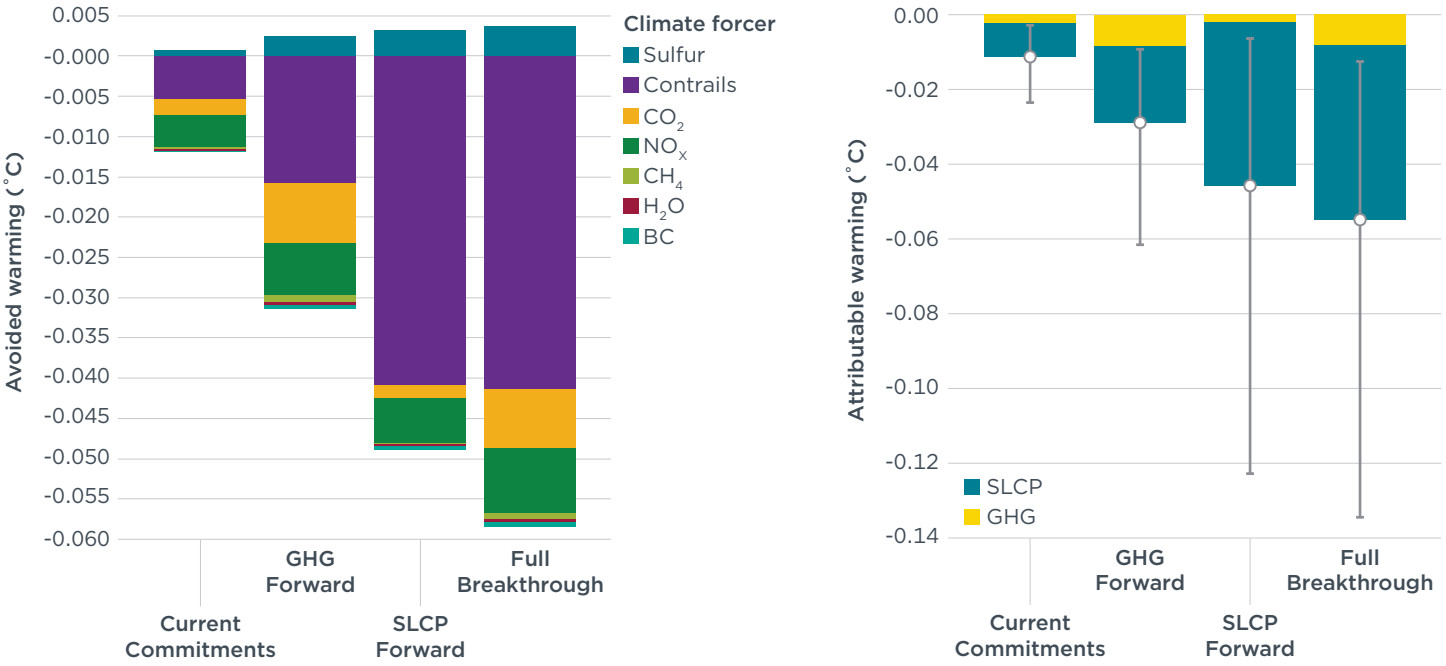

Note: Lines on the right represent the 95% confidence interval for the SLCP temperature response.

The 95% confidence intervals for the SLCP warming shown on the right were produced using the analyses detailed in Appendix C and Appendix D. They reflect the uncertainty in the ERF of each SLCP and do not account for uncertainties in emission quantities or traffic growth rates. The confidence intervals in all scenarios are larger than the mean GHG contribution. In the scenarios without SLCP mitigation (Historical Trends, Current Commitments, and GHG Forward), projected SLCP-attributable warming in 2050 can range from about 14% of the GHG contribution to more than 3 times the GHG contribution. In the scenarios with SLCP mitigation (SLCP Forward and Full Breakthrough), SLCP-attributable warming in 2050 ranges from about 5% of the GHG contribution to roughly 1.2 times the GHG contribution. Thus, the benefits of action on SLCPs rely greatly on the expected ERF from each pollutant.

This raises the question of whether action to control SLCPs, which often incurs a fuel burn penalty, is still recommended if the ERF is on the lower end of our confidence interval. To interrogate this, we looked at the increase in GHG-attributable warming in 2050 when SLCP controls are applied together with GHG controls (Full Breakthrough scenario) compared with when only GHG controls are applied (GHG Forward scenario). SLCP controls increase GHG-attributable warming by less than 0.0001 °C. In the case that SLCP ERFs are on the lower end of our confidence interval (i.e., 1.04E-10 mW/m^2/km), SLCP controls reduce their contribution to warming in 2050 by 0.0034 °C, bringing a benefit that is 40 times greater than the increase from the GHG penalty of the measures. The same is true when comparing the Current Commitments and the SLCP Forward scenarios, in which GHG control measures are minimal. In these cases, the benefit of SLCP measures is similar (0.0039 °C), but in the absence of GHG controls, the absolute GHG penalty is greater, at 0.0003 °C. However, the benefit of

the SLCP control measures is still 10 times greater than the GHG penalty. This shows that even if the ERF estimates of SLCPs are on the lower end of the 95% confidence interval, SLCP mitigation measures are projected to bring climate benefits despite the expected increase in GHG from enacting the measures. Based on IPCC guidance on communicating the likelihood of uncertain phenomenon, we can say that it is "extremely likely" that SLCP control measures as described in this report would result in a climate benefit in 2050 (Mastrandrea et al., 2011; IPCC, 2021).[12] The relative benefit is greater when SLCP measures are paired with GHG control measures.

Table 13 shows the relative share of total aviation warming in 2050 by pollutant and scenario. Each column sums to 100%; accordingly, sulfur's cooling impact is shown as a negative percent. The table shows relative consistency in the contributions of the various pollutants to the climate impact across the Historical Trends, Current Commitments, and GHG Forward scenarios, the latter because reductions in fuel burn reduce CO_2 while also generally reducing co-pollutants (NO_x and nvPM) associated with fuel combustion. Precipitous drops in contrail warming are seen in the SLCP Forward and Full Breakthrough scenarios, down to about one-seventh of total warming. Sulfur cooling falls significantly in the GHG Forward and Full Breakthrough scenarios as fuel efficiency improvements reduce the total volume of fuel burn and due to the use of low-sulfur SAF blends and hydrotreated fuel.

Table 13

Share of total aviation warming in 2050 by pollutant and scenario

Climate forcer	Scenario				
	Historical Trends	Current Commitments	GHG Forward	SLCP Forward	Full Breakthrough
Contrails	43%	43%	40%	14%	16%
CO_2	38%	41%	43%	60%	60%
NO_x	17%	15%	15%	20%	19%
CH_4	2.3%	2.3%	2.1%	3.5%	3.0%
H_2O	1.7%	1.6%	1.7%	2.4%	2.4%
BC	0.7%	0.7%	0.5%	0.5%	0.5%
N_2O	0.03%	0.03%	0.03%	0.04%	0.05%
Sulfur	-3.5%	-3.2%	-1.8%	-1.2%	-0.7%
Total	100%	100%	100%	100%	100%

Avoidable warming by mitigation lever

Figure 18 shows avoidable 2050 global warming by pollutant and scenario (left) and aggregated by long-lived GHGs versus SLCPs groups (right) in 2050. The figure on the left shows only the mean expected contribution from each pollutant, while the figure on the right also shows the 95% confidence interval for the SLCP contributions.

12 The International Panel on Climate Change uses the following terms to indicate the assessed likelihood of an outcome or result: "virtually certain 99–100% probability; very likely 90–100%; likely 66–100%; about as likely as not 33–66%; unlikely 0–33%; very unlikely 0–10%; and exceptionally unlikely 0–1%. Additional terms (extremely likely 95–100%; more likely than not >50–100%; and extremely unlikely 0–5%) are also used when appropriate."

In both figures, only four bars are shown as the Historical Trends scenario provides the comparison baseline. On the left we see that reduced contrail warming provides the largest potential abatement across all scenarios, even those that do not model targeted action on contrails (the Current Commitments and GHG Forward scenarios). This is due to reduced contrail warming as a function of SAF blending and fuel efficiency improvements, which reduce the amount of particulate matter formed and fuel precursors consumed, respectively. Contrail abatement provides virtually all net mitigation under the SLCP Forward scenario and almost four-fifths of potential mitigation under the Full Breakthrough scenario.

Figure 18

Avoidable 2050 global warming by pollutant and scenario and aggregated by GHGs versus SLCPs groups

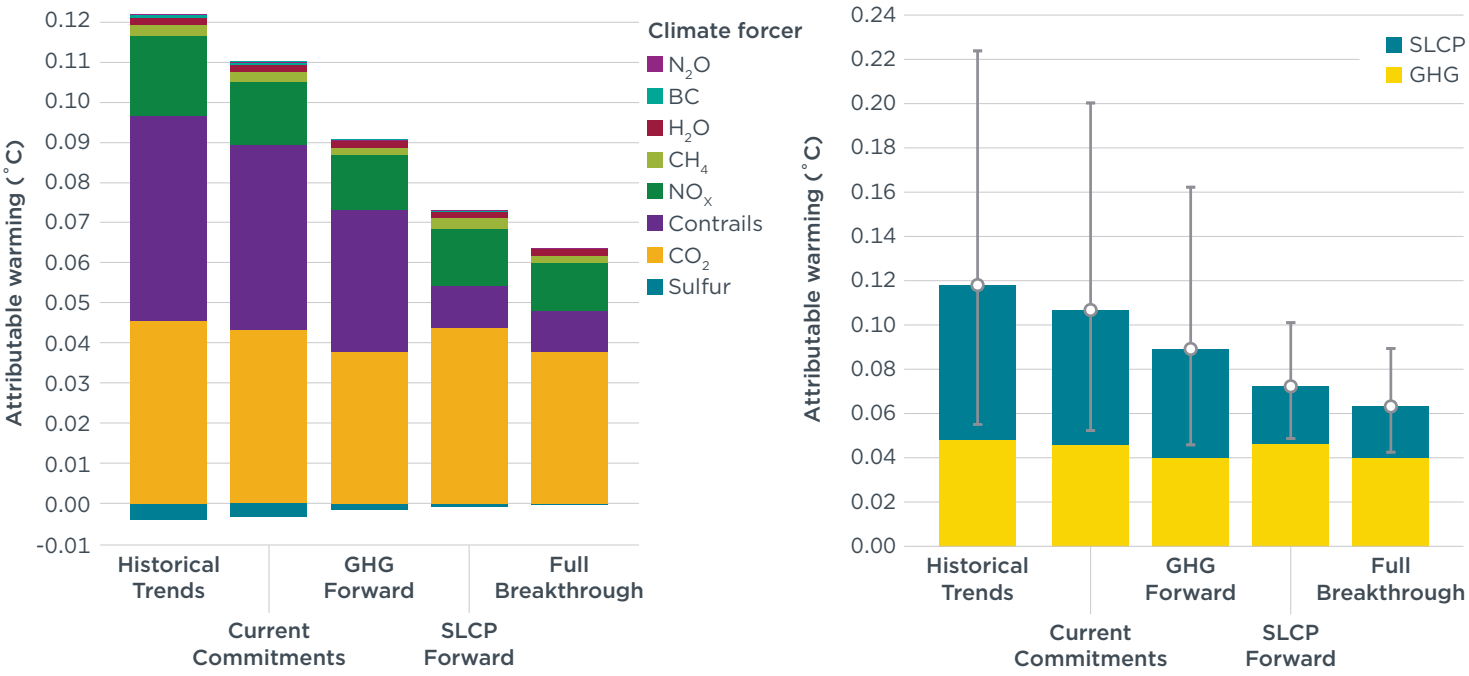

When the pollutants are aggregated (right), the 95% confidence intervals show the large uncertainty in the avoidable warming from SLCPs. If SLCP ERFs are on the lower end of the confidence interval, the avoidable warming from SLCPs is smaller than that from GHG in all scenarios but the SLCP Forward scenario. When GHG mitigation and SLCP mitigation are applied together in the Full Breakthrough scenario, the low end of the confidence interval still implies avoidable warming from SLCPs that is about 50% of that from GHGs.

Table 14 summarizes the relative contribution of different mitigation measures for the Full Breakthrough scenario. Avoided temperature response is shown for contrail avoidance, SAFs, hydrotreating, operational efficiency, advanced engine technologies, technical efficiency improvements, demand response, modal shift, and ZEPs. The levers are arranged in decreasing order of contribution to avoidable warming. Both the total warming and the GHG versus SLCP mitigation potential is shown, along with the percent of total mitigation. Attribution of avoidable warming to mitigation levers was

done by applying one lever at a time to the baseline scenario. When applied one at a time, the sum of the avoidable warming of all levers can exceed the total avoidable of the scenario. In that case, the individual avoidable warming values are normalized by the total avoidable warming.

Table 14

Share of avoidable warming by mitigation lever in 2050 under the Full Breakthrough scenario

Mitigation lever	Avoided warming (mC)			% of total
	GHGs	SLCPs	Total	
Contrail avoidance	0.07	-23.4	-23.3	42.5%
SAF	-5.90	-5.68	-11.6	21.1%
Hydrotreating	0.05	-6.35	-6.30	11.5%
Operational efficiency	-1.37	-4.58	-5.95	10.8%
Low NO_x/nvPM engines	0.00	-4.39	-4.39	8.0%
Technical efficiency	-0.84	-1.80	-2.62	4.8%
Demand response	-0.12	-0.30	-0.42	0.8%
Modal shift	-0.07	-0.17	-0.25	0.5%
ZEP	-0.02	-0.02	-0.05	0.1%
Total	**-8.20**	**-46.6**	**-54.9**	**100%**
% of total	**15%**	**85%**	**100%**	

As shown in Table 14, contrail avoidance contributes the largest share (23 mC, or about half) of all potential avoidable warming. That includes a small (0.07 mC) temperature increase due to the fuel burn penalty of rerouting. SAF contributes about one-fifth (21%) of avoided temperature, the second largest amount. Hydrotreating and operational efficiency are the third and fourth ranked levers, both contributing an estimated 11% of the total avoidable warming; interestingly, two-thirds of operational efficiency-driven mitigation comes from SLCPs, due in part to a reduction in kilometers flown.

In total, contrail avoidance, SAFs, hydrotreating, and operational efficiency account for 86% of expected avoidable warming in 2050, compared with only 14% from the other factors combined. Other levers, including low NO_x/nvPM engines, hydrotreating, technical efficiency, ZEPs, demand response, and modal shift contribute only modestly to avoidable warming. Overall, more than four-fifths (85%) of avoided temperature increase is linked to a reduction of SLCPs.

Comparing the cost of SAF, hydrotreating, and contrail avoidance in the context of their contribution to avoidable warming sheds light on the cost-effectiveness of each lever. Engine, airframe, and operational efficiency improvements were not compared in this study because the cost is likely to be internalized by the industry and have minimal impacts on consumer price. Contrail avoidance, as the lever with the most mitigation potential (23 mC under the Full Breakthrough scenario), would incur $28 billion in fuel cost increase between 2030 and 2050 because of fuel burn penalty. This is a fraction

of the $1.86 trillion SAF cost premium attributable to SLCP mitigation.[13] Moreover, SAF is estimated to reduce 5.7 mC of SLCP-incurred warming, or one-fourth of the potential reduction from contrail avoidance. Hydrotreating alone would deliver SLCP-attributable warming mitigation potential of 6.4 mC, and its unit cost of $17.53 billion per avoided mC increase is 17 times less than SAF's unit cost of $326.7 billion per mC.

13 Total SAF cost premium over conventional fossil jet fuel under the Full Breakthrough scenario is $3.7 billion; this total cost was attributed to SLCP mitigation based its share of total avoidable warming from SAF.

CONCLUSIONS

This paper updates the ICCT's net-zero technology roadmap to reflect recent industry trends in technology development and the latest science on mitigating short-lived climate pollutants. We employed simplified climate modeling using the FaIR model to generate an estimate of temperature response through 2050. Under the Historical Trends scenario, we expect aviation to contribute about 118 mC (0.118 °C) of global warming by 2050, with additional warming after 2023 consuming 18% of the remaining temperature budget to 1.7 °C. That would represent a quadrupling of aviation's pre-pandemic contribution of 4% of historical temperature change (Klöwer et al., 2022).

Our GHG Forward scenario resulted in cumulative GHG emission reductions about 48% below the business-as-usual Historical Trends scenario, and would set aviation on a pathway to contribute 89 mC (0.089 °C) of anthropogenic global warming by 2050, with continuing warming afterwards. This corresponds to an additional 31 mC of warming above 2025 levels, or 9% of a remaining climate budget of 340 mC to achieve 1.7 °C (Forster et al., 2024). Thus, even with a maximum level of GHG mitigation between now and 2050, aviation would more than double its share of the remaining climate budget, from 4% of historical temperature change in 2019 to 9%. This highlights the need to identify additional mitigation levers, such as SLCP control and explicit air transport demand management.

We found that targeted action in short-lived climate pollutants, notably contrail avoidance maneuvers and fuel composition improvements, provides the potential for deeper reductions in aviation warming. Under the SLCP Forward scenario, aviation warming plateaus after 2035 and is constrained to 14 mC of additional warming in 2050, a 76% reduction from the Historical Trends scenario. The SLCP Forward scenario avoids 1.5 times more warming than the GHG Forward scenario in 2050 and keeps aviation's share of global warming to 4% by 2050. Still, aviation's contribution to global warming begins to increase again after 2045 as warming from accumulating CO_2 overcomes short-term cooling from SLCP reductions.

Only the Full Breakthrough scenario, involving maximum efforts to reduce both GHGs and SLCPs, prevents aviation from exceeding its current 4% share of global warming. We estimate that additional aviation warming after 2025 can be reduced from 60 mC in the Historical Trends scenario to only 5.3 mC in the Full Breakthrough scenario through the introduction of clean fuels, contrails avoidance, and more fuel-efficient aircraft. This would offset more than 90% of all anticipated warming after 2025. This offers the potential for climate-neutral growth, since traffic is anticipated to increase by about 150%, to 2.5 times the 2023 levels, by 2050.[14]

To date, national and international policymakers have focused on achieving net-zero CO_2 emissions from aviation by 2050. This work fundamentally revises our understanding of the available mitigation levers and puts contrails on the map of key levers alongside SAF. Contrail mitigation provides at least 47%, and as much as 89%, of avoidable warming depending on the scenario. This is because of the short-term impacts of those pollutants and the fact that contrail avoidance and hydrotreating technologies are relatively mature. The near-term benefits of GHG mitigation, in contrast, are limited by the relative immaturity of control technologies such as e-fuels, the long atmospheric residence times of GHGs, and the entrenchment of fossil fuel as a cheap, abundant incumbent fuel.

14 We investigated the temperature trends beyond 2050 for all scenarios using simplified assumptions and will publish those in a separate blog.

This report did not model explicit demand reduction policies or the use of CO_2 removal technologies as measures to help reach the net-zero target. The results from the GHG Forward scenario highlight the challenges of achieving the industry's adopted 2050 net-zero CO_2 target solely through in-sector improvements to aircraft and fuels. In principle, the use of CO_2 removal technologies could be used to compensate for residual CO_2 emissions, especially if high-integrity removals such as direct air capture with geological storage become available at scale. However, significant uncertainties remain regarding the availability, cost, permanence, and governance of such removals (IPCC, 2022). For this reason, even though CO_2 removal technologies may play a role in balancing hard-to-abate emissions in the long term, policymakers should still prioritize scalable, near-term measures to reduce aviation-attributable warming.

At the level of individual mitigation, contrail avoidance maneuvers provide 43% of avoidable warming in 2050 under the Full Breakthrough scenario, double that of SAF (21%), the lever that delivers the second biggest reduction. Combined, contrail avoidance, SAF, hydrotreating, and operational efficiency accounted for almost 90% of avoidable warming in this scenario. Still, contrail avoidance alone is insufficient to stabilize aviation's contribution to global warming, as evidence by the fact that expected warming from aviation is projected to increase again after 2045 under the SLCP Forward scenario. This highlights the need for SLCP control for short and mid-term climate protection and GHG control for long-term climate stabilization.

POLICY IMPLICATIONS

Several policy findings can be drawn from this work. At the highest level, if climate stabilization by 2050 is the goal, action to cut SLCPs can contribute a majority of the estimated climate impact mitigation: 84% per the Full Breakthrough scenario. In particular, contrail avoidance is potentially the most effective means of reducing aviation's contribution to climate change and is twice as impactful as the second most effective measure (SAF). The third and fourth most effective factors, hydrotreating and operational efficiency, can contribute one-quarter of the benefit associated with contrail mitigation. The climate benefits of hydrotreating would be maximized if green hydrogen produced using additional renewable electricity were to be adopted on a wide scale at refineries to avoid the GHG penalty. Operational efficiency is expected to have significant contrail abatement benefits by reducing fossil jet fuel use and the number of flights per unit payload to be moved.

While SAF remains an essential long-term decarbonization strategy, its near-term temperature benefits are limited by high costs ($300+/tonne CO_2e) and the slow pace of scale-up. In our central estimate, SAF deployment in 2050 provides around 12 mC of temperature mitigation from CO_2 reductions alone; this benefit could be greater if SAF's potential to reduce contrail formation is also considered. By comparison, targeted contrail avoidance offers an estimated 23 mC of mitigation in 2050, though this is subject to greater scientific uncertainty. Together, SAF and contrail mitigation can form complementary levers—addressing both long-lived and short-lived climate impacts of aviation.

Public policies could provide funding support for contrail avoidance technologies. Such technologies could include: 1) monitoring, reporting, and verification programs; 2) on-board hardware, including humidity sensors; 3) flight planning approaches, including navigational software for avoidance and international cooperation by air navigation service providers; 4) weather forecasting and modeling approaches to predict the location of ice super-saturated regions; and 5) satellite monitoring approaches to

detect persistent contrails in real time so that other flights can be rerouted around those areas. The cost of avoidance maneuvers could be neutralized by integrating contrail and other SLCPs into emissions trading systems.

Public policies that could support fuel composition improvements include: establishing limits on aromatic, naphthalene, and sulfur content in conventional jet fuel, similar to the International Maritime Organization's sulfur limit on marine fuels, and implementing mandates or targets for hydrotreating, coupled with certification programs to ensure net climate benefits.

For GHGs, the majority of emission reductions are still expected to be provided by SAFs. Public policies to promote SAFs could include: 1) mandates to establish predictable demand for SAFs; 2) incentives to narrow the price gap between SAF and conventional jet fuel, including subsidies for SAF and taxation on fossil jet fuel; 3) direct project support through grants and loan guarantees to address high upfront capital investments needed for early SAF production facilities; and 4) derisking and revenue certainty policies such as long-term offtake agreements and contracts-for-difference to reduce market uncertainty and mobilize more private investments.

Fuel efficiency improvements are also expected to provide substantial GHG mitigation; more fuel-efficient aircraft and operations should modestly reduce SLCPs generated through the combustion of jet fuel. Given the CAEP/13 standard decision, which codifies existing airframe product lines but will not promote additional new types with higher fuel efficiency (Hameed & Rutherford, 2025), policymakers could consider economic incentives to create market pull for more fuel-efficient designs, including emissions trading and fuel taxation. Applying ICAO's CO_2 standard to the in-service fleet as a phase-out mechanism of older aircraft (Graver & Rutherford, 2018) could also be investigated; this approach could accelerate the introduction of more advanced airframe technologies. Direct research support for novel configurations could also be considered.

Even under the best-case Full Breakthrough scenario, additional warming is likely after 2050 unless further action is taken to reduce GHG emissions from aviation. That is the timeframe by which hydrogen aircraft, potentially in long-haul applications, may be sufficiently mature for widespread adoption. Public policies to support zero-emission planes could include government grants for hydrogen aircraft research and development and hydrogen infrastructure at airports, as well as fiscal incentives through integration into emissions trading systems and sustainable aviation fuel mandates.

FUTURE WORK

This study lays the groundwork for projecting aviation SLCP emissions out to 2050 and places these projections in the context of aviation's overall contribution to global warming, including its GHG emissions. While the SLCP mitigation modeling in this study draws from the most recent scientific literature, there are a few areas that could be strengthened in the future.

First, uncertainties in future-year meteorology and its effect on contrail formation were not explicitly modeled in this study. Thus, second-order effects wherein a warmer atmosphere creates feedback loops with contrail warming were not captured. The contrail uncertainty quantification illuminates the potential magnitude of the uncertainties, but the year-on-year variations have not yet been explored.

Second, future research could refine the quantification of climate and air quality benefits from SLCP control measures. Real-world data on how alternative fuels and next-generation engines (especially lean-burn engines) affect nvPM emissions and persistent contrail formation are limited. More data on the effectiveness and fuel burn impact of contrail avoidance maneuvers are also needed to increase modeling accuracy. Detailed cost assessments for each mitigation lever are also needed to evaluate the cost-effectiveness of policies.

Third, regional analysis is critical for informing mitigation policies. While this report presents global scenarios, the deployment of mitigation levers such as SAF blending, contrail avoidance, or hydrotreating will vary by region and require more detailed temperature response modeling that takes into account local atmospheric conditions and background emissions.

It is also important to evaluate post-2050 climate risks. While SLCP reductions can decrease near-term warming, they do not eliminate the long-term climate burden of CO_2. Future work could assess scenarios through 2100 through high-fidelity modeling and quantify the need for sustained GHG and SLCP reductions to prevent warming rebounds after mid-century. In addition, airline and consumer behavior remains an area of future modeling improvement. For example, shifts in fleet utilization patterns, strategies for handling green premiums, rebound effects associated with efficiency gains, and other topics could be further assessed.

REFERENCES

4AIR. (2024). *Policy watch: Sustainable aviation policy tracker.* https://www.4air.aero/policywatch

Aerospace Testing International. (2024, July 2). *Universal Hydrogen shut down after running out of cash*. https://www.aerospacetestinginternational.com/news/universal-hydrogen-shut-down-after-running-out-of-funding.html

Agarwal, A., Speth, R. L., Fritz, T. M., Jacob, S. D., Rindlisbacher, T., Iovinelli, R., Owen, B., Miake-Lye, R. C., Sabnis, J. S., & Barrett, S. R. H. (2019). SCOPE11 method for estimating aircraft black carbon mass and particle number emissions. *Environmental Science & Technology*, *53*(3), 1364–1373. https://doi.org/10.1021/acs.est.8b04060

Agarwal, A., Meijer, V. R., Eastham, S. D., Speth, R. L., & Barrett, S. R. (2022). Reanalysis-driven simulations may overestimate persistent contrail formation by 100%–250%. *Environmental Research Letters*, *17*(1). https://dspace.mit.edu/handle/1721.1/145280

Airbus. (2025, March 25). *Soaring towards future aircraft* [Press release]. https://www.airbus.com/en/newsroom/stories/2025-03-soaring-towards-future-aircraft

Airline Data Inc. (n.d.) *US DOT Form T-100*. Retrieved August 15, 2024, from https://airlinedatahub.com/

Albritton, D. L., Meira Filho, L. G., Cubasch, U., Dai, X., Ding, Y., Griggs, D. J., Hewitson, B., Houghton, J. T., Isaksen, I., Karl, T., McFarland, M., Meleshko, V. P., Mitchell, J. F. B., Noguer, M., Nyenzi, B. S., Oppenheimer, M., Penner, J. E., Pollonais, S., Stocker, T., … & Yap, K-S. (2001). Technical summary: A report accepted by Working Group I of the IPCC but not approved in detail. In J.T. Houghton, Y. Ding, D.J. Griggs, M. Noguer, P.J. van der Linden, X. Dai, K. Maskell, & C.A. Johnson (Eds.), *Climate change 2001: The scientific basis. Contribution of Working Group I to the third assessment report of the Intergovernmental Panel on Climate Change* (pp. 21-83). Cambridge University Press. https://archive.ipcc.ch/ipccreports/tar/wg1/pdf/WGI_TAR_full_report.pdf.

Andrews, S., Cathcart, J., Chen, A., Cornec, H., Kumar, S., Majholm, J., Meijers, M., Meijers, N., Miller, R., Mukhopadhaya, J., Sachdeva, N., Shapiro, M., Stern, C., & Wendling, Z. A. (2024). *Understanding contrail management: Opportunities, challenges, and insights*. RMI Contrail Impact Task Force. https://elib.dlr.de/209597/1/Final_RMI_CITF-Contrail-Management-Report_072524.pdf

ATR. (n.d.). *ATR EVO concept*. Retrieved August 13, 2025, from https://www.atr-aircraft.com/innovation/atr-evo-concept/

Baughcum, S. L., Begin, J. J., Franco, F., Greene, D. L., Lee, D. S., McLaren, M. L., Mortlock, A. K., Newton, P. J., Schmitt, A., Sutkus, D. J., Vedantham, A., & Wuebbles, D. J. (1999). *Aircraft emissions: Current inventories and future scenarios*. (Reprinted from *Aviation and the global atmosphere*, pp. 290–331, by J.E. Penner, D.H. Lister, D.J. Griggs, D.J. Dokken, & M. McFarland (Eds.), 1999, Cambridge University Press)

Barrett, S., Weibel, D., Brink, L., & Liu, M. (2021). *Project 039 naphthalene removal assessment*. FAA Center of Excellence for Alternative Jet Fuels & Environment. https://ascent.aero/documents/2019/07/ascent-project-039-2018-annual-report.pdf

Berntsen, T., & Fuglestvedt, J. (2008). Global temperature responses to current emissions from the transport sectors. *Proceedings of the National Academy of Sciences, 105*(49), 19154–19159. https://doi.org/10.1073/pnas.0804844105

Bickel, M., Ponater, M., Bock, L., Burkhardt, U., & Reineke, S. (2020). Estimating the effective radiative forcing of contrail cirrus. *Journal of Climate, 33*(5). https://doi.org/10.1175/JCLI-D-19-0467.1

Bickel, M. (2023). *Climate impact of contrail cirrus*. [Dissertation, Deutsches Zentrum für Luft- und Raumfahrt]. https://doi.org/10.57676/MZMG-R403

Bier, A., & Burkhardt, U. (2022). Impact of parametrizing microphysical processes in the jet and vortex phase on contrail cirrus properties and radiative forcing. *Journal of Geophysical Research: Atmospheres*, *127*(23). https://doi.org/10.1029/2022JD036677

Bock, L., & Burkhardt, U. (2016). Reassessing properties and radiative forcing of contrail cirrus using a climate model. *Journal of Geophysical Research: Atmospheres*, *121*(16), 9717-9736. https://doi.org/10.1002/2016JD025112

Bock, L., & Burkhardt, U. (2019). Contrail cirrus radiative forcing for future air traffic. *Atmospheric Chemistry and Physics*, *19*(12), 8163–8174. https://doi.org/10.5194/acp-19-8163-2019

Boyle, A. (2025, February 14). Eviation lays off employees and pauses development of electric-powered airplane. *GeekWire*. https://www.geekwire.com/2025/eviation-lays-off-employees-and-pauses-development-of-electric-powered-airplane/

Buffi, M., Scarlat, N., Hurtig, O., Motola, V., Georgakaki, A., Letout, S., Mountraki, A., & Joanny, G. (2022). *Clean Energy Technology Observatory: Renewable fuels of non-biological origin in the European Union – Status report on technology development, trends, value chains and markets.* Publications Office of the European Union. https://data.europa.eu/doi/10.2760/76717

Burkhardt, U., & Kärcher, B. (2011). Global radiative forcing from contrail cirrus. *Nature Climate Change*, *1*(1), 54–58. https://doi.org/10.1038/nclimate1068

Burkhardt, U., Bock, L., & Bier, A. (2018). Mitigating the contrail cirrus climate impact by reducing aircraft soot number emissions. *npj Climate and Atmospheric Science*, *1*(37). https://doi.org/10.1038/s41612-018-0046-4

CFM International. (n.d.). *Revolutionary Innovation for Sustainable Engines (RISE).* Retrieved August 13, 2025, from https://www.cfmaeroengines.com/rise

Chen, C. C., Gettelman, A., Craig, C., Minnis, P., & Duda, D. P. (2012). Global contrail coverage simulated by CAM5 with the inventory of 2006 global aircraft emissions. *Journal of Advances in Modeling Earth Systems*, *4*(2). https://doi.org/10.1029/2011MS000105

Chen, C. C., & Gettelman, A. (2013). Simulated radiative forcing from contrails and contrail cirrus. *Atmospheric Chemistry and Physics*, *13*(24), 12525-12536. https://doi.org/10.5194/acp-13-12525-2013

Ch-aviation. (n.d.) *Operator load factor data* [Dataset]. Retrieved September 12, 2024, from https://www.ch-aviation.com/

Debney, D., Beddoes, S., Foster, M., James, D., Kay, E., Kay, O., Shawki, K., Stubbs, E., Thomas, D., Weider, K., & Wilson, R. (2022). *Zero-carbon emission aircraft concepts*. Aerospace Technology Institute. https://www.ati.org.uk/wp-content/uploads/2022/03/FZO-AIN-REP-0007-FlyZero-Zero-Carbon-Emission-Aircraft-Concepts.pdf

DuBois, D. & Paynter, G. C. (2006). "Fuel Flow Method2" for estimating aircraft emissions. *SAE Transactions, 115*, 1–14. https://doi.org/10.4271/2006-01-1987

Eastham, S. D., Chossière, G. P., Speth, R. L., Jacob, D. J., & Barrett, S. R. H. (2024). Global impacts of aviation on air quality evaluated at high resolution. *Atmospheric Chemistry and Physics*, *24*(4), 2687–2703. https://doi.org/10.5194/acp-24-2687-2024

Embraer Commercial Aviation. (n.d.). *Future aircraft concepts*. Retrieved August 13, 2025, from https://embraercommercialaviationsustainability.com/concepts/

Eurocontrol. (n.d.). *Base of aircraft data* [Dataset]. Retrieved December 8, 2024, from https://www.eurocontrol.int/model/bada

Eurocontrol. (2023). *1.A.3.a Aviation -Annex 1 - Master emissions calculator - 2023 - Protected - v1.5_18_09_2024*. https://www.eea.europa.eu/publications/emep-eea-guidebook-2023/part-b-sectoral-guidance-chapters/1-energy/1-a-combustion/1-a-3-a-aviation.3/view

European Commission. (n.d.). *ReFuelEU Aviation*. Retrieved April 8, 2025, from https://transport.ec.europa.eu/transport-modes/air/environment/refueleu-aviation_en

European Union Aviation Safety Agency. (n.d.). *ICAO aircraft engine emissions databank* [Dataset]. Retrieved September 3, 2025, from https://www.easa.europa.eu/en/domains/environment/icao-aircraft-engine-emissions-databank

European Union Aviation Safety Agency. (2023). *Report on impact assessment of nvPM emissions from non-regulated engines*. https://www.easa.europa.eu/en/downloads/138846/en

Forster, P. M., Smith, C., Walsh, T., Lamb, W. F., Lamboll, R., Cassou, C., Hauser, M., Hausfather, Z., Lee, J-Y., Palmer, M. D., von Schuckmann, K., Slangen, A. B. A., Szopa, S., Trewin, B., Yun, J., Gillett, N., Jenkins, S., Matthews, H. D., Raghavan, K., Ribes, A., … & Zhai, P. (2025). Indicators of global climate change 2024: Annual update of key indicators of the state of the climate system and human influence. *Earth System Science Data*, *17*(6), 2641-2680. https://doi.org/10.5194/essd-17-2641-2025

Fuglestvedt, J. S., Berntsen, T. K., Myhre, G., Rypdal, K., & Schaefer, A. (2010). Transport impacts on atmosphere and climate: Metrics. *Atmospheric Environment, 44*(37), 4648–4677. https://doi.org/10.1016/j.atmosenv.2009.04.044

Gettelman, A., Chen, C. C., & Bardeen, C. G. (2021). The climate impact of COVID-19-induced contrail changes. *Atmospheric Chemistry and Physics*, *21*(12), 9405-9416. https://doi.org/10.5194/acp-21-9405-2021

Google Research. (n.d.). *Project contrails*. Retrieved August 8, 2025, from https://sites.research.google/contrails/

Government of Brazil. (2024, October 9). *Lula enacts Fuel of the Future law: "Brazil will drive the world's largest energy revolution"* [Press release]. https://www.gov.br/planalto/en/latest-news/2024/10/lula-enacts-fuel-of-the-future-law-201cbrazil-will-drive-the-worlds-largest-energy-revolution201d

Graham, D. (2025, April 22). Airbus delays hydrogen-electric plane by up to 10 years. *Skift*. https://skift.com/2025/04/22/airbus-delays-hydrogen-electric-plane-by-up-to-10-years/

Graver, B. (2022 January 5). Airline fuel efficiency: 'If you can't measure it, you can't improve it.' *International Council on Clean Transportation Staff Blog*. https://theicct.org/aviation-fuel-efficiency-jan22/

Graver, B., Mukhopadhaya, J., Zheng, X. S., Rutherford, D., Mukhopadhaya, J., & Pronk, E. (2022). *Vision 2050: Aligning aviation with the Paris Agreement*. International Council on Clean Transportation. https://theicct.org/publication/global-aviation-vision-2050-align-aviation-paris-jun22/

Graver, B., & Rutherford, D. (2018). *U.S. passenger jets under ICAO's CO2 standard: 2018–2038*. International Council on Clean Transportation. https://theicct.org/publication/u-s-passenger-jets-under-icaos-co2-standard-2018-2038/

Grobler, C. (2024). *Past, present, and future climate impacts of aviation* [Doctoral dissertation, Massachusetts Institute of Technology]. https://dspace.mit.edu/handle/1721.1/154000

Grewe, V., Gangoli Rao, A., Grönstedt, T., Xisto, C., Linke, F., Melkert, J., Middel, J., Ohlenforst, B., Blakey, S., Christie, S., Matthes, S., & Dahlmann, K. (2021). Evaluating the climate impact of aviation emission scenarios towards the Paris agreement including COVID-19 effects. *Nature Communications, 12*(3841). https://doi.org/10.1038/s41467-021-24091-y

Hameed, M., & Rutherford, D. (2025). *Fuel burn of new commercial jet aircraft: 1960 to 2024*. International Council on Clean Transportation. https://theicct.org/publication/fuel-burn-of-new-commercial-jet-aircraft-1960-to-2024-feb25/

Hepher, T. (2025). Airbus postpones development of new hydrogen aircraft. *Reuters*. https://www.reuters.com/business/aerospace-defense/airbus-postpones-development-new-hydrogen-aircraft-2025-02-07/

Hemmerdinger, J., & Hardee, H. (2023, March 2). Universal Hydrogen completes first flight of hydrogen-powered Dash 8. *FlightGlobal*. https://www.flightglobal.com/airframers/universal-hydrogen-completes-first-flight-of-hydrogen-powered-dash-8/152306.article

Hersbach, H., Bell, B., Berrisford, P., Biavati, G., Horányi, A., Muñoz Sabater, J., Nicolas, J., Peubey, C., Radu, R., Rozum, I., Schepers, D., Simmons, A., Soci, C., Dee, D., Thépaut, J-N. (2023). *ERA5 hourly data on single levels from 1940 to present* [Dataset]. Copernicus Climate Change Service Climate Data Store. 10.24381/cds.adbb2d47

IAGOS. (n.d.). *In-service aircraft for a global observing system*. Retrieved March 1, 2025, from https://www.iagos.org/

International Air Transport Association. (n.d.). *Aircraft technology roadmap to 2050*. https://www.sipotra.it/wp-content/uploads/2020/03/Aircraft-Technology-Roadmap-to-2050.pdf

International Air Transport Association. (2024a). *Aviation net-zero CO2 transition pathways: Comparative review*. https://www.iata.org/contentassets/8d19e716636a47c184e7221c77563c93/nz-roadmaps.pdf

International Air Transport Association. (2024b). *Disappointingly slow growth in SAF production* [Press release]. https://www.iata.org/en/pressroom/2024-releases/2024-12-10-03/

International Air Transport Association. (2024c). *Industry statistics*. https://www.iata.org/en/iata-repository/pressroom/fact-sheets/industry-statistics/

International Civil Aviation Organization. (2017). *Annex 16 to the Convention on International Civil Aviation: Environmental protection. Volume III — Aeroplane CO_2 emissions*. https://store.icao.int/en/annex-16-environmental-protection-volume-iii-aeroplane-co2-emissions

International Civil Aviation Organization. (n.d.-a) *CORSIA Central Registry (CCR)* [Dataset]. Retrieved February 20, 2025, from https://www.icao.int/CORSIA/CCR

International Civil Aviation Organization. (n.d.-b). *Traffic by flight stage* [Dataset]. Retrieved August 15, 2024, from http://dataplus.icao.int/Tools

International Civil Aviation Organization. (2019). *Independent expert integrated technology goals assessment and review for engines and aircraft*. https://store.icao.int/en/independent-expert-integrated-technology-goals-assessment-and-review-for-engines-and-aircraft-english-printed

International Civil Aviation Organization. (2022b, October 7). *States adopt net-zero 2050 aspirational goal for international flight operations* [Press release]. https://www2023.icao.int/Newsroom/NewsDoc2022/COM.49.22.EN.pdf

International Civil Aviation Organization. (2023a). *ICAO conference delivers strong global framework to implement a clean energy transition* [Press release]. https://www.icao.int/Newsroom/Pages/ICAO-Conference-delivers-strong-global-framework-to-implement-a-clean-energy-transition-for-international-aviation.aspx

International Civil Aviation Organization. (2023b). *Post-COVID-19 forecasts scenarios: Appendix A*. https://www2023.icao.int/sustainability/Documents/Post-COVID-19%20forecasts%20scenarios%20tables.pdf

International Civil Aviation Organization. (2023d). *Annex 16 to the Convention on International Civil Aviation: Environmental protection. Volume II — Aircraft engine emissions (4th edition)*.

International Council on Clean Transportation. (n.d.-a). *Jet and turboprop simulations for trajectory-based emissions and meteorological effects (JETSTREAM) model documentation*. https://theicct.github.io/JETSTREAM-doc/

International Council on Clean Transportation. (n.d.-b). *PACE model documentation*. https://theicct.github.io/PACE-doc/

Intergovernmental Panel on Climate Change. (2021). Summary for Policymakers. In V. Masson-Delmonte, P. Zhai, A. Pirani, S. L. Connors, C. Péan, S. Berger, N. Caud, Y. Chen, L. Goldfarb, M. I. Gomis, M. Huang, K. Leitzell, E. Lonnoy, J. B. R. Matthews, T. K. Maycock, T. Waterfield, O. Yelekçi, R. Yu, & B. Zhou (Eds.), *Climate change 2021: The physical science basis*: *Contribution of Working Group I to the sixth assessment report of the Intergovernmental Panel on Climate Change* (pp. 3–32). Cambridge University Press. https://doi.org/10.1017/9781009157896.001

Intergovernmental Panel on Climate Change. (2022). *Climate change 2022: Mitigation of climate change*. https://www.ipcc.ch/report/ar6/wg3/

Japan Ministry of Economy, Trade and Industry. (2025, July 15). 第7回 持続可能な航空燃料 (SAF) の導入促進に向けた官民協議会 [Seventh meeting of the public–private council to promote the introduction of sustainable aviation fuel]. https://www.meti.go.jp/shingikai/energy_environment/saf/007.html

JetZero. (n.d.). *United Airlines invests in JetZero* [Press release]. Retrieved August 13, 2025, from https://www.jetzero.aero/united-investment-announcement

Kärcher, B. (2018). Formation and radiative forcing of contrail cirrus. *Nature Communications*, *9*(1824). https://doi.org/10.1038/s41467-018-04068-0

Klöwer, M., Allen, M. R., Lee, D. S., Proud, S. R., Gallagher, L., & Skowron, A. (2021). Quantifying aviation's contribution to global warming. *Environmental Research Letters*, *16*(10). https://doi.org/10.1088/1748-9326/ac286e

Kaminski-Morrow, D. (2024). Airbus aims hydrogen-fuelled aircraft at low end of market. *FlightGlobal.* https://www.flightglobal.com/aerospace/airbus-aiming-hydrogen-fuelled-aircraft-at-low-end-of-market/156945.article

Leach, N. J., Jenkins, S., Nicholls, Z., Smith, C. J., Lynch, J., Cain, M., Walsh, T., Wu, B., Tsutsui, J., & Allen, M. R. (2021). FaIRv2.0.0: a generalized impulse response model for climate uncertainty and future scenario exploration. *Geoscientific Model Development*, *14*(5), 3007–3063. https://doi.org/10.5194/gmd-14-3007-2021

Lee, D. S., Fahey, D. W., Skowron, A., Allen, M. R., Burkhardt, U., Chen, Q., Doherty, S.J., Freeman, S., Forster, P.M., Fuglestvedt, J., Gettelman, A., De León, R.R., Lim, L.L., Lund, M.T., Millar, R.J., Owen, B., Penner, J.E., Pitari, G., Prather, M.J., … & Wilcox, L. J. (2021). The contribution of global aviation to anthropogenic climate forcing for 2000 to 2018. *Atmospheric environment*, *244*. https://doi.org/10.1016/j.atmosenv.2020.117834

Märkl, R. S. (2025). *Properties of contrails from aircraft with modern engines and alternative fuels* [Doctoral dissertation, Johannes Gutenberg-Universität Mainz]. https://openscience.ub.uni-mainz.de/items/dfa71e51-4b70-4ae2-9253-9b31ee547ed5

Märkl, R. S., Voigt, C., Sauer, D., Dischl, R. K., Kaufmann, S., Harlaß, T., Hahn, V., Roiger, A., Weiß-Rehm, C., Burkhardt, U., Schumann, U., Marsing, A., Scheibe, M., Dörnbrack, A., Renard, C., Gauthier, M., Swann, P., Madden, P., Luff, D., Stallinen, R., … & Le Clercq, P. (2024). Powering aircraft with 100% sustainable aviation fuel reduces ice crystals in contrails. *Atmospheric Chemistry and Physics*, *24*(6), 3813–3837. https://doi.org/10.5194/acp-24-3813-2024

Mastrandrea, M. D., Field, C. B., Stocker, T. F., Edenhofer, O., Ebi, K. L., Frame, D. J., Held, H., Kriegler, E., Mach, K. J., Matschoss, P. R., Plattner, G. K., Yohe, G. W., & Zwiers, F. W. (2010). *Guidance note for lead authors of the IPCC fifth assessment report on consistent treatment of uncertainties*. Intergovernmental Panel on Climate Change. https://www.ipcc.ch/site/assets/uploads/2017/08/AR5_Uncertainty_Guidance_Note.pdf

Mithal, S., & Rutherford, D. (2023). *ICAO's 2050 net-zero CO2 goal for international aviation*. International Council on Clean Transportation. https://theicct.org/wp-content/uploads/2022/12/global-aviation-ICAO-net-zero-goal-jan23.pdf

Mukhopadhaya, J., & Graver, B. (2022). *Performance analysis of regional electric aircraft*. International Council on Clean Transportation. https://theicct.org/wp-content/uploads/2022/07/global-aviation-performance-analysis-regional-electric-aircraft-jul22-1.pdf-1.pdf

Mukhopadhaya, J. (2023). *Performance analysis of fuel cell retrofit aircraft*. International Council on Clean Transportation. https://theicct.org/wp-content/uploads/2023/08/Aircraft-retrofit-white-paper-A4-v3.pdf

Myhre, G., Kvalevåg, M., Rädel, G., Cook, J., Shine, K. P., Clark, H., Karcher, F., Markowicz, K., Kardas, A. E., Wolkenberg, P., Balkanski, Y., Ponater, M., Forster, P., Rap, A., Rodriguez de Leon, R. (2009). Intercomparison of radiative forcing calculations of stratospheric water vapour and contrails. *Meteorologische Zeitschrift*, *18*(6), 585–596. https://doi.org/10.1127/0941-2948/2009/0411

National Civil Aviation Industry. (n.d.) *Microdados* [Microdata]. https://www.gov.br/anac/pt-br/assuntos/regulados/empresas-aereas/Instrucoes-para-a-elaboracao-e-apresentacao-das-demonstracoes-contabeis/envio-de-informacoes

Norris, G., & Warwick, G. (2025, February 8). *Airbus delays hydrogen but expands engine test plan*. Aviation Week Network. https://aviationweek.com/aerospace/emerging-technologies/airbus-delays-hydrogen-expands-engine-test-plan

O'Shea, C. (2023, June 12). *Next generation experimental aircraft becomes NASA's newest X-Plane* [Press release]. NASA. https://www.nasa.gov/news-release/next-generation-experimental-aircraft-becomes-nasas-newest-x-plane/

OAG. (n.d.) *Global airline schedules data* [Dataset]. Retrieved September 14, 2024, from https://www.oag.com/airline-schedules-data

Platt, J. C., Shapiro, M., Engberg, Z., McCloskey, K., Geraedts, S., Sankar, T., Stettler, M.E.J., Teoh, R., Schumann, U., & Rohs, S. (2024). The effect of uncertainty in humidity and model parameters on the prediction of contrail energy forcing. *Environmental Research Communications, 6*(9). https://doi.org/10.1088/2515-7620/ad6ee5

Ponater, M., Bickel, M., Bock, L., & Burkhardt, U. (2021). Towards determining the contrail cirrus efficacy. *Aerospace 8*(2). https://doi.org/10.3390/aerospace8020042

Ponater, M., Marquart, S., Sausen, R., & Schumann, U. (2005). On contrail climate sensitivity. *Geophysical Research Letters, 32*(10). https://doi.org/10.1029/2005GL022580

Priestley Centre for Climate Futures. (2023, June 14). *Scientists find three years left of remaining carbon budget for 1.5°C*. University of Leeds. https://climate.leeds.ac.uk/news/scientists-find-three-years-left-of-remaining-carbon-budget-for-1-5c/

Quadros, F. D., Snellen, M., & Dedoussi, I. C. (2022, January 3). *Recent and projected trends in global civil aviation fleet average NOX emissions indices* [Conference presentation]. AIAA SCITECH 2022 Forum, San Diego, CA. https://doi.org/10.2514/6.2022-2051

Quaas, J., Gryspeerdt, E., Vautard, R., & Boucher, O. (2021). Climate impact of aircraft-induced cirrus assessed from satellite observations before and during COVID-19. *Environmental Research Letters, 16*(6), 064051. https://doi.org/10.1088/1748-9326/abf686

Rap, A., Forster, P. M., Haywood, J.M., Jones, A., & Boucher, O. (2010). Estimating the climate impact of linear contrails using the UK Met Office climate model. *Geophysical Research Letters 37*(20). https://doi.org/10.1029/2010GL045161

Rhode, D. (2025). Zero-emission planes hit turbulence: What do recent delays mean for net-zero aviation by 2050? *International Council on Clean Transportation Staff Blog*. http://theicct.org/zero-emission-planes-hit-turbulence-what-do-recent-delays-mean-for-net-zero-aviation-by-2050-may25/

Rolls-Royce. (n.d.). *UltraFan*. Retrieved August 13, 2025, from https://www.rolls-royce.com/innovation/ultrafan.aspx

Rutherford, D. (2024 April 15). Net-zero aviation: How it started and how it's going. *International Council on Clean Transportation Staff Blog*. https://theicct.org/net-zero-aviation-how-it-started-and-how-its-going-apr24/

Schumann, U., Penner, J. E., Chen, Y., Zhou, C., & Graf, K. (2015). Dehydration effects from contrails in a coupled contrail–climate model. *Atmospheric Chemistry and Physics*, *15*(19), 11179-11199. https://doi.org/10.5194/acp-15-11179-2015

Shapiro, M., Engberg, Z., Teoh, R., Stettler, M., Dean, T., & Abbott, T. (2025). *Pycontrails: Python library for modeling aviation climate impacts*. Zenodo. https://doi.org/10.5281/zenodo.14714880.

Smith, C. J., Forster, P. M., Allen, M., Leach, N., Millar, R. J., Passerello, G. A., & Regayre, L. A. (2018). Understanding rapid adjustments to diverse forcing agents. *Geophysical Research Letters, 45*(21), 12023–12031. https://doi.org/10.1029/2018GL079826

Sonabend-W, A., Elkin, C., Dean, T., Dudley, J., Ali, N., Blickstein, J., Brand, E., Broshears, B., Chen, S., Engberg, Z., Galyen, M., Geraedts, S., Goyal, N., Grenham, R., Hager, U., Hecker, D., Jany, M., McCloskey, K., Ng, J., … & Platt, J. C. (2024). Feasibility test of per-flight contrail avoidance in commercial aviation. *Communications Engineering*, *3*(1), 184. https://doi.org/10.1038/s44172-024-00329-7

Spire. (n.d.) *Automatic Dependent Surveillance-Broadcast (ADS-B) data* [Dataset]. Retrieved October 2, 2024, from https://spire.com/aviation/

Teoh, R., Schumann, U., Gryspeerdt, E., Shapiro, M., Molloy, J., Koudis, G., Voigt, C., & Stettler, M. E. J. (2022). Aviation contrail climate effects in the North Atlantic from 2016 to 2021 [Supplemental Material]. *Atmospheric Chemistry and Physics*, *22*(16), 10919–10935. https://doi.org/10.5194/acp-22-10919-2022

Teoh, R., Schumann, U., Voigt, C., Schripp, T., Shapiro, M., Engberg, Z., Molloy, J., Koudis, G., & Stettler, M. E. (2022). Targeted use of sustainable aviation fuel to maximize climate benefits. *Environmental science & technology*, *56*(23), 17246-17255. https://doi.org/10.1021/acs.est.2c05781

Teoh, R., Engberg, Z., Schumann, U., Voigt, C., Shapiro, M., Rohs, S., & Stettler, M. E. (2024). Global aviation contrail climate effects from 2019 to 2021. Atmospheric Chemistry and Physics, 24(10), 6071-6093. https://doi.org/10.5194/acp-24-6071-2024

Terrenoire, E., Hauglustaine, D., Cohen, Y., Cozic, A., Valorso, R., Lefèvre, F., & Matthes, S. (2022). Impact of present and future aircraft NOX and aerosol emissions on atmospheric composition and associated direct radiative forcing of climate. *Atmospheric Chemistry and Physics 22*(18): 11987–23. https://doi.org/10.5194/acp-22-11987-2022.

Transport & Environment. (2024). *Contrail avoidance: Aviation's climate opportunity of the decade*. https://www.transportenvironment.org/uploads/files/Contrails-Briefing-2.pdf

UK Department for Transport. (2024, December 19). *Sustainable Aviation Fuel (SAF) Mandate*. https://www.gov.uk/government/collections/sustainable-aviation-fuel-saf-mandate

U.S. Department of Transportation. (n.d.) Bureau of Transportation Statistics Form 41. https://www.transtats.bts.gov/databases.asp?Z1qr_VQ=E&Z1qr_Qr5p=N8vn6v10&f7owrp6_VQF=D

van Seters, D., Grebe, S., & Faber, J. (2024). *Health impacts of aviation UFP emissions in Europe*. CE Delft. https://cedelft.eu/wp-content/uploads/sites/2/2024/06/CE_Delft_220396_Health_Impacts_of_Aviation_def.pdf

World Bank. (n.d.) World Bank country and lending groups. Retrieved April 10, 2025, from https://datahelpdesk.worldbank.org/knowledgebase/articles/906519-world-bank-country-and-lending-groups

Yim, S. H. L., Lee, G. L., Lee, I. H., Allroggen, F., Ashok, A., Caiazzo, F., Eastham, S. D., Malina, R., & Barrett, S. R. H. (2015). Global, regional and local health impacts of civil aviation emissions. *Environmental Research Letters*, *10*(3), 034001. https://doi.org/10.1088/1748-9326/10/3/034001

Zhang, W., Van Weverberg, K., Morcrette, C. J., Feng, W., Furtado, K., Field, P. R., … & Rap, A. (2025). Impact of host climate model on contrail cirrus effective radiative forcing estimates. *Atmospheric Chemistry and Physics*, *25*(1), 473-489. https://doi.org/10.5194/acp-25-473-2025

APPENDIX A: TRAFFIC SENSITIVITY ANALYSIS

All results in the main text were modeled under a mid traffic case with an annual traffic growth rate of 3.4% for passenger transport and 3.6% for dedicated freight transport. Due to the uncertainties associated with future air traffic growth, we modeled aviation's warming contribution over time to both high and low traffic growth assumptions. In the high traffic case, annual passenger traffic growth is assumed to be 3.7% and dedicated freight traffic growth 3.9%. In the low traffic case, we assumed 2.8% annual growth for passenger transport and 3.1% annual growth for freight. All traffic growth rates were taken from ICAO (2023b).

As shown in Figure A1, traffic uncertainties are projected to lead to minimal overlap of future warming contributions under the different scenarios. Only the low-traffic Historical Trends and the high-traffic Current Commitments scenarios see a small overlap. For the remaining scenarios (GHG Forward, SLCP Forward, and Full Breakthrough), traffic uncertainties do not affect the overall trend of increasing, inflecting, or stabilizing warming trends, respectively.

Figure A1
Traffic sensitivity of aviation's warming contribution, 1940–2050

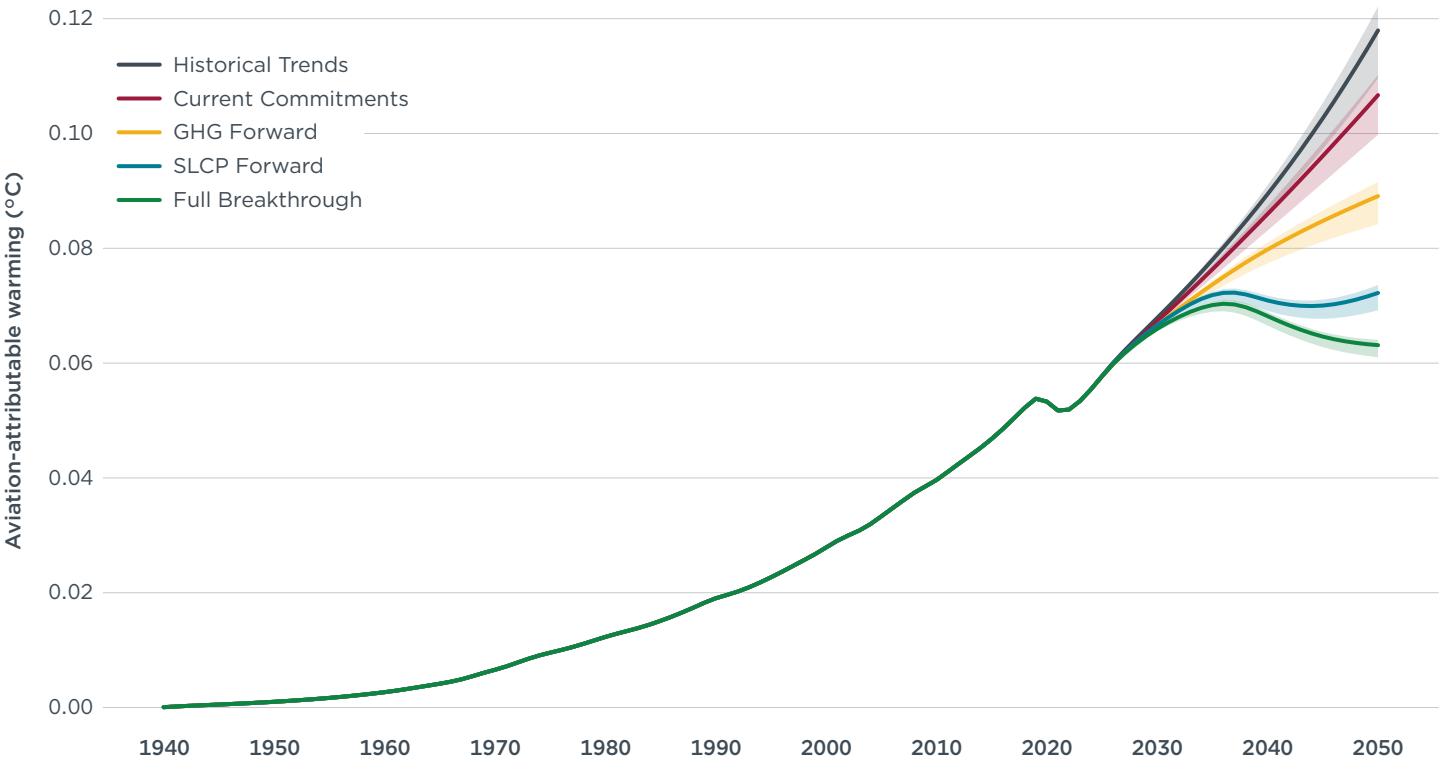

THE INTERNATIONAL COUNCIL ON CLEAN TRANSPORTATION **THEICCT.ORG**

APPENDIX B: CONTRAIL ABATEMENT PROPERTIES OF SAFS AND HYDROTREATED FOSSIL JET FUEL

Existing data points from studies investigating relationships between nvPM emissions, ice particle number, and annual mean contrail RF in rich-burn engines were used to develop correlations for modeling impacts of SAF on contrail radiative forcing. A three-step approach was taken to do so using studies across a range of geographical scopes.

First, data from studies quantifying percent change in nvPM number EI relative to SAF blend percentage were collected. Points from Teoh, Schumann, Voigt, et al. (2022) and Markl et al. (2024) were fitted to a polynomial curve, as shown in Figure B1. The resulting curve provides a 43% reduction in nvPM emissions for a 100% SAF blend, which is in line with experimental and modeling results that have shown reductions between 35% and 52%. We did not use the results of Caizzo et al. (2017) because this study considers mean contrail net RF, while the others looked at annual mean values.

Hydrotreated jet fuel was assumed to have the same nvPM reductions as SAF, as a similar fuel composition was assumed. These reductions in nvPM emissions from fuel composition were applied after any engine-level reductions from future engine technologies in the SLCP Forward and Full Breakthrough scenarios.

Figure B1

Correlation between SAF blending rate and nvPM emission index

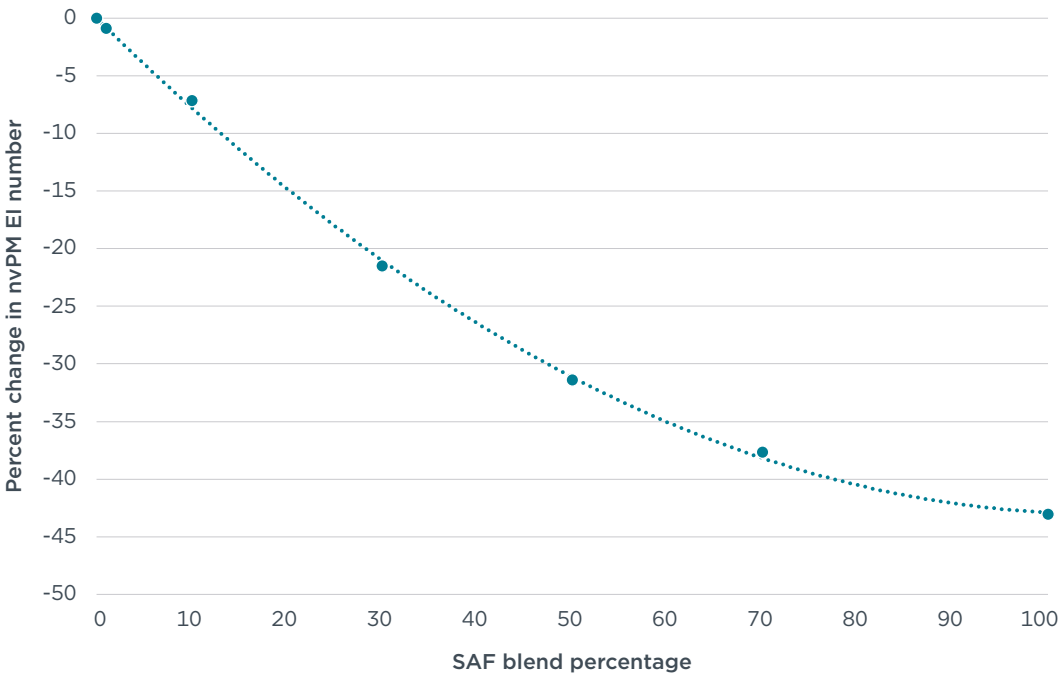

THE INTERNATIONAL COUNCIL ON CLEAN TRANSPORTATION **THEICCT.ORG**

Next, a linear relationship between percent change in nvPM number EI and ice particle number was developed using data points gathered from the same studies (Figure B2). This results in a roughly 50% reduction in nvPM ice particle number for a 43% reduction in nvPM number EI, which is the estimate when using 100% SAF. Preliminary studies have shown that engines emitting less than 10^{12} particles per kilogram of jet fuel may not exhibit this trend. Volatile particulate matter (vPM) begins to activate and interact

with the exhaust plume when soot emissions are significantly lowered. Because of this, ice particle numbers in the lean-burn combustion mode could be similar to the rich-burn mode even though the nvPM numbers per kilogram of fuel are up to 99% lower. This phenomenon is described in Karcher et al. (2018), and this relationship is seen in the experimental results of the VOLCAN2 flight trials conducted by the European Union. This is an area of ongoing study and preliminary research indicates the possibility for reductions in vPM formation from fuels with low sulfur content.

Figure B2

Correlation between change in nvPM emission index and change in ice particle number

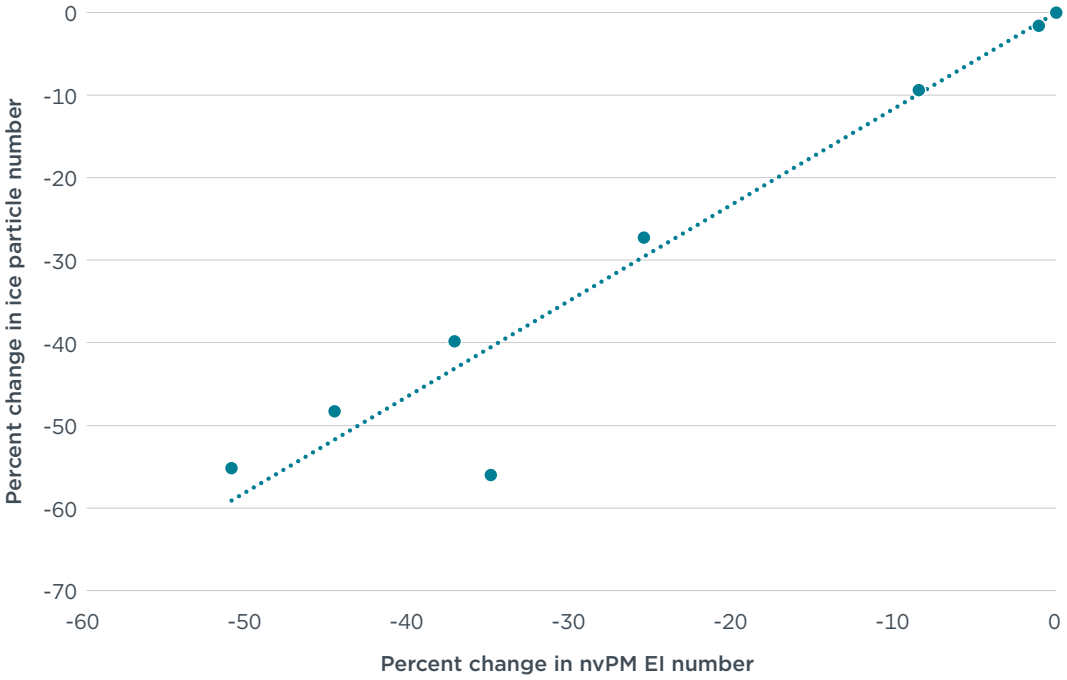

THE INTERNATIONAL COUNCIL ON CLEAN TRANSPORTATION **THEICCT.ORG**

In our modeling, if the average fleet nvPM number EI were to go below 10^{12} particles per kilogram of jet fuel, which we assume to be the threshold value for the soot-poor regime, a constant ice crystal number of 10^{14} ice crystals per kilogram of jet fuel was used to approximate the ice nucleation. This is an average of the ice particle number seen in the soot-poor regime in Markl et al. (2025). After running PACE with low-soot engines entering service in the SLCP Forward and Full Breakthrough scenarios, we did not reach this lower limit of 10^{12} particles per kilogram of fuel due to the slow uptake of advanced engines through 2050 relative to the existing engines in the fleet, with the vast majority operating in the soot-rich regime (nvPM number EI greater than 10^{12} particles per kilogram of jet fuel).

The third correlation that was formed was a linear relationship between percent change in ice particle number and annual mean net contrail RF. To do this, we used data points from Teoh et al. (2024), Markl et al. (2024), Burkhardt et al. (2018), and Bock and Burkhardt (2019).

We used these three relationships leveraging data points from a range of studies to form our correlation between SAF blend percentage and percent change in contrail RF, shown in Figure B3.

Figure B3

Correlation between change in ice particle number and change in annual mean contrail radiative forcing

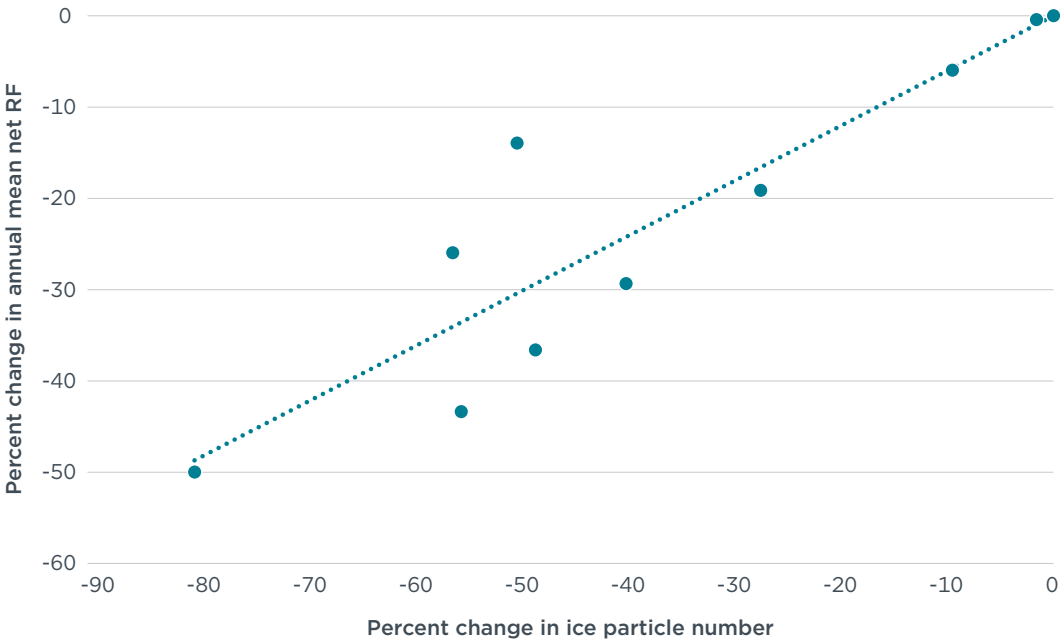

THE INTERNATIONAL COUNCIL ON CLEAN TRANSPORTATION **THEICCT.ORG**

APPENDIX C: CONTRAIL UNCERTAINTY ANALYSIS

Modeling the climate impact of aviation contrail cirrus remains a significant scientific challenge due to the complex, nonlinear interactions between aircraft emissions, atmospheric conditions, and radiative processes. We used CoCiP to create our contrail inventory for 2023, but we also recognize that the climate impact of contrails is uncertain and using one single model for contrail climate assessment may not be appropriate. To remedy this, we carried out a meta-analysis, like that of Lee et al. (2021), of multiple analyses of the climate impact of contrail cirrus. This analysis included studies since 2021 (including our own CoCiP analysis), which expanded the number of estimates from the four that were used in Lee et al. (2021) to 19. Like the previous meta-analysis, we scaled the estimates from each study to be directly comparable and expressed them in ERF per flight kilometer. The meta-analysis was used to perform Monte-Carlo-based uncertainty propagation to yield an output distribution for the global ERF of contrails per kilometer flown. The mean and 95% confidence interval of this output distribution is used for the projection of contrail's climate impact.

Studies estimating the global impact of contrail cirrus have employed either global climate models, contrail process models, or Earth observations. One observational study relied on satellite observations to infer aviation-induced changes in cirrus coverage and optical properties by comparing years with normal aviation activity to COVID-19-related air traffic reductions in 2020 (Quass et al., 2021). Process-based models such as CoCiP simulate contrail formation, dispersion, and decay using detailed flight trajectory and meteorological data, enabling spatio-temporal resolution of contrail radiative effects (Teoh et al., 2024). Global climate models integrate simplified contrail parameterizations, capturing the contrail cirrus life-cycle, microphysical processes (e.g., advection, deposition, sublimation, sedimentation), and their interactions with natural clouds, thereby estimating contrail cirrus radiative forcing at a global scale (Burkhardt & Kärcher, 2011; Chen & Gettelman, 2013; Schumann et al., 2015; Bock & Burkhardt, 2016; Gettelman et al., 2021; Bier & Burkhardt, 2022; Zhang et al., 2025).

The Lee et al. (2021) meta-analysis of the available literature at the time provided an estimate and a 5%–95% confidence interval for the RF (111.4 mW/m^2 ± 70%) and ERF (57.4 mW/m^2 ± 70%) for contrail cirrus. It employed four estimates that were based on aviation activity data from 2002 and 2006 and only used results from global climate models (Burkhardt & Kärcher, 2011; Chen & Gettelman, 2013; Schumann et al. 2015; Bock & Burkhardt, 2016).[15] Table C1 lists the studies considered in this meta-analysis along with the years that they analyze, the models that they employ, the aviation inventories that are used, the corresponding flight kilometers, and the estimated radiative forcing. We treated the Bier and Burkhardt (2022) estimate of 44 mW/m^2 for 2006 as an update of the Bock and Burkhardt (2016) estimate of 56 mW/m^2 for 2006 and we discarded the older value.

15 The study used an update to the Chen and Gettelman, 2013 study that used a smaller ice crystal radius and a bigger contrail cross-sectional area, which resulted in an increase from 13 mW/m^2 to 57 mW/m^2

Table C1

Modeling details and estimated global contrail cirrus RF of all the studies used in this study

Study	Model	Aviation inventory	Year	Flight kilometers (km)	Reported RF or ERF (mW/m²)
Burkhardt and Kaercher (2011)	ECHAM4-CCMod	AERO2K	2002	3.28E+10	38
Bock and Burkhardt (2016)	ECHAM5-CCMod	AERO2K	2002	3.28E+10	35
Chen and Gettelman (2013) [a]	CAM5	AEDT	2006	3.87E+10	57
Schumann et al. (2015)	CAM3+-IMPACT, CoCiP	AEDT	2006	3.87E+10	63
Bier and Burkhardt (2022)	ECHAM5-CCMod	AEDT	2006	3.87E+10	44 (31, 49)
Gettelman et al. (2021) [a]	CAM6	AEDT	2019	5.72E+10	90 (40, 140)
	CAM6	AEDT	2020	6.23E+10	33 (-2, 68)
Grewe et al. (2021)	AirClim	WeCare	2005	3.71E+10	45
Markl et al. (2024)	ECHAM5-CCMod	AEDT	2018	5.26E+10	72
Quass et al. (2021)	Satellite imaging		2019	6.09E+10	61 (22, 100)
Teoh et al. (2024)	CoCiP	ADS-B	2019	6.09E+10	62.1 (13.7, 74.8)
	CoCiP	ADS-B	2020	3.45E+10	27.3
	CoCiP	ADS-B	2021	4.19E+10	31.7
Zhang et al. (2025) [a]	CAM6	AEDT	2006	3.87E+10	52.5
	CAM6	AEDT	2018	6.11E+10	60.1
	UM	AEDT	2006	3.87E+10	25.7
	UM	AEDT	2018	6.11E+10	40.8
ICCT, forthcoming	CoCiP	ADS-B	2023	5.68E+10	41.5 (7.13, 176.1)

[a] The results of these simulation results are considered closer to ERF rather than RF.

Six of the estimates have an uncertainty interval associated with them. The source of the uncertainties that inform these intervals is different for each study. For Bier and Burkhardt (2022), the upper and lower interval boundary are the results of running the model with -66% and +100% nvPM number emissions. Similarly, Teoh et al. (2024) ran the analysis of 2019 using nvPM number EI of 10^{14} to 10^{15} particles per kg of fuel burned, informing the upper and lower interval of the analysis. Since the sensitivity analysis was not done for 2020 and 2021 results, the percentage change in the contrail RF from the 2019 results is applied to the 2020 and 2021 results. The ICCT analysis did a similar sensitivity analysis but varied the nvPM number EI by 0.1x to 10x, resulting in a higher upper bound. Gettelman et al. (2021) used ensemble members to run multiple Earth system simulations and used 2 standard deviations to report the uncertainty interval. For these studies we take the uncertainty interval as the 95% confidence interval. For studies without any uncertainty or sensitivity analysis, we adopted the assumption that the 95% confidence interval is ± 70% of the central estimate (Lee et al., 2021). We acknowledge that in Lee et al. (2021), the ± 70% assumption is for the 5%–95% confidence interval, which would be slightly smaller than the 95% confidence interval, but we kept the same assumption in the absence of a more rigorous uncertainty analysis.

In addition to scaling by flight kilometers flown, we employed scaling factors to account for some differences between the model estimates:

- S_1 = 1.4 to account for differences in base aviation inventory (studies using AERO2K used a factor of 1.4 to be comparable to AEDT; Bock & Burkhardt, 2016);
- S_2 = 1.14 to scale on-ground track distance to flown "slant" distance (only for studies using AERO2K as the base inventory; Bock & Burkhardt, 2016);
- S_3 = 0.87 if a model used monthly instead of hourly resolved air traffic data (Chen et al., 2012); and
- S_4 = 1.15 if a model is using frequency bands for the radiative transfer calculations instead of line-by-line calculations (Myhre et al., 2009).

We introduced two new scaling factors for the CoCiP-based studies:

- S_5 = 0.85 to account for the dehydration effect that contrails have on ice super-saturated regions and that is currently missed by CoCiP (Schumann et al., 2015); and
- S_6 = 0.95 to account for contrail-contrail overlap (Teoh et al., 2024).

The scaled RF per km estimates are listed in Table C2 along with the associated uncertainty interval.

Table C2

Scaling details for each study with the processed RF per km values and associated uncertainty bands

Study	Scaling factors applied	Year	RF per km (mW/m²/km)	Lower RF per km (mW/m²/km)	Upper RF per km (mW/m²/km)
Burkhardt and Kaercher (2011)	S_1, S_2, S_4	2002	2.12E-09	6.38E-10	3.61E-09
Bock and Burhardt (2016)	S_1, S_2, S_3,S_4	2002	1.70E-09	5.11E-10	2.90E-09
Chen and Gettelman (2013)	S_3,S_4	2006	1.47E-09	4.42E-10	2.51E-09
Schumann et al. (2015)	S_4, S_6	2006	1.87E-09	5.61E-10	3.18E-09
Bier and Burkhardt (2022)	S_3,S_4	2006	1.14E-09	8.01E-10	1.27E-09
Gettelman et al. (2021)	S_3,S_4	2019	1.57E-09	7.00E-10	2.45E-09
	S_3,S_4	2020	5.30E-10	-3.21E-11	1.09E-09
Grewe et al. (2021)	S_3,S_4	2005	1.21E-09	3.64E-10	2.06E-09
Markl et al. (2024)	S_3,S_4	2018	1.37E-09	4.11E-10	2.33E-09
Quass et al. (2021)		2019	1.00E-09	3.61E-10	1.64E-09
Teoh et al. (2024)	S_4, S_5, S_6	2019	9.46E-10	2.09E-11	1.14E-09
	S_4, S_5,S_6	2020	7.34E-10	1.62E-11	8.85E-10
	S_4, S_5, S_6	2021	7.03E-10	1.55E-11	8.46E-10
Zhang et al. (2025)	S_3, S_4	2006	1.36E-09	4.07E-10	2.31E-09
	S_3, S_4	2018	9.84E-10	2.95E-10	1.67E-09
	S_3, S_4	2006	6.65E-10	1.99E-10	1.13E-09
	S_3, S_4	2018	6.68E-10	2.00E-10	1.13E-09
ICCT, forthcoming	S_4, S_5, S_6	2023	6.78E-10	1.17E-11	2.88E-09

Radiative forcing from contrails is not as effective as CO_2 in changing the Earth's surface temperature. To account for this, we used an efficacy factor (ERF/RF) to convert all RF estimates to ERF estimates. There are four studies that quantify the efficacy of contrails (listed in Table C3), of which three provide 95% confidence intervals for their estimate.[16] With such few estimates, a statistical analysis is difficult. Instead, a triangular distribution with a minimum, midpoint, and maximum of 0.14, 0.36, and 0.7 was used. The midpoint is the average of the central estimates. The maximum is the highest end of the confidence intervals. The minimum is 33% lower than the lowest estimate since the lower confidence interval of the other studies was, on average, 33% lower than the central estimate. Chen and Gettelman (2013), Gettelman et al. (2021), and Zhang et al. (2025) report ERF, so the efficacy factor is not applied to these studies.

Table C3

Studies that quantify efficacy with provided 95% confidence intervals in parenthesis

Study	Efficacy
Ponater et al. (2005)	0.59 (0.48, 0.7)
Rap et al. (2010)	0.31 (0.17, 0.45)
Bickel et al. (2020)	0.35 (0.23, 0.51)
Bickel (2023)	0.21
Triangular distribution used for this study	0.36 (0.14, 0.7)

To propagate the uncertainty in each individual estimate to the combined result, we treated each estimate as an independent random variable that is distributed within the uncertainty intervals. There is no prior distribution associated with these estimates, so we assumed they may be uniformly, triangularly, or normally distributed. For the normal distribution, it must be assumed that the mean is centered in the interval bound and the upper and lower bounds are 2 standard deviations from the mean. No such assumption is required for the triangle and uniform distributions, which have finite intervals and do not have to be centered. This yielded 18 individual estimates with 3 distributions each, resulting in 54 distributions.

For the uncertainty propagation, we took 100,000 samples from each of the 54 distributions and treated each as an individual estimate of the RF per km. We also took 100,000 samples of the efficacy factor and multiplied it by the samples from the relevant studies. The resulting samples form the final distribution of the ERF per km used in this paper (Figure C1). The shape of the distribution is neither smooth nor centered. The resulting mean of the distribution is 7.03E-10 $mW/m^2/km$ with a 95% confidence interval of [1.04E-10, 20.1E-10] $mW/m^2/km$. The mode of the distribution is 2.72E-10 $mW/m^2/km$.

16 Bickel 2023 does not provide a confidence interval as his estimate is the quotient of two ratio distributions which makes statistical parameters difficult to calculate analytically.

Figure C1
Distribution of the ERF per km used in this study

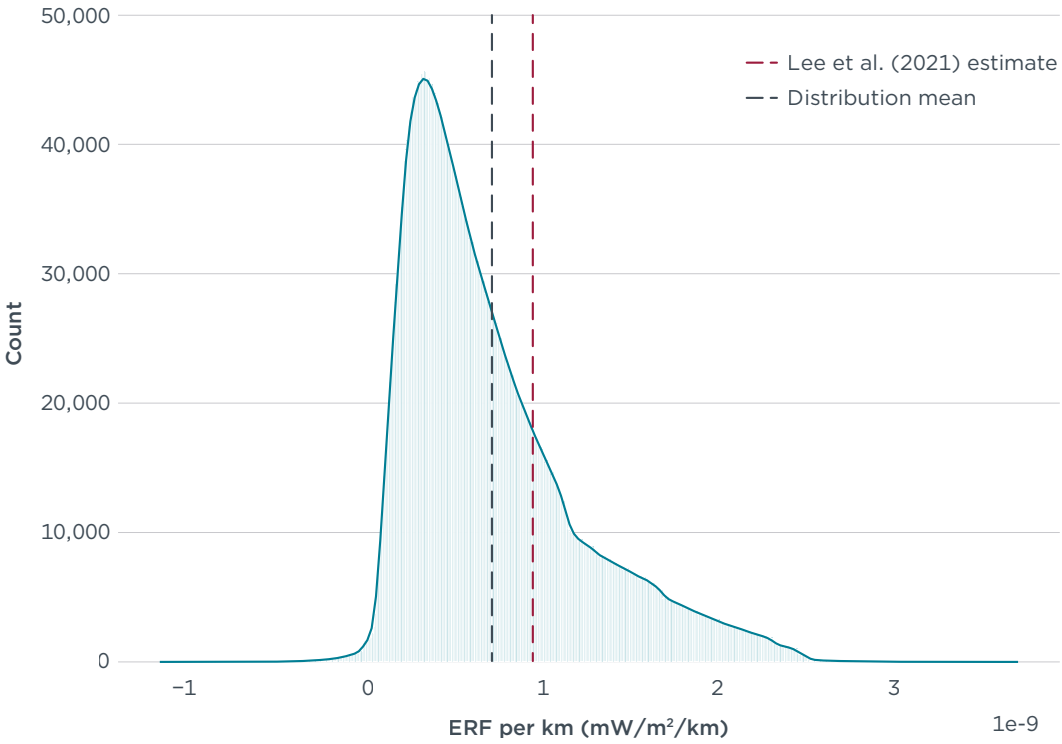

THE INTERNATIONAL COUNCIL ON CLEAN TRANSPORTATION **THEICCT.ORG**

The mean of the distribution is ~25% lower than the central estimate of 9.36E-10 mW/m²/km from Lee et al. (2021) and the 95% confidence interval is bigger than the 5-95% confidence interval calculated by Lee et al., 2021. Comparing this combined estimate to our CoCiP results for 2023, the contrail warming impact in 2023 could be more than 2.3 times (42.2 mW/m² [7.4, 118.1]) higher than predicted by CoCiP (17.8 mW/m²). Figure C2 plots the ERF per km estimates from all the different studies and compares them to the Lee et al. (2021) meta-analysis and this analysis. This report uses the last entry in the plot, labeled "This analysis (Combined distribution)," which is the output from this meta-analysis; this is preferred over the results from our own CoCiP analysis, labeled "ICCT, forthcoming," as it incorporates the results of multiple models and different years of analysis. There has been a tendency for newer contrail impact estimates since 2021 to be lower than the Lee et al. (2021) values, except for simulations run using the CAM6 model.

Figure C2

Central estimate and uncertainty intervals used for this meta-analysis

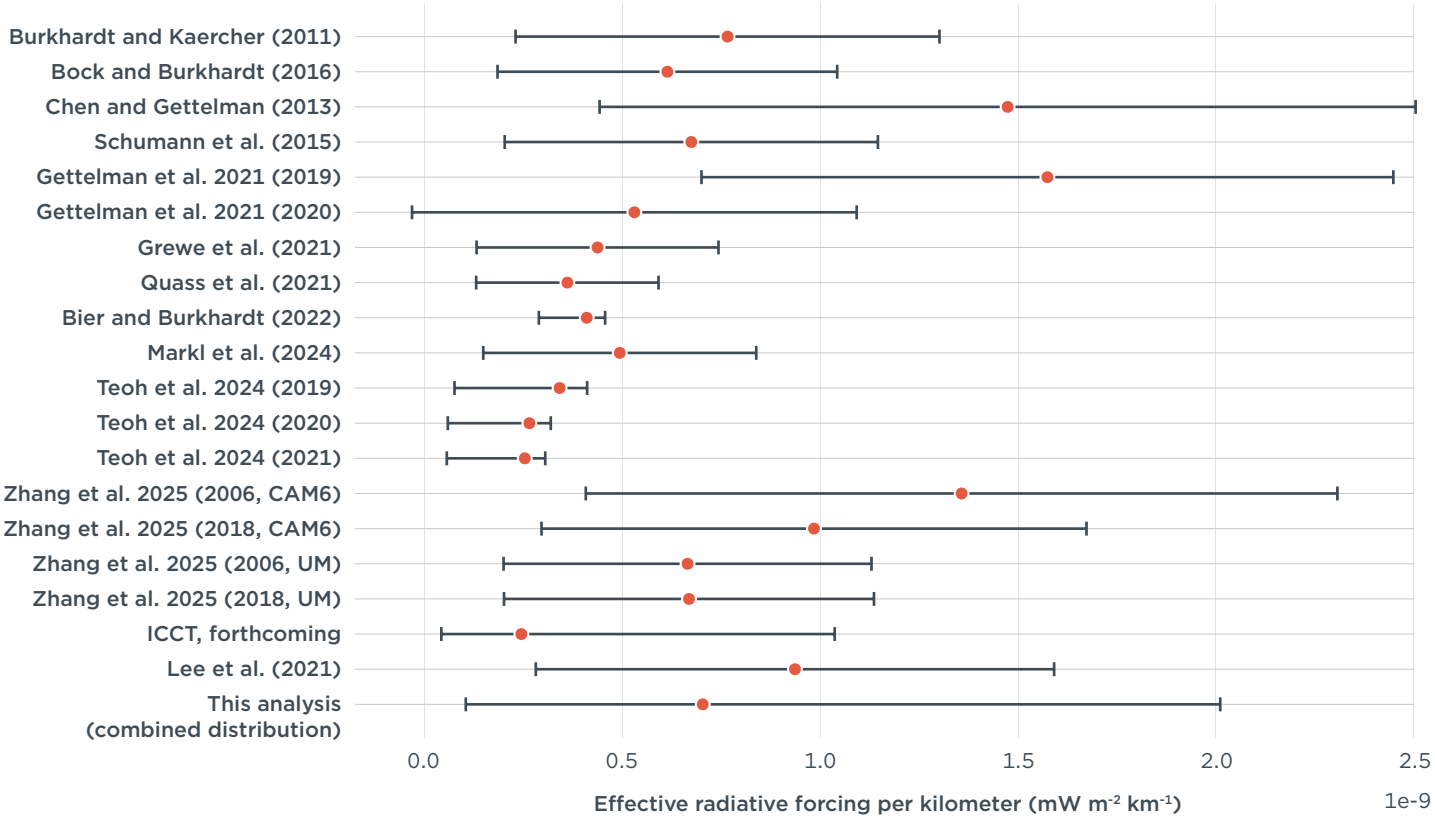

THE INTERNATIONAL COUNCIL ON CLEAN TRANSPORTATION **THEICCT.ORG**

APPENDIX D: UNCERTAINTY ANALYSIS OF ALL SLCPS

In addition to the meta-analysis for contrails and their uncertainties (Appendix C), we also used 5%–95% confidence intervals from Lee et al. (2021) to propagate the uncertainty in the ERF of all SLCPs. Table D1 lists the central estimate and the upper and lower bounds for the ERF per unit of emission of each SLCP. Note that the contrail cirrus values are the mean and 95% confidence interval from our analysis, while all others are the median and 5%–95% confidence interval from Lee et al. (2021).

Table D1

Values used in uncertainty analysis of climate impact of contrails

Pollutant	Central estimate for ERF	Lower bound for ERF	Upper bound for ERF
Contrail cirrus [mW/m²/km]	7.03E-10	1.04E-10	20.1E-10
NO_x [mW/m²/Tg(N) /yr]	12.25	0.41	19.91
SO_x [mW/m²/Tg(SO_2) /yr]	-19.91	-49.78	-6.87
nvPM [mW/m²/Tg(nvPM) /yr]	100.67	7.95	428.65
Water vapor [mW/m²/Tg(H_2O) /yr]	0.0052	0.0021	0.0083

The values presented are multiplied by the annual emissions of each pollutant in each modeled scenario to create time series for the central, lower, and upper estimates. These are then passed through the FaIR climate model as explained in the Temperature Response section. The temperature response in 2050, including the upper and lower bounds, is shown for all of the scenarios in Table D2. The Historical Trends and Full Breakthrough scenario results are also plotted in Figure D1. The range in temperature response due to uncertainty in SLCP climate impact is greater than the range due to variable traffic growth rates, as shown in Figure A1.

Table D2

Temperature response in 2050 with bounds that account for the uncertainty in the climate impact of SLCPs

Scenario	Temperature response in 2050 (°C)
Historical Trends	0.118 [0.055, 0.224]
Current Commitments	0.107 [0.052, 0.200]
GHG Forward	0.089 [0.046, 0.162]
SLCP Forward	0.072 [0.049, 0.101]
Full Breakthrough	0.063 [0.042, 0.089]

Figure D1

Temperature response for the Historical Trends and the Full Breakthrough scenarios

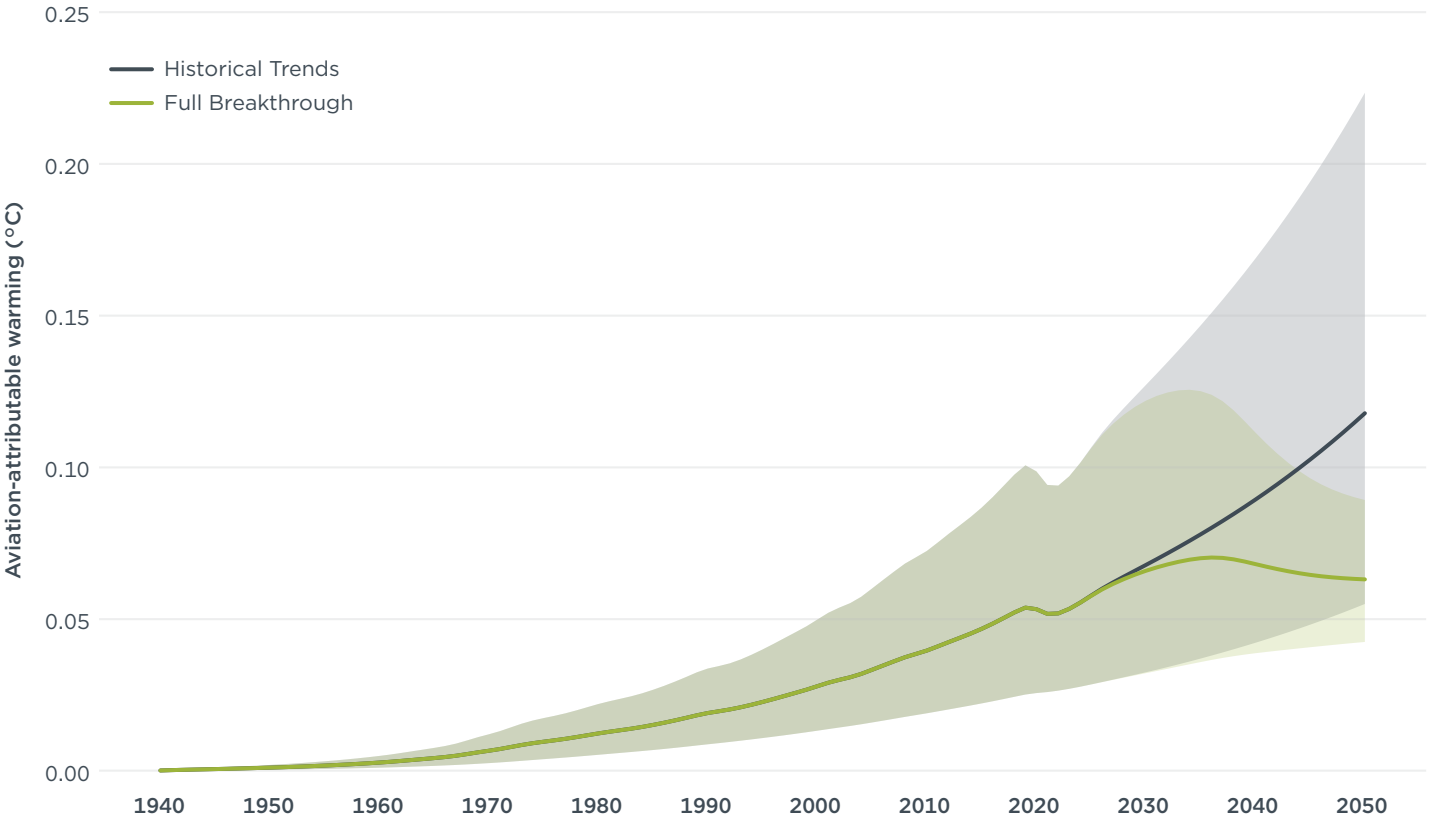

Note: The shaded area representing the range of possible responses due to uncertainty in the climate impact of SLCPs.

www.theicct.org

communications@theicct.org

@theicct.org

icct
THE INTERNATIONAL COUNCIL
ON CLEAN TRANSPORTATION

BEIJING | BERLIN | NEW DELHI | SAN FRANCISCO | SÃO PAULO | WASHINGTON DC